National Library of Canada
Canadian Theses Service
Ottawa, Canada
K1A 0N4

Bibliothèque nationale du Canada
Services des thèses canadiennes

CANADIAN THESES

THÈSES CANADIENNES

NOTICE

The quality of this microfiche is heavily dependent upon the quality of the original thesis submitted for microfilming. Every effort has been made to ensure the highest quality of reproduction possible.

If pages are missing, contact the university which granted the degree.

Some pages may have indistinct print especially if the original pages were typed with a poor typewriter ribbon or if the university sent us an inferior photocopy.

Previously copyrighted materials (journal articles, published tests, etc.) are not filmed.

Reproduction in full or in part of this film is governed by the Canadian Copyright Act, R.S.C. 1970, c. C-30.

AVIS

La qualité de cette microfiche dépend grandement de la qualité de la thèse soumise au microfilmage. Nous avons tout fait pour assurer une qualité supérieure de reproduction.

S'il manque des pages, veuillez communiquer avec l'université qui a conféré le grade.

La qualité d'impression de certaines pages peut laisser à désirer, surtout si les pages originales ont été dactylographiées à l'aide d'un ruban usé ou si l'université nous a fait parvenir une photocopie de qualité inférieure.

Les documents qui font déjà l'objet d'un droit d'auteur (articles de revue, examens publiés, etc.) ne sont pas microfilmés.

La reproduction, même partielle, de ce microfilm est soumise à la Loi canadienne sur le droit d'auteur, SRC 1970, c. C-30.

THIS DISSERTATION HAS BEEN MICROFILMED EXACTLY AS RECEIVED

LA THÈSE A ÉTÉ MICROFILMÉE TELLE QUE NOUS L'AVONS REÇUE

NL-339 (r.86/06)

Canada

THE UNIVERSITY OF ALBERTA

THE EFFECTS OF CLAY FINES ON OIL/WATER DISPERSIONS

by

(C) JONATHAN R. SPENCE

A THESIS

SUBMITTED TO THE FACULTY OF GRADUATE STUDIES AND RESEARCH

IN PARTIAL FULFILMENT OF THE REQUIREMENTS FOR THE DEGREE

OF MASTER OF SCIENCE

DEPARTMENT OF CHEMICAL ENGINEERING

EDMONTON, ALBERTA

SPRING 1987

Permission has been granted to the National Library of Canada to microfilm this thesis and to lend or sell copies of the film.

The author (copyright owner) has reserved other publication rights, and neither the thesis nor extensive extracts from it may be printed or otherwise reproduced without his/her written permission.

L'autorisation a été accordée à la Bibliothèque nationale du Canada de microfilmer cette thèse et de prêter ou de vendre des exemplaires du film.

L'auteur (titulaire du droit d'auteur) se réserve les autres droits de publication; ni la thèse ni de longs extraits de celle-ci ne doivent être imprimés ou autrement reproduits sans son autorisation écrite.

ISBN 0-315-37802-6

THE UNIVERSITY OF ALBERTA

RELEASE FORM

NAME OF AUTHOR JONATHAN R. SPENCE

TITLE OF THESIS THE EFFECTS OF CLAY FINES ON OIL/WATER DISPERSIONS

DEGREE FOR WHICH THESIS WAS PRESENTED MASTER OF SCIENCE

YEAR THIS DEGREE GRANTED SPRING 1987

Permission is hereby granted to THE UNIVERSITY OF ALBERTA LIBRARY to reproduce single copies of this thesis and to lend or sell such copies for private, scholarly or scientific research purposes only.

The author reserves other publication rights, and neither the thesis nor extensive extracts from it may be printed or otherwise reproduced without the author's written permission.

(SIGNED) Jon Spence

PERMANENT ADDRESS:

1369 Hermitage Road
Edmonton, Alberta
T5A 4N5

DATED April 6 1987

THE UNIVERSITY OF ALBERTA

FACULTY OF GRADUATE STUDIES AND RESEARCH

The undersigned certify that they have read, and recommend to the Faculty of Graduate Studies and Research, for acceptance, a thesis entitled The Effects of Clay Fines On Oil/Water Dispersions submitted by Jonathan R. Spence in partial fulfilment of the requirements for the degree of Master of Science in Chemical Engineering.

.....

Supervisor

.....

.....

.....

.....

Date.....March 30/87.....

Abstract

The purpose of this work is to investigate the effects of clay and fines on the size of oil drops in oil/water dispersions. The study was motivated by the need to understand why low grade oil sands result in a surprisingly low bitumen recovery in the Hot Water Process for recovering bitumen from oil sand. A stirred vessel with a flat bladed impeller was used to create the dispersions. A photographic method, using an image analyzer, was used to determine the average drop sizes and the drop size distributions.

Results were obtained using a light hydrocarbon (hexane), a medium viscosity paraffin oil, and a heavy Cold Lake bitumen. Pure kaolinite was used for the solids, as well as an unpurified mixture of clay fines recovered from Athabasca oil sand. Runs were carried out with and without clay fines over a range of Weber numbers. Different methods of introducing the fines were studied, as well as the effects of the presence of NaCl in the continuous water phase.

The addition of clay was found to increase the drop size for both the hexane and the paraffin oil, approximately doubling the drop size for hexane. The addition of the kaolinite to the bitumen/water dispersions was found to have little effect.

Acknowledgement

The author would like to thank Dr. Jacob Masliyah for his invaluable support and guidance during the course of this work. Thanks are also due to the workshop staff, the instrument shop staff, and all other individuals who assisted with this work.

The author would also like to thank and acknowledge the financial support provided by the Alberta Oil Sands Technology and Research Authority.

Table of Contents

Chapter		Page
1.	Objectives	1
2.	Introduction	2
3.	Literature Review	4
	3.1 Oil/Water Dispersions	4
	3.2 Colloid Theory	12
	3.3 The Effect of Solid Additives	12
	3.4 Experimental Techniques	14
4.	Experimental Apparatus and Procedure	20
	4.1 Experimental Apparatus	20
	4.2 Experimental Materials	27
	4.3 Experimental Procedure	29
5.	Results and Discussion	32
	5.1 Average Drop Diameters	53
	5.2 Drop Size Distributions	54
	5.3 Maximum Drop Sizes	65
	5.4 Experimental Errors	69
6.	Conclusions	73
7.	Recommendations	74
8.	References	75
9.	Appendix A : Material Properties	83
	9.1 Properties of Kaolinite used in this work	83
	9.2 Properties of Athabasca Fines	85
	9.3 Properties of Cold Lake Bitumen used in this work	86
10.	Appendix B : Experimental Data	88
11.	Appendix C : Experimental Drop Size Distributions	93

List of Tables

Table		Page
4.1	Properties of hexane, paraffin oil, and bitumen.	28
4.2	Clay Composition of Athabasca Fines.....	28
5.1	Theoretical and experimental maximum drop diameters (at a nominal agitation speed of 408 rpm).....	66
5.2	Comparison of average values of d_{32}/d_{max}	68
10.1	Drop size parameters.....	88

List of Figures

Figure		Page
3.1	Comparison of experimental data of Gnanasundaram et al. [16], (Information adapted from source)	10
3.2	Experimental data for paraffin oil/water dispersions, Ward and Knudsen [44], (Information adapted from source)	11
4.1	Schematic Diagram of Experimental Apparatus	21
4.2	Schematic Diagram of Optical Probe	24
5.1	Sauter mean drop size as a function of impeller speed for 5% hexane/water, paraffin oil/water, and bitumen/water dispersions	33
5.2	The effect of the addition of 0.04wt% kaolinite to a 5% hexane water dispersion	37
5.3	The effect of the addition of 0.04wt% Athabasca fines to a 5% hexane/water dispersion	40
5.4	Variation in sauter mean drop size with two different modes of kaolinite addition to hexane/water dispersions	42
5.5	Variation in sauter mean drop size with increasing NaCl concentration for hexane/water dispersions	43
5.6	The effect of the addition of 0.04wt% kaolinite to a hexane/water dispersion at 0.02M NaCl	45
5.7	The effect of the addition of 0.04wt% kaolinite to a 5% paraffin oil/water dispersion	46
5.8	The effect of the addition of 0.04wt% kaolinite to a 5% bitumen/water dispersion	49
5.9	Comparison of experimental data for hexane/water, paraffin oil/water and bitumen/water dispersions to the predictions of Equation 5.3	51
5.10	Comparison of the results of other work with the predictions of Equation 5.5, Wang and Calabrese [43], (Information adapted from source)	52
5.11	Drop size distribution for a 5% hexane, 95% water dispersion, 0.001M NaCl, 389 rpm	55

5.12 Drop size distribution for a 5% hexane, 95% water dispersion, 0.04 wt% kaolinite, 0.001M NaCl, 384 rpm.....56

5.13 Drop size distribution for a 5% paraffin oil, 95% water dispersion, 0.001M NaCl, 368 rpm.....57

5.14 Drop size distribution for a 5% paraffin oil, 95% water dispersion, 0.04 wt% kaolinite, 0.001M NaCl, 375 rpm.....58

5.15 Drop size distribution for a 5% bitumen, 95% water dispersion, 0.001M NaCl, 389 rpm.....59

5.16 Drop size distribution for a 5% bitumen, 95% water dispersion, 0.04 wt% kaolinite, 0.001M NaCl, 381 rpm.....60

5.17 Log-normal probability plot showing the effect of kaolinite addition to a 5% hexane/water dispersion at 0.001M NaCl (not all points are shown).....62

5.18 Log-normal probability plot showing the effect of kaolinite addition to a 5% paraffin/water dispersion at 0.001M NaCl (not all points are shown).....63

5.19 Log-normal probability plot showing the effect of kaolinite addition to a 5% bitumen/water dispersion at 0.001M NaCl (not all points are shown).....64

5.20 Experimental and theoretical maximum drop sizes at 408 rpm.....67

11.1.1 Drop size distribution for a 5% hexane, 95% water dispersion, 0.001M NaCl, 325 rpm.....94

11.1.2 Drop size distribution for a 5% hexane, 95% water dispersion, 0.001M NaCl, 349 rpm.....95

11.1.3 Drop size distribution for a 5% hexane, 95% water dispersion, 0.001M NaCl, 372 rpm.....96

11.1.4 Drop size distribution for a 5% hexane, 95% water dispersion, 0.001M NaCl, 385 rpm.....97

11.1.5 Drop size distribution for a 5% hexane, 95% water dispersion, 0.001M NaCl, 410 rpm.....98

11.1.6 Drop size distribution for a 5% hexane, 95% water dispersion, 0.001M NaCl, 436 rpm.....99

11.1.7 Drop size distribution for a 5% hexane, 95% water dispersion, 0.04 wt% kaolinite, 0.001M NaCl, 325 rpm.....100

11.1.8 Drop size distribution for a 5% hexane, 95% water dispersion, 0.04 wt% kaolinite, 0.001M NaCl, 329 rpm.....101

11.1.9 Drop size distribution for a 5% hexane, 95% water dispersion, 0.04 wt% kaolinite, 0.001M NaCl, 347 rpm.....102

11.1.10 Drop size distribution for a 5% hexane, 95% water dispersion, 0.04 wt% kaolinite, 0.001M NaCl, 352 rpm.....103

11.1.11 Drop size distribution for a 5% hexane, 95% water dispersion, 0.04 wt% kaolinite, 0.001M NaCl, 383 rpm.....104

11.1.12 Drop size distribution for a 5% hexane, 95% water dispersion, 0.04 wt% kaolinite, 0.001M NaCl, 385 rpm.....105

11.1.13 Drop size distribution for a 5% hexane, 95% water dispersion, 0.04 wt% kaolinite, 0.001M NaCl, 420 rpm.....106

11.1.14 Drop size distribution for a 5% hexane, 95% water dispersion, 0.04 wt% kaolinite, 0.001M NaCl, 423 rpm.....107

11.1.15 Drop size distribution for a 5% hexane, 95% water dispersion, 0.04 wt% kaolinite, 0.001M NaCl, 440 rpm.....108

11.1.16 Drop size distribution for a 5% hexane, 95% water dispersion, 0.04 wt% kaolinite, 0.001M NaCl, 450 rpm.....109

11.1.17 Drop size distribution for a 5% hexane, 95% water dispersion, 0.04 wt% Athabasca fines, 0.001M NaCl, 344 rpm.....110

11.1.18 Drop size distribution for a 5% hexane, 95% water dispersion, 0.04 wt% Athabasca fines, 0.001M NaCl, 374 rpm.....111

11.1.19 Drop size distribution for a 5% hexane, 95% water dispersion, 0.04 wt% Athabasca fines, 0.001M NaCl, 393 rpm.....112

11.1.20 Drop size distribution for a 5% hexane, 95% water dispersion, 0.04 wt% Athabasca fines, 0.001M NaCl, 417 rpm.....113

11.1.21 Drop size distribution for a 5% hexane, 95% water dispersion, 0.04 wt% Athabasca fines, 0.001M NaCl, 435 rpm.....114

11.1.22 Drop size distribution for a 5% hexane, 95% water dispersion, 0.04 wt% kaolinite (added to the oil phase), 0.001M NaCl, 327 rpm.....115

11.1.23 Drop size distribution for a 5% hexane, 95% water dispersion, 0.04 wt% kaolinite (added to the oil phase), 0.001M NaCl, 365 rpm.....116

11.1.24 Drop size distribution for a 5% hexane, 95% water dispersion, 0.04 wt% kaolinite (added to the oil phase), 0.001M NaCl, 369 rpm.....117

11.1.25 Drop size distribution for a 5% hexane, 95% water dispersion, 0.04 wt% kaolinite (added to the oil phase), 0.001M NaCl, 410 rpm.....118

11.1.26 Drop size distribution for a 5% hexane, 95% water dispersion, 0.04 wt% kaolinite (added to the oil phase), 0.001M NaCl, 434 rpm.....119

11.1.27 Drop size distribution for a 5% hexane, 95% water dispersion, 0.02M NaCl, 346 rpm.....120

11.1.28 Drop size distribution for a 5% hexane, 95% water dispersion, 0.02M NaCl, 371 rpm.....121

11.1.29 Drop size distribution for a 5% hexane, 95% water dispersion, 0.02M NaCl, 372 rpm.....122

11.1.30 Drop size distribution for a 5% hexane, 95% water dispersion, 0.02M NaCl, 377 rpm.....123

11.1.31 Drop size distribution for a 5% hexane, 95% water dispersion, 0.02M NaCl, 407 rpm.....124

11.1.32 Drop size distribution for a 5% hexane, 95% water dispersion, 0.02M NaCl, 435 rpm.....125

11.1.33 Drop size distribution for a 5% hexane, 95% water dispersion, 0.02M NaCl, 457 rpm.....126

11.1.34 Drop size distribution for a 5% hexane, 95% water dispersion, 0.04 wt% kaolinite, 0.02M NaCl, 350 rpm.....127

11.1.35 Drop size distribution for a 5% hexane, 95% water dispersion, 0.04 wt% kaolinite, 0.02M NaCl, 374 rpm.....128

11.1.36 Drop size distribution for a 5% hexane, 95% water dispersion, 0.04 wt% kaolinite, 0.02M NaCl, 377 rpm.....129

11,1.37 Drop size distribution for a 5% hexane, 95% water dispersion, 0.04 wt% kaolinite, 0.02M NaCl, 400 rpm.....130

11.1.38 Drop size distribution for a 5% hexane, 95% water dispersion, 0.04 wt% kaolinite, 0.02M NaCl, 420 rpm.....131

11.2.1 Drop size distribution for a 5% paraffin oil, 95% water dispersion, 0.001M NaCl, 305 rpm.....132

11.2.2 Drop size distribution for a 5% paraffin oil, 95% water dispersion, 0.001M NaCl, 327.5 rpm...133

11.2.3 Drop size distribution for a 5% paraffin oil, 95% water dispersion, 0.001M NaCl, 349 rpm.....134

11.2.4 Drop size distribution for a 5% paraffin oil, 95% water dispersion, 0.001M NaCl, 403 rpm.....135

11.2.5 Drop size distribution for a 5% paraffin oil, 95% water dispersion, 0.04 wt% kaolinite, 0.001M NaCl, 308 rpm.....136

11.2.6 Drop size distribution for a 5% paraffin oil, 95% water dispersion, 0.04 wt% kaolinite, 0.001M NaCl, 325 rpm.....137

11.2.7 Drop size distribution for a 5% paraffin oil, 95% water dispersion, 0.04 wt% kaolinite, 0.001M NaCl, 345 rpm.....138

11.2.8 Drop size distribution for a 5% paraffin oil, 95% water dispersion, 0.04 wt% kaolinite, 0.001M NaCl, 349 rpm.....139

11.2.9 Drop size distribution for a 5% paraffin oil, 95% water dispersion, 0.04 wt% kaolinite, 0.001M NaCl, 401 rpm.....140

11.3.1 Drop size distribution for a 5% bitumen, 95% water dispersion, 0.001M NaCl, 319 rpm.....141

11.3.2 Drop size distribution for a 5% bitumen, 95% water dispersion, 0.001M NaCl, 360 rpm.....142

11.3.3 Drop size distribution for a 5% bitumen, 95% water dispersion, 0.001M NaCl, 410 rpm.....143

11.3.4 Drop size distribution for a 5% bitumen, 95% water dispersion, 0.001M NaCl, 450 rpm.....144

11.3.5 Drop size distribution for a 5% bitumen, 95% water dispersion, 0.04 wt% kaolinite, 0.001M NaCl, 304 rpm.....145

11.3.6 Drop size distribution for a 5% bitumen, 95% water dispersion, 0.04 wt% kaolinite, 0.001M NaCl, 356 rpm.....146

11.3.7 Drop size distribution for a 5% bitumen, 95% water dispersion, 0.04 wt% kaolinite, 0.001M NaCl, 380 rpm.....147

11.3.8 Drop size distribution for a 5% bitumen, 95% water dispersion, 0.04 wt% kaolinite, 0.001M NaCl, 414 rpm.....148

11.3.9 Drop size distribution for a 5% bitumen, 95% water dispersion, 0.04 wt% kaolinite, 0.001M NaCl, 437 rpm.....149

List of Photographic Plates

Plate		Page
4.1	Photograph of Experimental Apparatus	25
4.2	Photograph of Optical Probe	26
5.1	Photograph of a 5% hexane/water dispersion at 349 rpm (no clay, 0.001M NaCl)	35
5.2	Photograph of a 5% paraffin oil/water dispersion at 375 rpm (no clay, 0.001M NaCl)	35
5.3	Photograph of a 5% bitumen/water dispersion at 450 rpm (no clay, 0.001M NaCl)	36

List of Symbols, Nomenclature or Abbreviations

a	interfacial area, m^2/m^3
$C_1, C_2, \ldots$	dimensionless constants
d	drop diameter, m
$\bar{d}$	average drop diameter, m
d_{32}	sauter mean drop diameter, m
D	impeller diameter, m
D_t	vessel diameter, m
F	a force parameter used in Equations 3.6 and 3.7 to describe the force of interaction between two particles
g_c	Newton's law conversion factor, $1 kg \cdot m/N \cdot s^2$
n	number of drops
N	impeller speed, rps
Re	Reynolds number
s	standard deviation
t_c	circulation time, s
v	Kolmogoroff's velocity scale, Equation 3.2
Vi	viscosity group, Equation 5.4
We	Weber number
We_{crit}	critical Weber number

Greek Symbols

β	$0.052e^{4\phi}$, Equation 3.15
ϵ	average energy dissipation rate per unit mass, J/sec·kg
η	Kolmogoroff's length, Equation 3.1

μ	viscosity, kg/m·s
ν	kinematic viscosity, m^2/s
ρ	density, kg/m^3
σ	interfacial tension, N/m
ϕ	dispersed phase volume fraction

Subscripts

c	continuous phase
d	dispersed phase
e	mixture
max	maximum
min	minimum

1. Objectives

The objectives of this work are:

1. To construct an experimental set-up to determine the drop size and drop size distribution of oil drops in oil/water dispersions.
2. To investigate the effects of adding pure kaolinite to dispersions of:
   - hexane/water
   - paraffin oil/water
   - bitumen/water
3. To study the effects of unpurified Athabasca fines on hexane/water dispersions.

2. Introduction

An understanding of the mechanisms of drop breakup and coalescence is an important part of learning how industrial mixing and separation processes work. This understanding can lead to more accurate control and better design for future processes.

One process where fluid mechanics and colloid chemistry play an important role is the Hot Water Process for recovering bitumen from oil sand. In this process, the mined oil sand is first mixed with hot water, steam, and caustic soda in a large cylindrical tumbler. The oil sand lumps of various sizes are ablated away into a slurry consisting of bitumen, water, and solids (both coarse and fine), at a temperature of about 80 °C. This mixture is sent to a large gravity separation vessel, where the bitumen forms drops which rise to the top of the vessel to form a froth. Most of the coarse solids and water report to a tailings stream, and the fines, water and small bitumen drops report to a middlings stream, which is withdrawn near the middle of the vessel. Bitumen is further recovered from the three exit streams via secondary recovery processes. It has been found that oil sands with exceptionally high fines content (those solids less than 44 microns) usually result in a very low bitumen recovery. One possible explanation for this is that the fine particles, which are mostly silica and various types of clays, somehow affect the coalescence of small

bitumen drops and impede the formation of a rich bitumen froth.

This work involved studying drop sizes and drop size distributions in an idealized three component system. A stirred cylindrical vessel was used to create the dispersions. The dispersions were stirred with a flat bladed impeller over a range of Weber numbers. Three different oil/water systems were studied; hexane/water, paraffin oil/water, and bitumen/water. Pure kaolinite was primarily used as the solid phase, but unpurified Athabasca fines were also used for the hexane/water system. The sauter mean drop size and the drop size distributions were measured with a photomicrographic probe. Photographs of the dispersions were taken and subsequently analyzed on an image analyzer.

3. Literature Review

The stability and formation of oil/water emulsions have been extensively studied by many researchers. The effects of solid additives on the emulsions have been well documented. Emulsions are generally defined as being made up of stable drops with sizes ranging from 0.1 to 50 microns. A great deal of research has also been performed on oil/water dispersions. Dispersions are systems with larger size drops which can coalesce and break up much more readily than in the case of emulsions.

3.1 Oil/Water Dispersions

In the field of oil/water dispersions, theoretical and experimental studies were conducted on drop breakup and drop coalescence. Kolmogoroff [20] defined the concept of local isotropy to describe drop breakup. Local isotropy refers to high levels of uniform local turbulence. Kolmogoroff used two parameters, a length scale,

$$\eta = (\nu^3/\epsilon)^{1/4} \tag{3.1}$$

and a velocity scale,

$$v = (\nu\epsilon)^{1/4} \tag{3.2}$$

For drops larger than Kolmogoroff's length η, inertial forces are said to dominate drop breakup. Viscous forces dominate breakup of drops smaller than η.

Shinnar [36] stated that local isotropy is present when the bulk flow has a high Reynolds number, and the width of the fluid ejected by the impeller is much higher than the length scale η. The width of the agitator is used as the width of fluid ejected by the impeller.

Shinnar et al. [36],[37] used Kolmogoroff's theory of local isotropy to predict some of the properties of dispersions, such as particle size distributions. Shinnar also extensively studied the breakup and coalescence of drops in a dispersion, developing an equation for maximum stable drop size when breakup is due to inertial effects ($d>>\eta$),

$$d_{max} = C_1 N^{-6/5} D^{-4/5} \left(\frac{\sigma}{\rho_c}\right)^{3/5} \qquad (3.3)$$

For a dispersion consisting of very small drops with $d<\eta$, breakup is due to viscous shear, and the maximum drop diameter is given by

$$d_{max} = \frac{(\nu_c)^{1/2}\sigma}{N^{3/2} D \mu_c} f\left(\frac{\mu_d}{\mu_c}\right) \qquad (3.4)$$

Equations 3.3 and 3.4 have been verified experimentally by Sprow [38] and Vermeulen [42].

The Weber number [41] is also used extensively to characterize oil/water dispersions. It is normally given as

$$We = \frac{D^3 N^2 \rho_c}{\sigma} \tag{3.5}$$

The Weber number is the ratio of kinetic energy of a drop to the surface energy. There is a critical Weber number, We_{crit}, above which drops become unstable and break up as the drop's kinetic energy overcomes the surface energy.

Equations have also been developed to predict the minimum drop sizes required for coalescence to take place, Sprow [38]. It is found that in the region where inertial forces dominate, the minimum drop size is given by

$$d_{min} = C_2 \frac{F^{3/8}}{(\rho_c)^{1/2} N^{3/4} D^{1/2}} \tag{3.6}$$

In the region where the viscous forces dominate, d_{min} is given by

$$d_{min} = C_3 \frac{F^{1/2} \mu^{1/4}}{(\mu_c)^{1/2} N^{3/4} D^{1/2}} \tag{3.7}$$

F is a force parameter defined by Sprow to describe the force of interaction between two particles.

Hinze [18] studied the mechanisms of drop deformation and breakup both experimentally and theoretically. He found three basic types of deformation. "Lenticular" deformation, where the drop is flattened to a lens shape, can take place

under conditions of parallel flow, axisymmetric-hyperbolic flow, and rotating flow. "Cigar-shaped" deformation was found in plane-hyperbolic flow and couette flow. The third type of deformation found by Hinze was "bulgy" deformation, in which the drop surface is deformed locally, which is caused by irregular flow patterns.

The parameter most used to describe drop sizes in oil/water dispersions is the sauter mean drop size, given as

$$d_{32} = \frac{\Sigma n d^3}{\Sigma n d^2} \tag{3.8}$$

The sauter mean diameter is also called a volume to surface mean diameter. The sauter mean diameter is especially useful because it can be related to interfacial area $a(m^2/m^3)$, where it is given as

$$a = \frac{6\phi_d}{d_{32}} \tag{3.9}$$

Experimental data for the sauter mean diameter of drops are normally correlated using an equation of the form

$$d_{32} = C_4 D(1+C_5\phi)We^{C_6} \tag{3.10}$$

A typical system, showing the order of magnitude of the constants, is that of Mlynek and Resnick [25],

$$d_{32} = 0.058D(1+5.4\phi)(We)^{-0.6} \tag{3.11}$$

Mlynek and Resnick developed Equation 3.11 to describe their experimental results for dispersions of isooctane and carbon tetrachloride in water. They used a baffled cylindrical vessel and a 6-blade turbine impeller to create the dispersions. Drop sizes were determined from photographs taken through a periscope which was inserted directly into the mixing vessel. A drop encapsulation method was also used to determine drop size parameters. Correlations similar to Equation 3.11 have also been developed by Brown and Pitt [3], Calderbank [7], and Coulaloglou and Tavlarides [12].

Other examples of correlations are those of Weinstein and Treybal [46],

$$d_{32} = 10^{-2.316+0.672\phi} (\nu_c)^{0.0722} \epsilon^{-0.194} \left(\frac{\sigma g_c}{\rho_c}\right)^{0.196} \qquad (3.12)$$

and that of Brown and Pitt [4],

$$d_{32} = C_7 \left(\frac{\sigma}{\rho} \epsilon^{2/3} \frac{(D_t)^{2/3}}{\epsilon^{-1/3} t_c}\right)^{3/5} \qquad (3.13)$$

In Equation 3.13, t_c is the circulation time, and ϵ is the average energy dissipation rate per unit mass.

The study of Tavlarides and Stamatoudis [41] provides an extensive list of various correlations used to predict the sauter mean drop size.

Gnanasundaram et al. [16] carried out experiments with hexane/water dispersions created in an agitated vessel. Drop sizes were determined from photographs taken through the

glass wall of the experimental vessel. Their results are shown in Figure 3.1. The correlation Gnanasundaram et al. used to describe their experimental results is

$$d_{32} = \beta(We)^{-0.6} \qquad (3.14)$$

where

$$\beta = 0.052e^{4\phi} \qquad (3.15)$$

Ward and Knudsen [44] conducted an experimental study in which drop sizes in a paraffin oil/water dispersion were measured. They created the dispersions in an agitated vessel, and then circulated the mixed liquids through a pipe loop. Drop size distributions, velocity profiles and pressure drops were also measured. Photographs of the dispersions were taken through a glass window in the pipe section , and were then analyzed by hand for the drop size parameters. The equation developed by Ward and Knudsen [44] to correlate their experimental results is

$$Re\ \left(\frac{d_{32}}{D}\right)\ \frac{\rho_d}{\rho_c} \leq 2 \qquad (3.16)$$

The experimental results of Ward and Knudsen [44] are shown in Figure 3.2.

The physical design aspects of mixing vessels have been extensively studied, including impeller type, impeller size

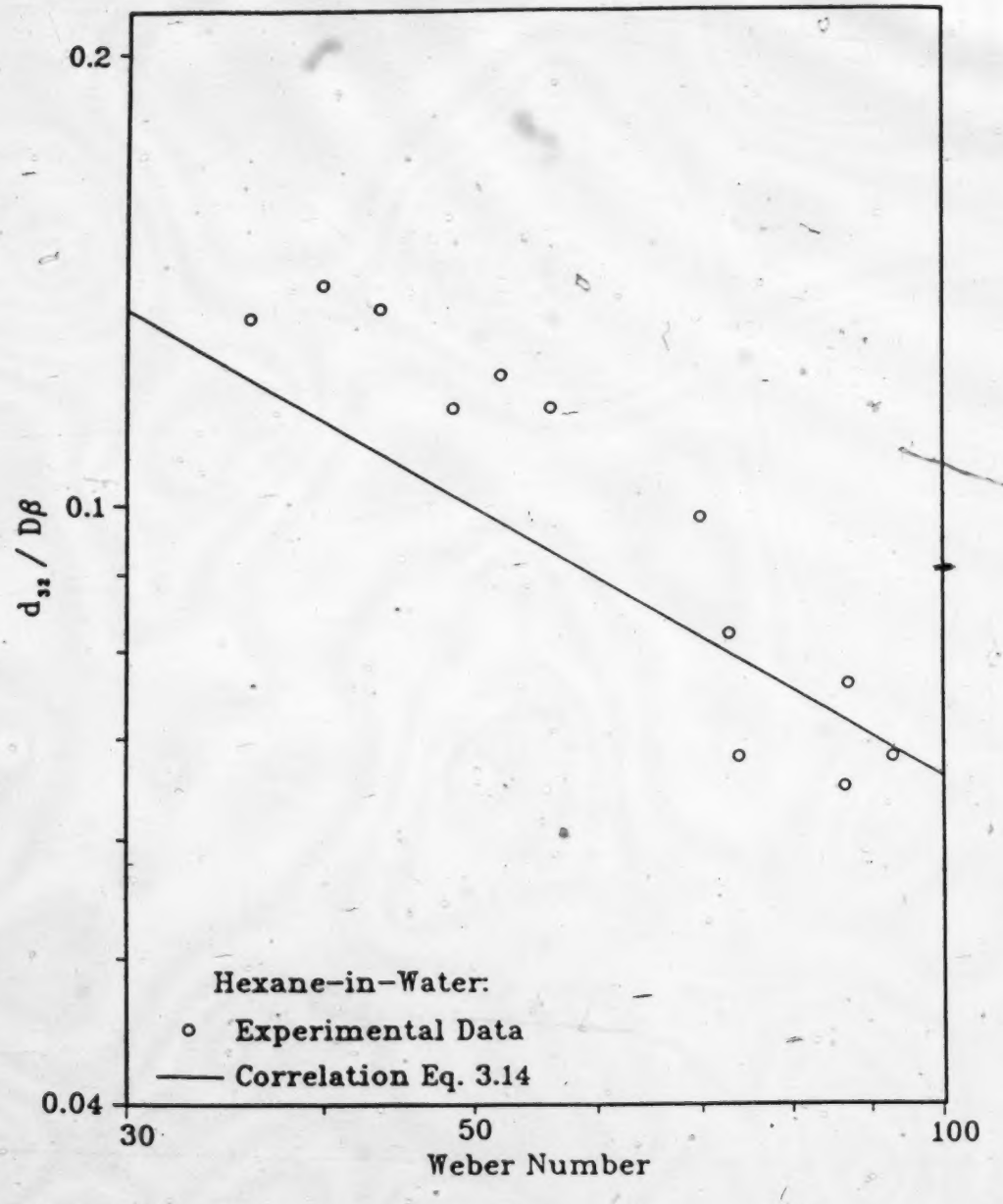

Figure 3.1 : Experimental data for hexane/water dispersions, Gnanasundaram et al. [16] (Information adapted from source)

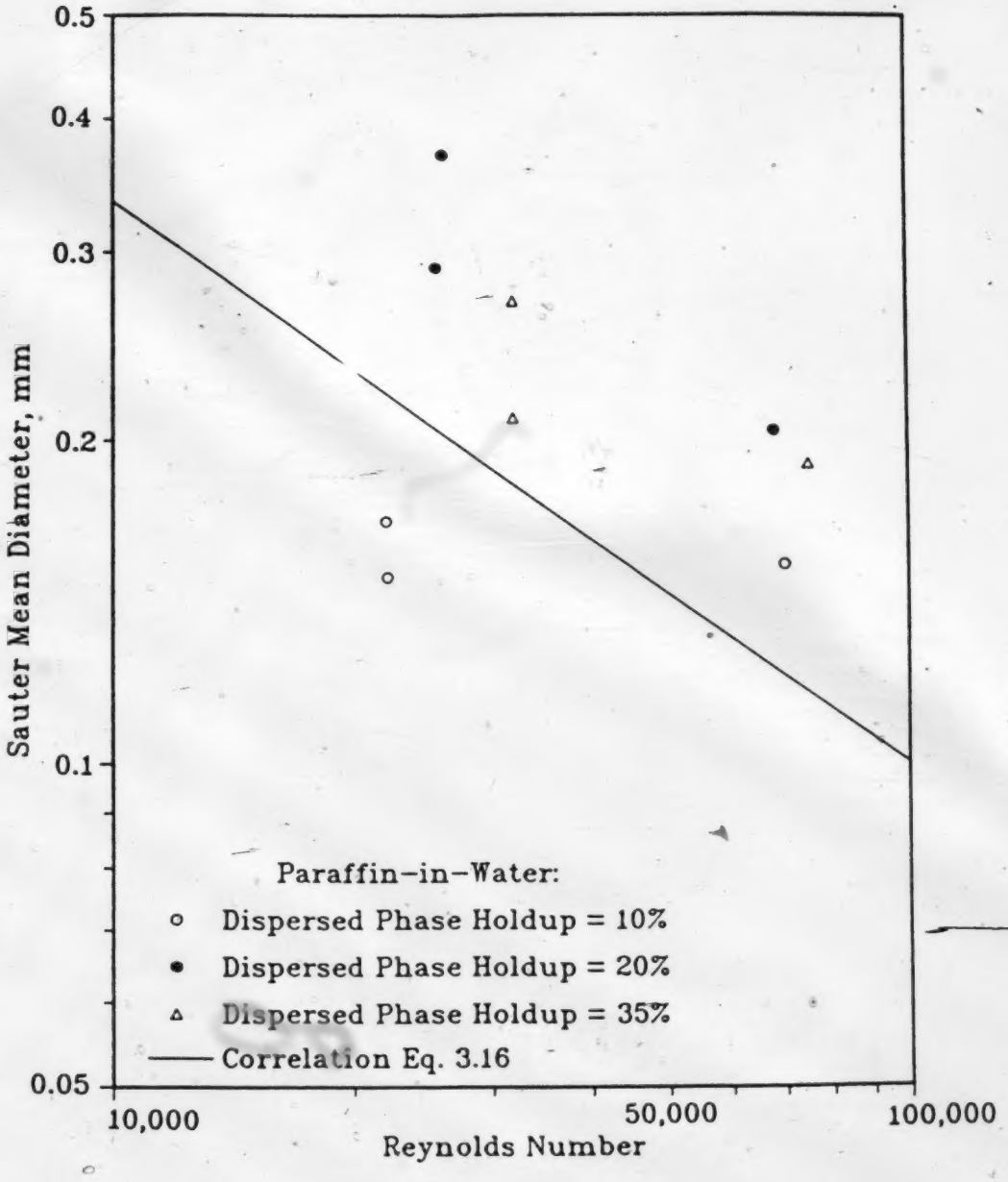

Figure 3.2 : Experimental data for paraffin oil/water dispersions, Ward and Knudsen [44] (Information adapted from source)

and location, and baffle design [26],[27]. As well, drop circulation patterns, velocities, local drop size variation at different points in the vessel, and other parameters have been examined [17],[19],[29],[46].

3.2 Colloid Theory

There are three main types of forces acting on small (colloidal) particles or drops. These are Van der Waal's attractive forces, Born repulsion forces, and electrostatic repulsion forces. The Van der Waal's forces are effective over a short range, whereas the the other two are long range forces. The Born repulsion forces are due to overlapping electron clouds, while the Van der Waal's attraction can be due to the polarization of one molecule by fluctuations in the charge distribution of a second molecule (Shaw [35]). The electrostatic forces are due to the electric double layer which surrounds most particles. The build up of electric charge of a particle attracts ions with the opposite charge towards the surface, and repels similarly charged ions away.

3.3 The Effect of Solid Additives

A large amount of work has been carried out studying fine solid particles both as emulsifiers and as emulsion breakers. A small number of studies have been conducted on the effects of fine solids in non-emulsified dispersions. Pickering [30], in 1907, determined the solid particle size

required to form emulsions. Alternatively, Collopy and Mueller [10] have used fine solids as an aid to coalescence, and to break emulsions.

Mizrahi and Barnea [24] reviewed various studies which have dealt with the effects of solids on various aspects of emulsions. They also performed a variety of experiments, both batch and continuous, using various solids to either break up or form emulsions. Their results indicated that if solids were preferentially wetted by the continuous phase, then the solids would aid in emulsification. Alternatively, if they were prefentially wetted by the dispersed phase, the solids would aid in coalescence. Gelot, Friesen, and Hamza [15] studied the effects of clays and other fines, as well as surfactants on toluene/water emulsions. Calcium kaolinite was found not to be an effective emulsifier for toluene/water systems, although calcium bentonite did stabilize a toluene in water emulsion. When calcium kaolinite was added with an anionic surfactant, it was able to stabilize the emulsions.

Dippenar [13],[14] studied the mechanism for liquid film rupture by solids in the process of froth flotation of minerals using a water/air froth. High speed cinematography was used to study froth cells in which single solid particles were placed on a single liquid/air froth cell. The effects of particle size and shape were studied for several different types of solids. It was found that a contact angle of greater than 90° was generally required for film rupture,

using both round and irregular shaped particles, such as hydrophobic quartz. Particles with orthorhombic shapes were able to break the froth film at contact angles even lower than 90°.

In the area of oil sand processing, Sanford and Levine [22],[23],[33] have published a series of papers on the effects of fines and other process variables on the recovery of bitumen from oil sand. They developed a thermodynamic theory to explain the stabilization of bitumen emulsions by fine solids. It was shown that oil sands with increasingly higher fines content had a decreasing bitumen recovery with the Hot Water Process. While Sanford and Levine acknowledged that clays were not the only fine particles present in oil sand fines, they believed that the clays were the most important type of small particles. They explained that the clay particles "are attached to the bitumen drops by un-ionized strong polar groups which form part of certain organic constituents of the bitumen. The addition of NaOH to the oil sand produces an anionic surfactant which bears the same sign as the clay particles (negative), and these forces tend to stabilize the emulsions formed."

3.4 Experimental Techniques

There are several different methods available for measuring drop sizes in liquid/liquid dispersions. The three basic categories are chemical methods, light transmittance and reflectance methods, and photographic methods. Each

method has its own intrinsic advantages and disadvantages. A major difference is that while all of the methods can be used to determine sauter mean drop size and interfacial area, only certain of the photographic methods will give a drop size distribution.

The chemical method is probably the most accurate for determining interfacial area and sauter mean drop size. Though mainly used for gas/liquid systems, the chemical method has also been used for liquid/liquid systems, as detailed in reviews by Sharma and Dankwerts [34] and also by Tavlarides and Stamatoudis [41]. This method uses a fast reaction of known kinetics, for which the rate of reaction can accurately be measured. The kinetic parameters of the reaction can then be used to determine the interfacial area, and hence the sauter mean drop size.

With the chemical method it is very important to choose the correct reaction for a given set of conditions. It is not always possible to find an applicable reaction for a given liquid/liquid system. A major disadvantage found by Tavlarides and Stamatoudis [41] is that mass transfer can affect the interfacial tension of a system, and therefore change its interfacial area. Also, no drop size distributions can be obtained with the chemical method.

Stokes and Harvey [39] measured the size of oil drops in oil water dispersions using a Coulter counter. The Coulter counter determines drop sizes by measuring variations in electrolyte concentration as a dispersion is

passed through it. A limitation of this method is that the dispersions have to be electrolytes [39].

The light transmittance techniques are among the most widely used. This is because of their simplicity both in use and in analysis of the results. The basis of the method is that when a parallel beam of light is passed through a dilute dispersion, the dispersed particles will scatter the light. By measuring the amount of light which is passed unaffected through the dispersion, is is possible to determine the interfacial area. There are several different ways to measure the light scattering; Calderbank [7] and others such as Vermeulen [42] have used optical probes which could be inserted directly into the vessel. This allows measurements to be made over a relatively short and localised path length.

Others such as Landau et al. [21] measured the amount of light transmitted through the width of the entire vessel. Some of the limitations of this method include a minimum measurable drop or bubble diameter of 0.0001 meters (Calderbank [7]), and a maximum determinable interfacial area of 700 square meters per cubic meter (Reith [31]). Also, the technique can only be used when the effects of multiple and forward scattering are negligible. When using the light scattering technique, generally the results must be verified by another method because of the possibilities for large systematic errors.

A variation on the light scattering technique is the light reflectance method. This method was developed by Calderbank, Evans and Rennie [8] for use with optically dense solutions. In this technique a light is shone through the vessel wall, and the amount reflected back by the dispersed phase of the solution is measured. This method only works for very optically dense solutions, and also has the drawback of measuring conditions only at the vessel wall, which may not be representative of the entire vessel.

As well as not measuring the drop size distributions, both the light scattering and light reflectance techniques do not work well when a third solid phase is added to the solution.

The third major category of drop size measurement techniques involves photographic methods. The simplest of these methods involves photographing the dispersion through the vessel wall. To prevent distortions caused by using a circular vessel, a square column or vessel can be used (Akida and Yoshida [1]), or the vessel can be fitted with a rectangular perspex jacket, such as that used by Landau et al. [21].

A problem photographing the dispersion through the vessel wall is that conditions at the wall may not represent those in the bulk of the solution, as with the light reflectance technique. To overcome this problem, various researchers have developed photographic probes which can be inserted directly into the vessel to determine drop sizes at

almost any desirable position. Photomicrographic probes as well as fibre optic probes have been used by some researchers such as Coulalaglou and Tavlarides [11],[12] and Park and Blair [28],[29]. Both still photography and high speed cinematography have been used by several different researchers. A disadvantage of using a probe is that the hydrodynamic conditions in the vessel may be changed with the insertion of the probe. Also, only a small volume can be examined at a time (Landau et al. [21]).

Another method used succesfully by some researchers such as Mlynek and Resnick [25] is to withdraw a portion of the dispersion from the vessel for analysis. Various methods have been used fo prevent the drops from coalescing after withdrawal, including the use of surfactants, and encapsulation of the drops with polymers (Mlynek and Resnick [25]). The major disadvantage with sample withdrawal methods is that the hydrodynamic conditions of the system are changed. Once withdrawn from vessel, the drops can be photographed using a microscope, or other similar apparatus.

The final step in any photographic technique is the analysis of the photographs or images produced. In the past this analysis has often been done by hand, using a ruler or other similar measurement technique, which could be very time consuming. With the current image analysis technology the analysis process has become much faster. However, with both methods of analysis there can be subjective errors introduced into the results, such as determining whether to

include certain drops.

4. Experimental Apparatus and Procedure

The method chosen in this work for measuring the required dispersion parameters was the photographic technique. This represented a method that would not change the interfacial properties of the oil/water system, and would be adaptable to adding clay. Also, both the sauter mean drop size and the drop size distributions could be determined. The inherent disadvantages of the the sample withdrawal method and the method of photographing through the vessel walls ruled out those particular methods.

It was decided to use a photographic probe similar to that of Coulaloglou and Tavlarides [11],[12], though a fibre optic probe was also considered.

4.1 Experimental Apparatus

The dispersions were prepared in a 20 litre Pyrex vessel having an inside diameter of 30 centimeters. The vessel was elevated on a 41.5 centimeter high platform so that the light probe could be inserted through the bottom of the vessel, and various light sources used underneath. A 0.75 horsepower variable speed direct current motor was used to drive the impeller. From Figure 4.1 it can be seen that the motor was connected to the agitator shaft with a belt and pulleys. This was done in order to leave as much free space as possible on top of the vessel in which to work with the camera and optical probe. A flat bladed impeller was

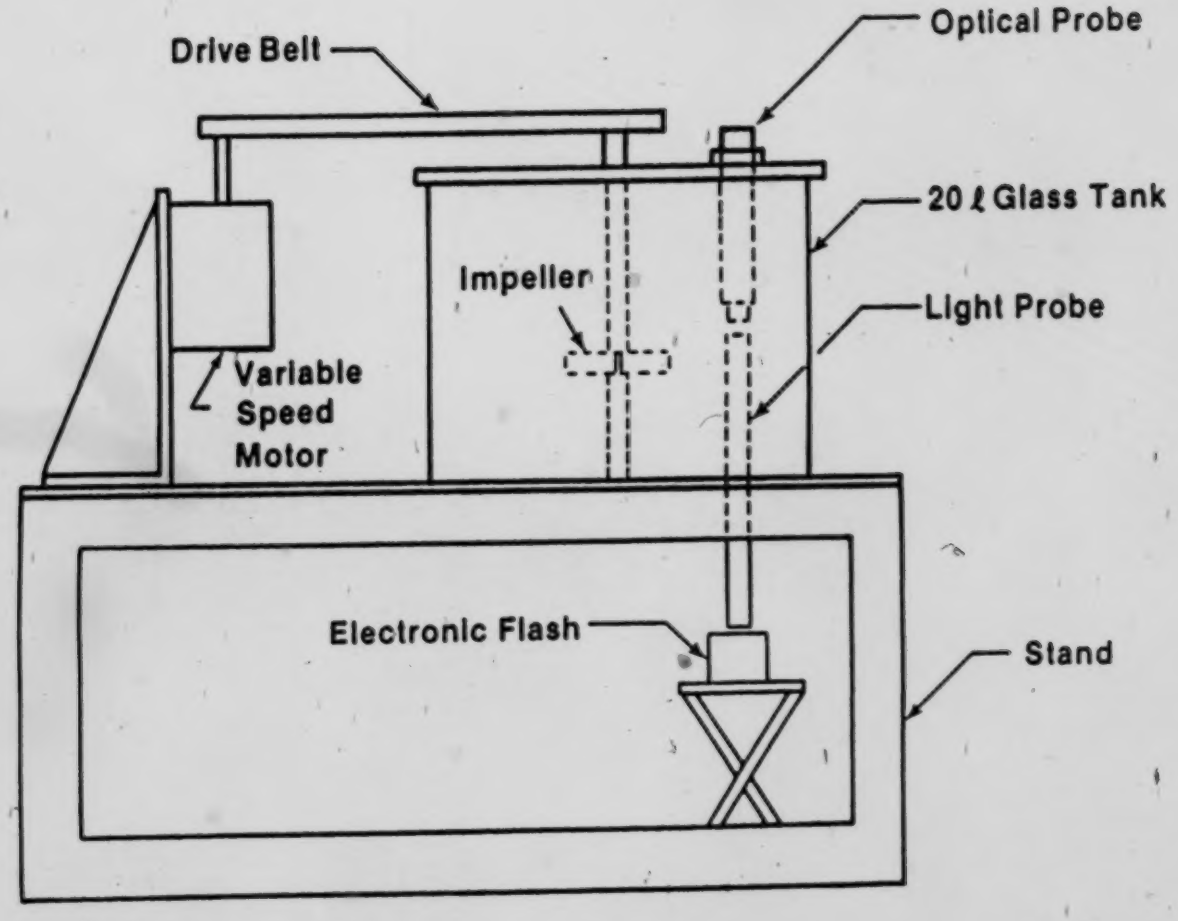

Figure 4.1 : Schematic Diagram of Experimental Apparatus

used to agitate the dispersion. This impeller had six blades, with an overall diameter of 10 centimeters. It was positioned 10.5 centimeters above the bottom of the vessel. A removable set of four baffles was used in the vessel. Each baffle had a width of 2.9 centimeters, and the baffles were equally spaced around the vessel. The vessel was fitted with an aluminum lid which had holes drilled in it for the optical probe, a heating element, and a thermocouple. The bottom of the vessel was fitted with a teflon cup in which the impeller shaft rested.

The stirred vessel apparatus was modified for the runs with bitumen/water dispersions in order to enable the runs to be performed at 70°C. A thermocouple and a 1000 watt immersion heater were inserted through the top of the vessel, and were attached to a temperature controller.

As mentioned previously, an optical probe and a light probe were used to photograph the dispersions. The optical probe was inserted through the lid of the vessel, while the light probe was inserted through the bottom of the vessel. The light probe was sealed in place with two "O" rings set in a stainless steel holder. Both probes were free to move up and down to any desired depth in the vessel.

The light probe was a 23 centimeter long plexiglass rod which was highly polished at each end. The rod was inserted into a stainless steel tube.

The optical probe used in this work was similar to that of Coulaloglou and Tavlarides [11],[12]. A schematic diagram

of this probe is shown in Figure 4.2. The probe was fitted with an objective lens and an eyepiece from a microscope. A composite eyepiece was used, which had a magnification of 6X. The objective lens used for most of this work had a magnification of 5X and a numerical aperature of 0.15. The probe was constructed with a tube length of 200 millimeters (Figure 4.2), in order to provide maximum flexibility of use. This was longer than the 160 millimeters for which the eyepiece and objective lens were designed, but the images were still very clear (as also found by Coulaloglou [11]). The overall magnification for the optical probe was 56X normal size. The optical probe was inserted in the vessel to a depth of 15 centimeters.

The plane of focus of the objective lens was approximately 25 millimeters away from the lens itself. When the probe was inserted in the dispersion, the drops between the tip of the lens and its plane of focus were found to interfere, so that a sharp image could not be obtained. Therefore the objective lens was fitted with an extension tube similar to that of Coulaloglou [11] (Figure 4.2). The extension tube was sealed with a cover glass of 0.15 millimeter thickness.

Photographs of the apparatus and of the optical probe are shown in Plates 4.1 and 4.2.

A Polaroid MP-4 Land camera was initially used to photograph the dispersion through the optical probe. However, because of the limited range of flexibility of the

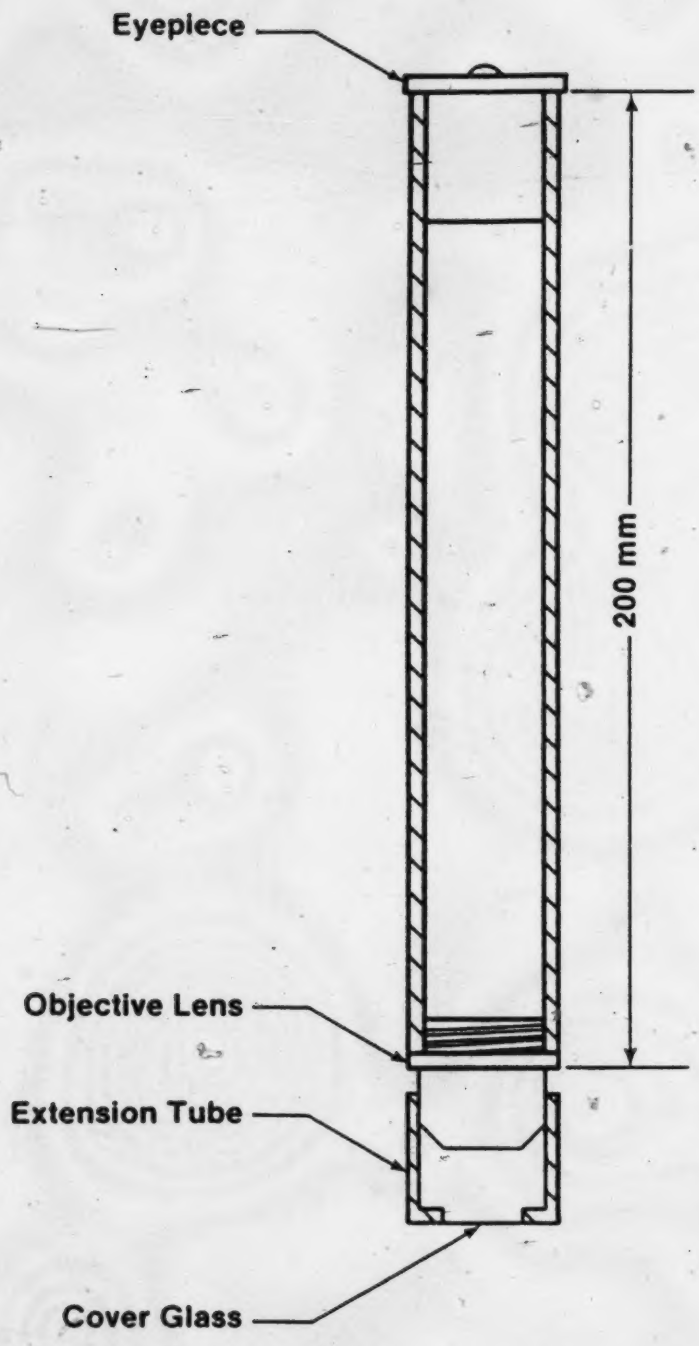

Figure 4.2 : Schematic Diagram of Optical Probe

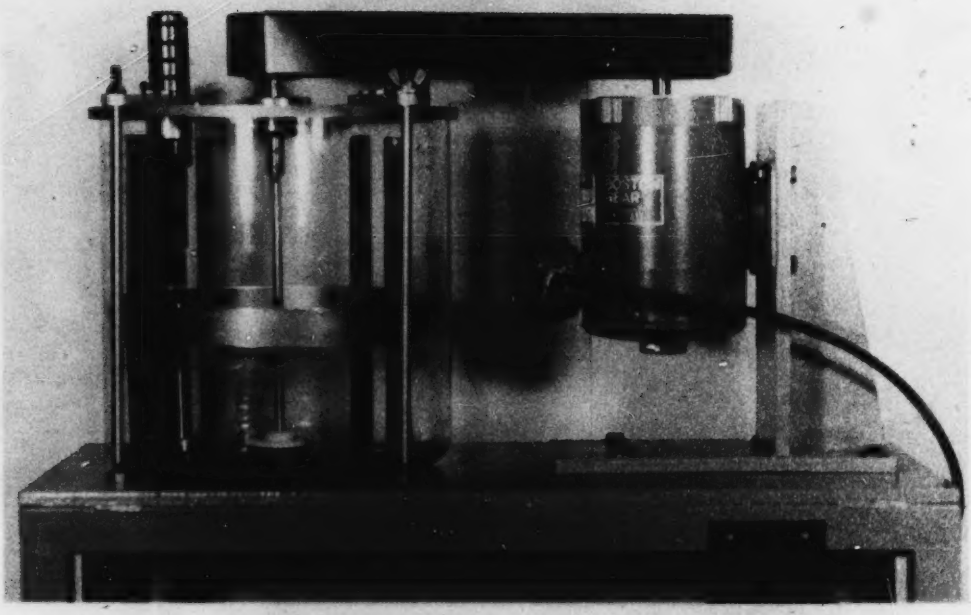

Plate 4.1 : Photograph of Experimental Apparatus

Plate 4.2 : Photograph of Optical Probe

Polaroid films in terms of contrast and film types available, it was decided to switch to a 35 millimeter Single Lens Reflex camera. The camera chosen was a Nikon F2-A, with a 55 millimeter Micro-Nikkor lens. Various films were experimented with, and the one finally chosen was Kodak Technical Pan 2415. This was a high contrast, fine grained film when developed in Kodak D-19 developer. The photographs were printed on 12.7 X 17.8 centimeter sheets of Kodak Polycontrast paper. Contrast of the individual prints was varied with a set of Kodak Polycontrast filters.

4.2 Experimental Materials

Experiments were carried out with three different hydrocarbons: n-hexane, paraffin oil (white, heavy), and a Cold Lake bitumen. The physical properties of these three hydrocarbons are shown in Table 4.1. Further bitumen properties are given in Appendix A. Hexane/water and paraffin oil/water interfacial tensions were measured with a Fisher Surface Tensiomat, which uses a platinum ring. The viscosity of the paraffin oil was measured with a Canon U-tube viscometer.

Two types of clay were used, a pure kaolinite (Hydrite UF) and an unpurified mixture of Athabasca fines. The pure kaolinite particles had a median size of 0.2 microns. Other properties of the kaolinite are given in Appendix A. The Athabasca fines were an unpurified mixture of solids recovered by solvent extraction from an Athabasca oil sand.

Hydrocarbon Type	Temp. °C	Density kg/m³	Viscosity kg/m·s	Interfacial Tension, N/m
Hexane	23	657	0.00030	0.051
Paraffin Oil	23	866	0.177	0.0279
Bitumen	70	990	0.520	0.016

Table 4.1 : Properties of hexane, paraffin oil, and bitumen

The particle size distribution for the Athabasca fines is given in Appendix A. The median particle size was approximately 10 microns. The fines were a mixture of sand, silt and clay. The clay composition is given in Table 4.2.

Constituent	Composition
Illite	30%
Kaolinite	30%
Montmorillonite	25%
Chlorite	15%

Table 4.2 : Clay composition of Athabasca fines

The water used for all the experimental runs was double distilled and deionized.

4.3 Experimental Procedure

The first step in performing an experimental run was to thoroughly clean the vessel, baffles, agitator, and all other apparatus which might come in contact with the dispersion. This was done by first scrubbing the apparatus with a soap solution, and then rinsing at least five times with water. The final rinse was performed with distilled water.

For the runs with hexane or paraffin oil, the vessel was cleaned before each run. However, for the bitumen system, the cleanup time was several hours. Therefore, to save time, up to five runs were done consecutively with the same bitumen/water system before the vessel was emptied and cleaned.

The 16 litres of distilled water used for each run was next measured into the vessel, and the required amount of salt was added. The salt was dissolved by stirring the water for five minutes. The required amount of hydrocarbon was then added to the vessel. For the experimental runs where solids were added, the next step involved mixing the solids with approximately 100 millilitres of water using a high speed Kinematica mixer. This was done to break up any lumps of particles which might have formed.

The next step was to turn on the dispersion vessel mixer and to set the required mixer speed with a stroboscope. If solids were to be added, that was done at this time. At least one hour was required for the dispersion

to reach equilibrium, so the total mixing time was set at two hours to ensure equilibrium.

Though the increased salt concentration helped to prevent the drops from sticking to the coverglass on the optical probe, washing the glass thoroughly before inserting the probe into the vessel was found most effective. Also, when working with bitumen, the probe was heated before insertion into the vessel.

After two hours of stirring, the optical and light probe positions were set as required for a given run. The electronic flash was then positioned, and the flash strength set according to the visibility conditions in the vessel. After positioning the camera and setting the correct exposure, 20 to 30 photographs were then taken. The film was developed before stopping the run in order to determine whether the photographs were acceptable for analysis.

The films were developed with Kodak D-19, a high contrast developer. However, for several of the runs it was necessary to use a set of Kodak Polycontrast filters to enhance the contrast even further. A photograph of a shaded calibration circle on a slide, as viewed through the optical probe, was printed with each roll of film. This was done to allow for calibration of the image analyzer in determining the drop diameters. Once the photographs were ready, they were prepared for image analysis using a procedure developed in the Mining, Metallurgical and Petroleum Engineering Department at the University of Alberta. First, a black ink

mechanical drafting pen and a series of circle templates were used to circle each drop which was in focus on a photograph. The outer diameter of the ink circles was chosen so as to coincide with the outer diameter of each drop. The number of photographs chosen for each run was that which would give a total of at least 200 drops. The final step in photograph preparation was to bleach the photograph with an Iodine/Potassium Iodide based bleach. This process left only the ink circles on each photograph and turned the background white.

Finally, the bleached photographs were analyzed on an image analyzer in order to determine the sauter mean drop diameter and the drop size distribution. A Bausch & Laumb Omnicon Alpha Image Analysis System and later a Beuhler Omnimet Image Analyzer were used for the analysis. The first step in the calibration procedure was to use the light pen to measure the projected diameter of the shaded calibration circle. A calibration factor was then determined by dividing the actual calibration circle diameter by the measured diameter. The individual diameters of all the drops on the experimental photographs were then determined using the light pen. The final results were then entered into data files on the computer, and each run was analyzed for the sauter mean drop size and the various parameters of the drop size distributions.

5. Results and Discussion

The experimental results are primarily presented as the variation of sauter mean drop size with impeller speed for the given conditions being studied. For the three basic oil/water systems - hexane/water, paraffin oil/water and bitumen/water, the results are shown in Figure 5.1. These results compare base case conditions for each type of dispersion at 0.001M NaCl, and with no solids added. For all three types of dispersions, drop size was found to decrease with increasing agitation speed. The bitumen drops were the largest of the three oils, while the hexane drops were the smallest. The paraffin oil drop size was in between those of bitumen and hexane. In this study, the highest interfacial tension was for the hexane/water system and the lowest was for the bitumen/water system. According to Equation 3.11, the sauter mean drop diameter decreases with decreasing interfacial tension and consequently we should have observed the opposite trends in the sauter mean diameter. However, the dispersed phase viscosity was lowest for the hexane and highest for the bitumen. Therefore the dispersed phase viscosity plays a more important role than interfacial tension in the systems being studied. Because dispersed phase viscosity plays an important role in the breakup process but has much less effect on coalescence, this indicates that drop breakup may be the controlling process in our system.

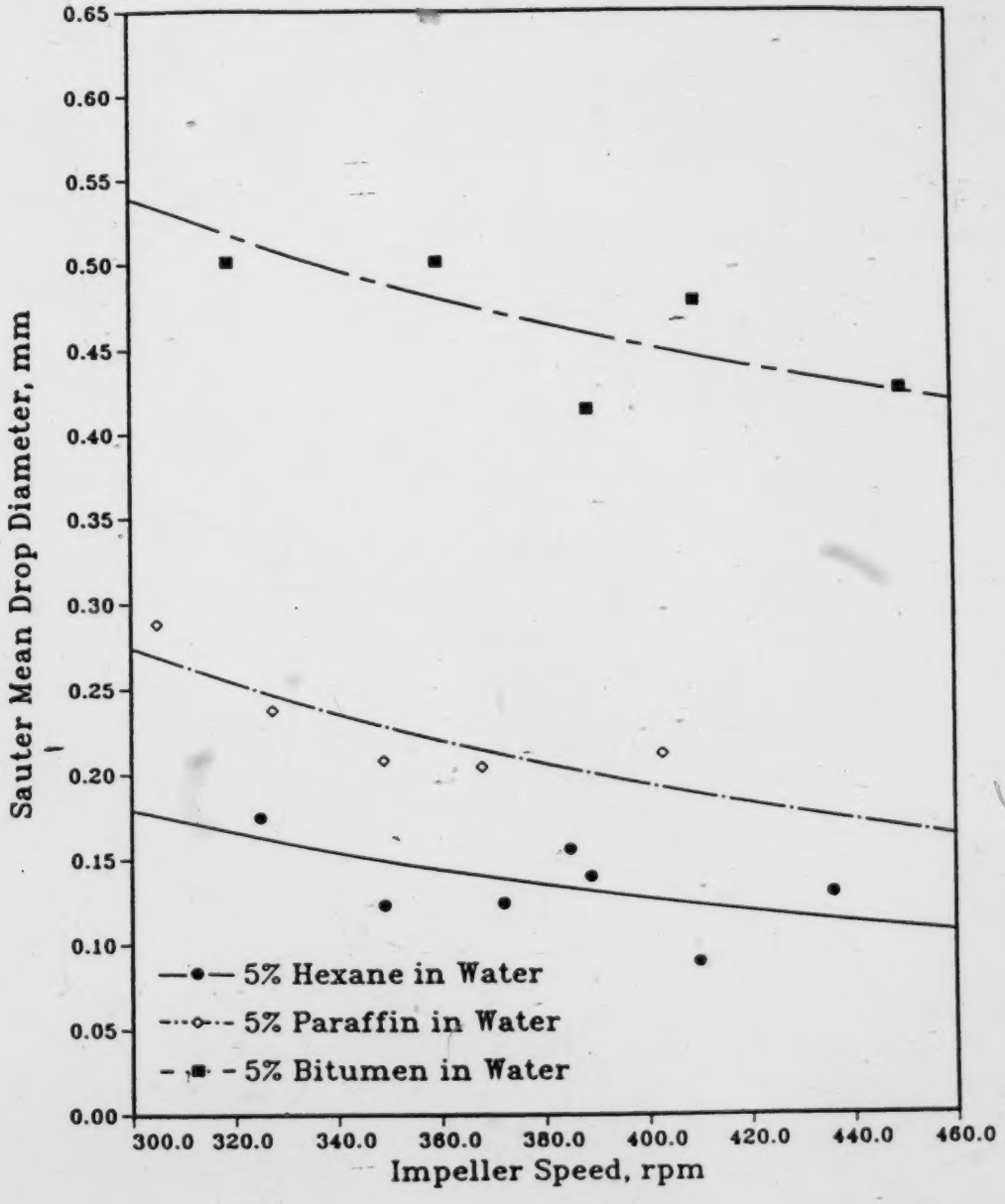

Figure 5.1 : Sauter mean drop size as a function of impeller speed for 5% hexane/water, paraffin oil/water, and bitumen/water dispersions (0.001M NaCl)

Photographs of the drops in the three different types of dispersions are shown in Plates 5.1, 5.2 and 5.3.

The hexane/water system was the first to be studied. All runs were carried out with 5% by volume hexane in water. Two NaCl concentrations were studied, 0.001M and 0.02M, and two different clays were examined, pure kaolinite and an unpurified mixture of Athabasca fines. The results for the hexane/water dispersion at 0.001M NaCl are shown in Figure 5.2. The range of impeller speeds was determined by two factors. The minimum speed was chosen so that all of the floating hexane from the upper surface of the liquid would be drawn down and mixed uniformly within the dispersion. The maximum speed was chosen so as to allow a wide range of speeds, but not to produce extremely small drops. For the first set of hexane/water runs this resulted in a range of agitation speeds from 320 to 450 revolutions per minute. From Figure 5.2 it can be seen that the results with the hexane/water dispersion with no added clay are scattered fairly evenly about the line representing Equation 3.11, the correlation of Mlynek and Resnick [25],

$$d_{32} = 0.058D(1+5.4\phi)(We)^{-0.6} \qquad (5.1)$$

This correlation has been compared to other researchers work with similar systems, so this would seem to indicate that the results of this work compare well with that of other researchers [3],[7].

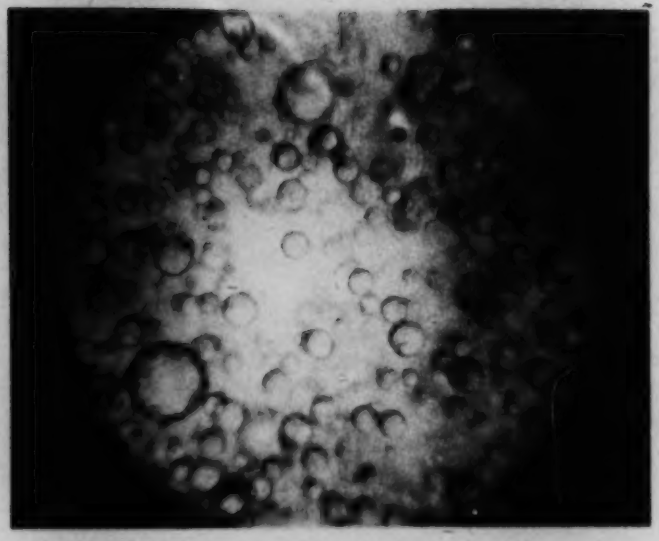

Plate 5.1 : Photograph of a 5% hexane/water dispersion at 349 rpm (no clay, 0.001M NaCl)

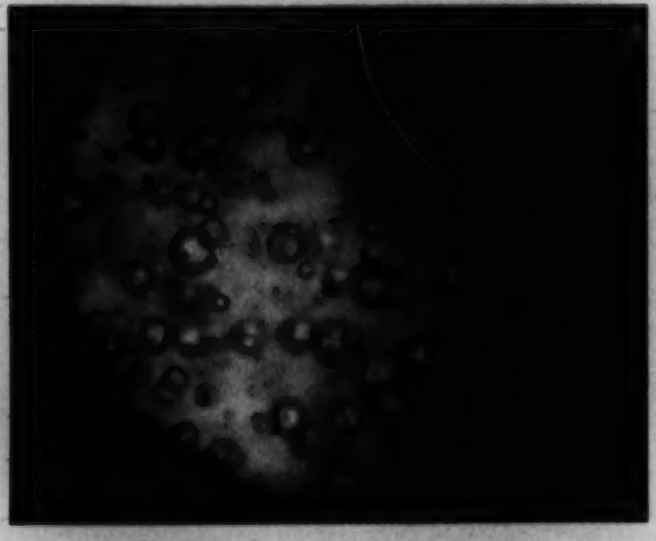

Plate 5.2 : Photograph of a 5% paraffin oil/water dispersion at 375 rpm (no clay, 0.001M NaCl)

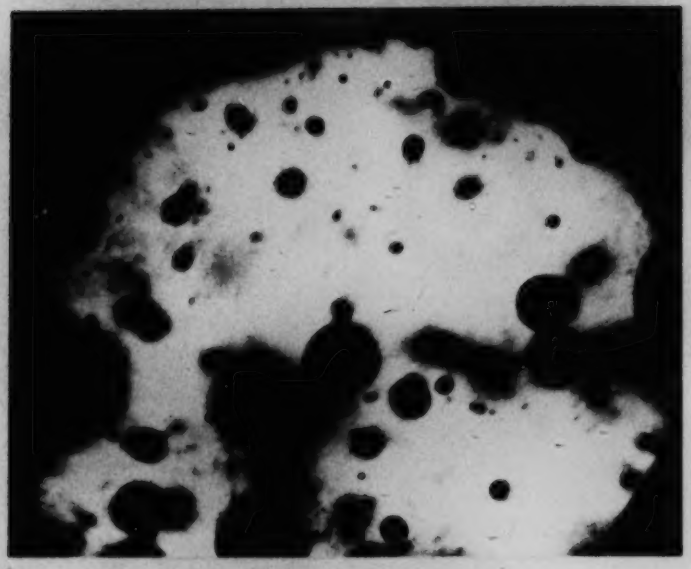

Plate 5.3 : Photograph of a 5% bitumen/water dispersion at 450 rpm (no clay, 0.001M NaCl)

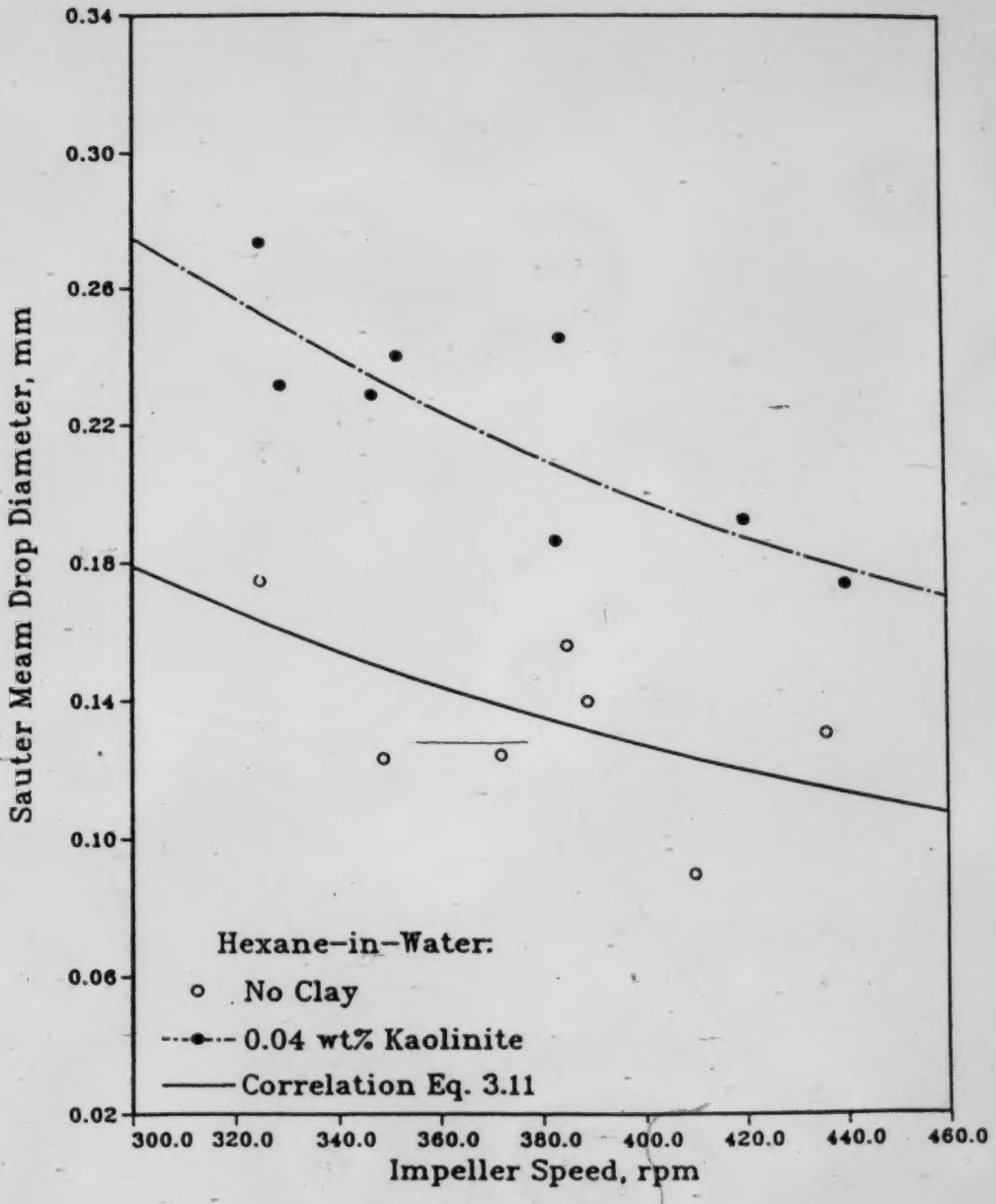

Figure 5.2 : The effect of the addition of 0.04wt% kaolinite to a 5% hexane/water dispersion (0.001M NaCl)

Figure 5.2 shows the results when 0.04% by weight pure kaolinite was added to the system. It can be seen that the sauter mean drop size greatly increased over the entire range of agitation speeds studied. The kaolinite used in this work had a median particle size of 0.2 microns. Therefore, the kaolinite particles were much smaller than the hexane drops, with an approximate kaolinite particle to hexane drop size ratio of 0.001. The kaolinite used is also primarily a water wet solid, although it does have some affinity for oil. From the experimental work it was observed that long after agitation had been stopped and most of the oil and water phases had separated, most of the kaolinite remained in the water phase, with less in the oil phase. Therefore, during agitation, most of the kaolinite must have remained suspended in the water phase or at the interface between the continuous phase (water) and the dispersed phase (hexane). The amount of kaolinite added was not enough to completely cover all of the surface area of the hexane drops, and therefore completely stabilize them. However, the kaolinite particles may have acted as nucleate sites which would aid in the coalescence of drops. Without any clay added, when two drops collided they may not have had sufficient momentum to overcome the capillary pressure, and so would not coalesce. The presence of the kaolinite may have lowered the capillary pressure, and so made it easier for two colliding drops to coalesce.

Another possible explanation of the increase in sauter mean diameter with the addition of kaolinite is related to the effect of kaolinite on drop breakup. As discussed earlier, breakup may be the most important factor controlling the drop size in the systems being studied. Therefore, by this argument, the increase in drop size caused by the addition of kaolinite must have been related to the effect of kaolinite particles on drop breakup, which is assumed to be the controlling process. This may have been made possible if the kaolinite particles surrounded the hexane drops, and therefore stabilized the drops during breakup.

The results for the addition of 0.04wt% Athabasca fines are shown in Figure 5.3. It can be seen that only a slight increase in the drop size occurs in comparison to the runs with no clay added. This increase is much less than when the pure kaolinite is added. The Athabasca fines had a median size of 10 microns, which was much larger than the kaolinite particles. This means that for the same weight of solids, there would be fewer Athabasca fines particles than kaolinite. This would mean that the number concentration is less, and so the Athabasca fines would have less effect on drop coalescence.

Alternatively, because the Athabasca fines were unpurified after their recovery from oil sand, there could have been some organics present on the surface of the particles. This may have made the Athabasca fines more oil

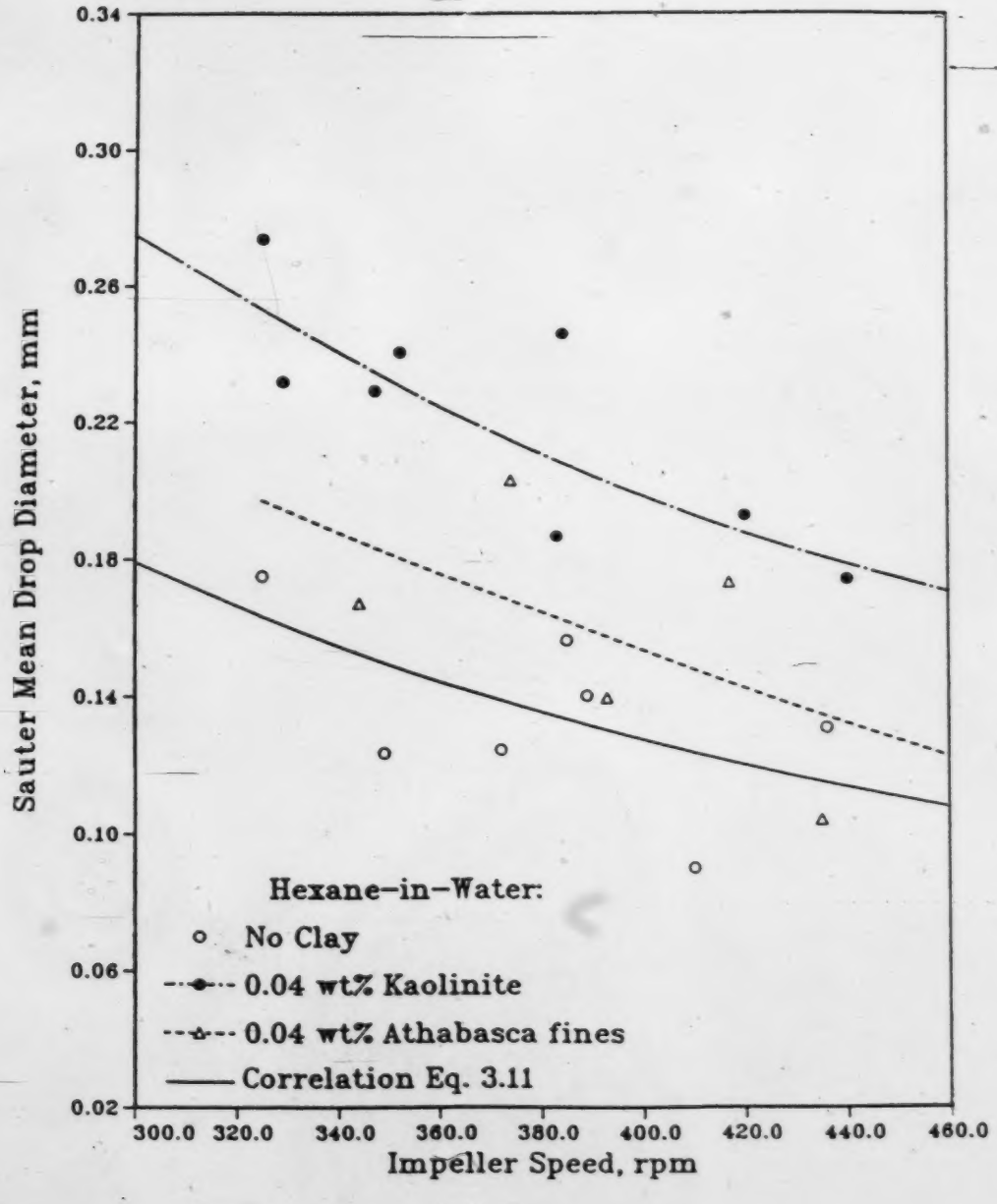

Figure 5.3 : The effect of the addition of 0.04wt% Athabasca fines to a 5% hexane/water dispersion (0.001M NaCl)

wet than water wet and so decreased the effect the fines had on coalescence.

The method used to add the clay for the first series of runs was to first disperse the clay in approximately 0.5 litres of the water to be used in the experiment using a high speed homogenizer. Once the hexane was added to the vessel and the stirring started, the 0.5 litres of clay/water mixture would then be added. However, some runs were also carried out in which the kaolinite was first dispersed in the hexane before addition to the main vessel. These results are shown in Figure 5.4, and the results seem to be fairly close to those when the kaolinite was first dispersed in the water phase. It was observed that the kaolinite did not disperse very well in the hexane, probably as a result of it being primarily water wettable.

A series of runs were performed with the hexane/water system in which the NaCl concentration was raised from 0.001 to 0.02M. The runs with no clay added showed a slight increase in the sauter mean diameter with the increased NaCl concentration, shown in Figure 5.5. This increase in drop size was probably due to the effect of the NaCl on the electrical double layer surrounding the oil drops. Watanabe [45] found that NaCl can in some cases decrease the strength of the electrical double layer surrounding oil drops. The electrical double layers of the hexane drops would all have the same charge, causing a repulsion between drops. Decreasing the strength of the double layer decreases the

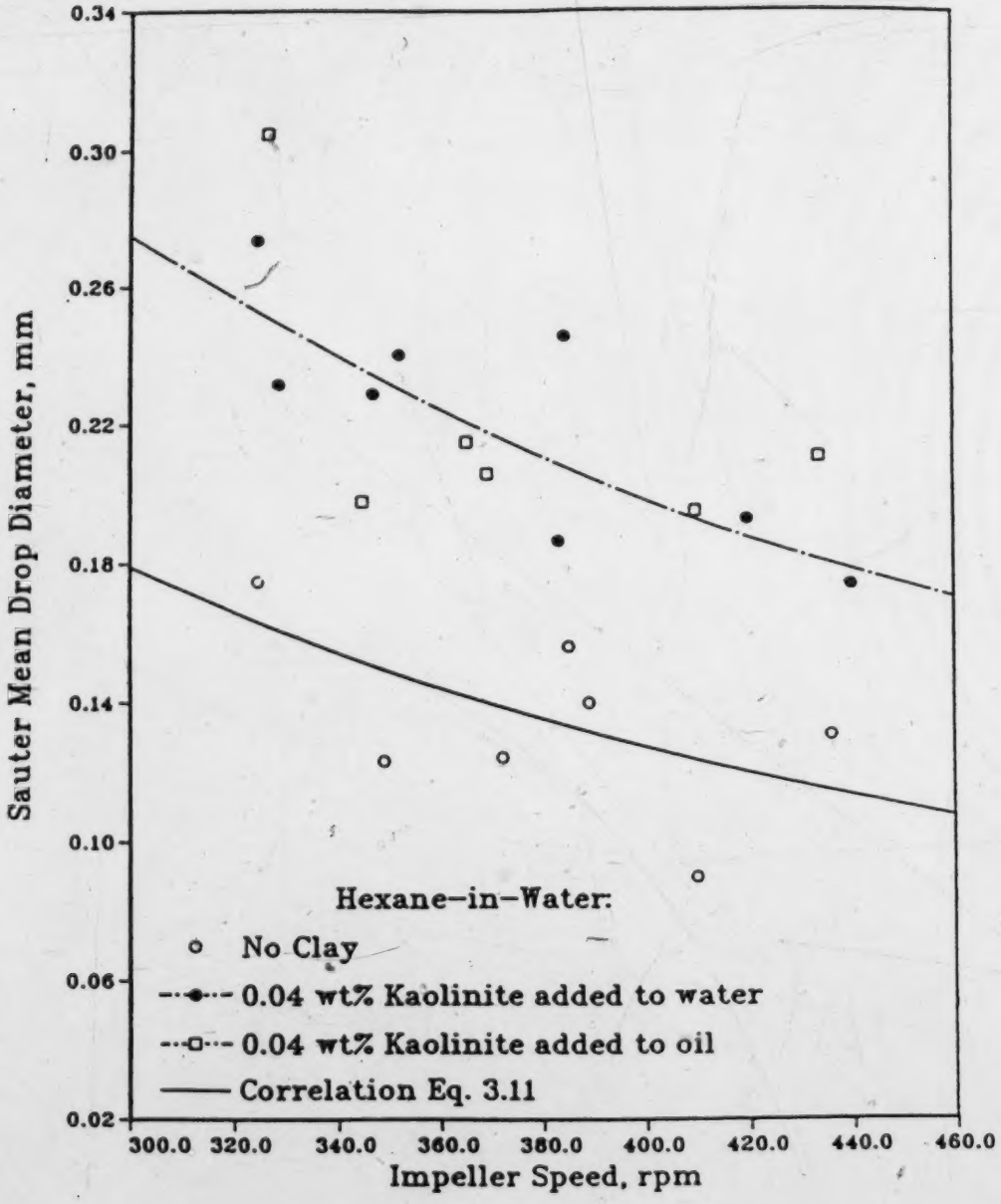

Figure 5.4 : Variation of sauter mean drop size with two different modes of kaolinite addition to hexane/water dispersions

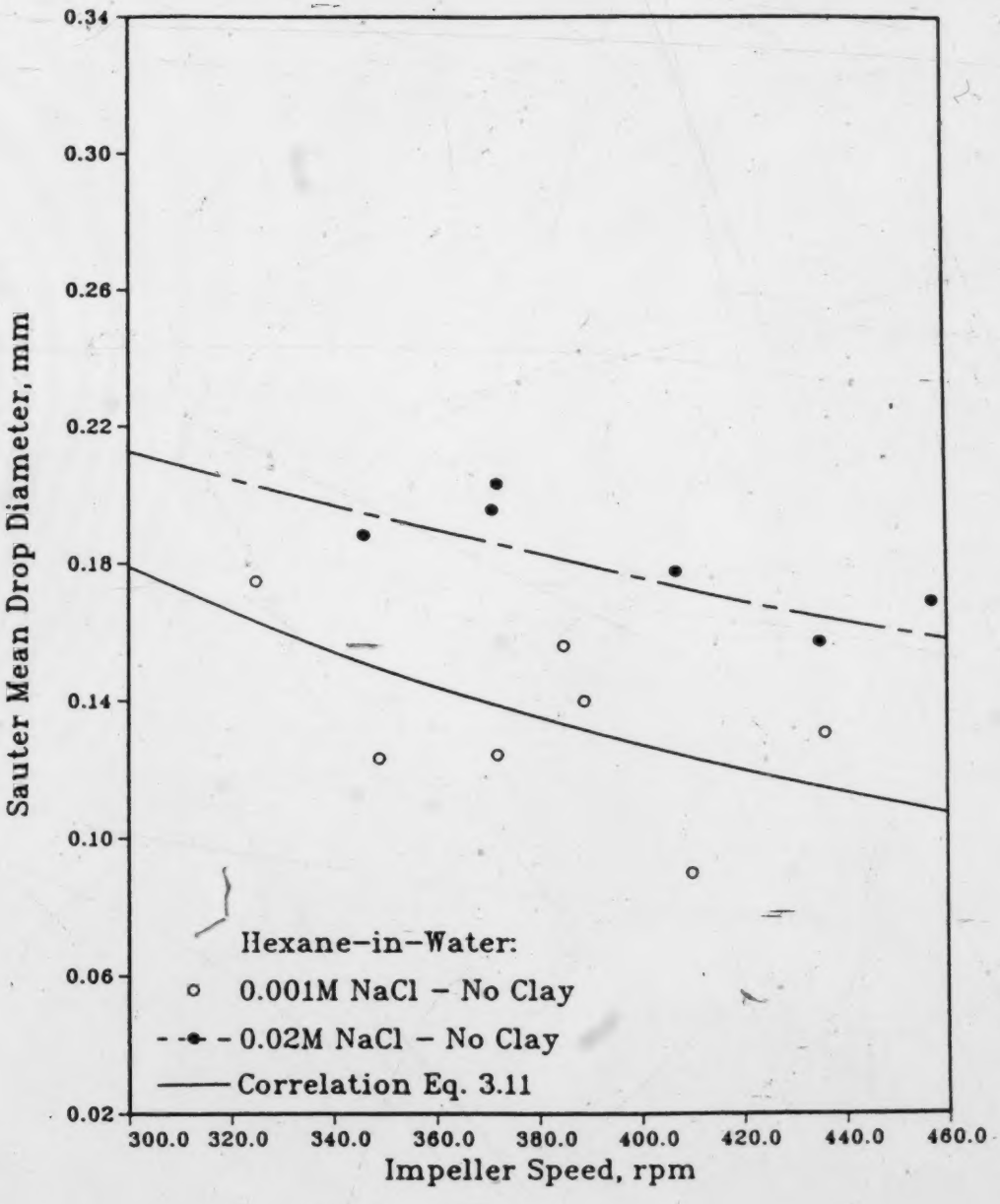

Figure 5.5 : Variation in sauter mean drop size with increasing NaCl concentration for hexane/water dispersions

repulsive force, thus allowing drops to coalesce more readily.

When 0.04 wt% kaolinite was added at the higher NaCl concentration, the sauter mean drop size again showed a slight increase, Figure 5.6. However, this increase was not as large as that produced by adding kaolinite at the lower NaCl concentration. The reason for the smaller increase in sauter mean drop size at 0.02M NaCl could be related to the electrical double layer surrounding the kaolinite particles. The increased NaCl concentration may decrease the strength of the double layer surrounding the kaolinite particles, causing them to form aggregates, and therefore decreasing their net concentration (by number). The smaller number of particles would have less effect on the dispersion.

The results for most of the hexane/water runs showed the expected trend of decreasing drop size with increasing impeller speed. This is because the higher impeller speed imparts more shear into the dispersion, which increases the breakup frequency, and hence decreases the drop size.

Figure 5.7 shows the results from the paraffin oil/water runs. The NaCl concentration for these runs was kept at 0.001M, and the temperature was 23°C. The amount of paraffin oil used in the dispersion was 5% by volume. The paraffin oil drop sizes are larger than those with the hexane/water system. The experimental points are also somewhat less scattered than those found with the hexane/water system. For this system, the correlation shown

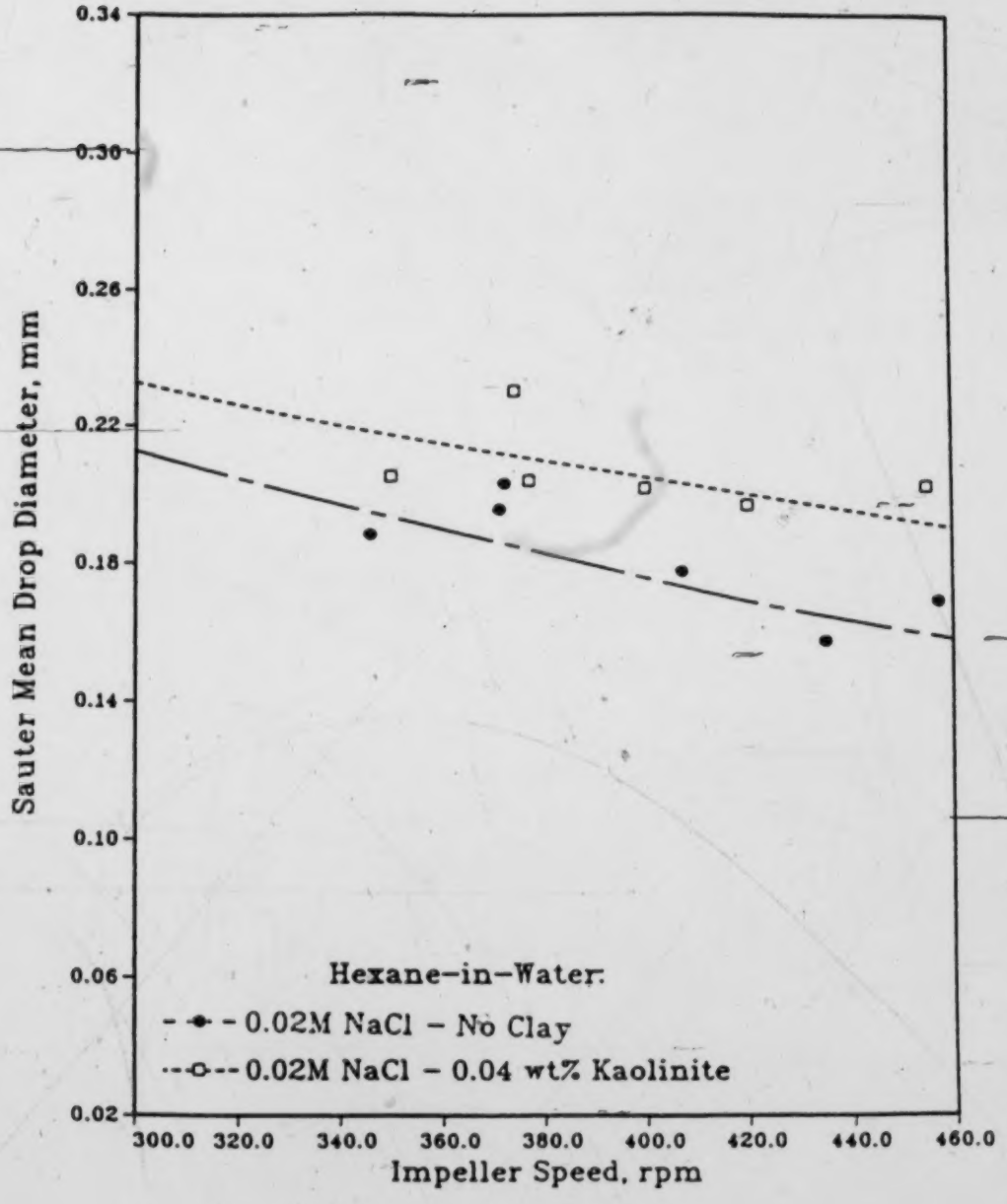

Figure 5.6 : The effect of the addition of 0.04wt% kaolinite to a hexane/water dispersion at 0.02M NaCl

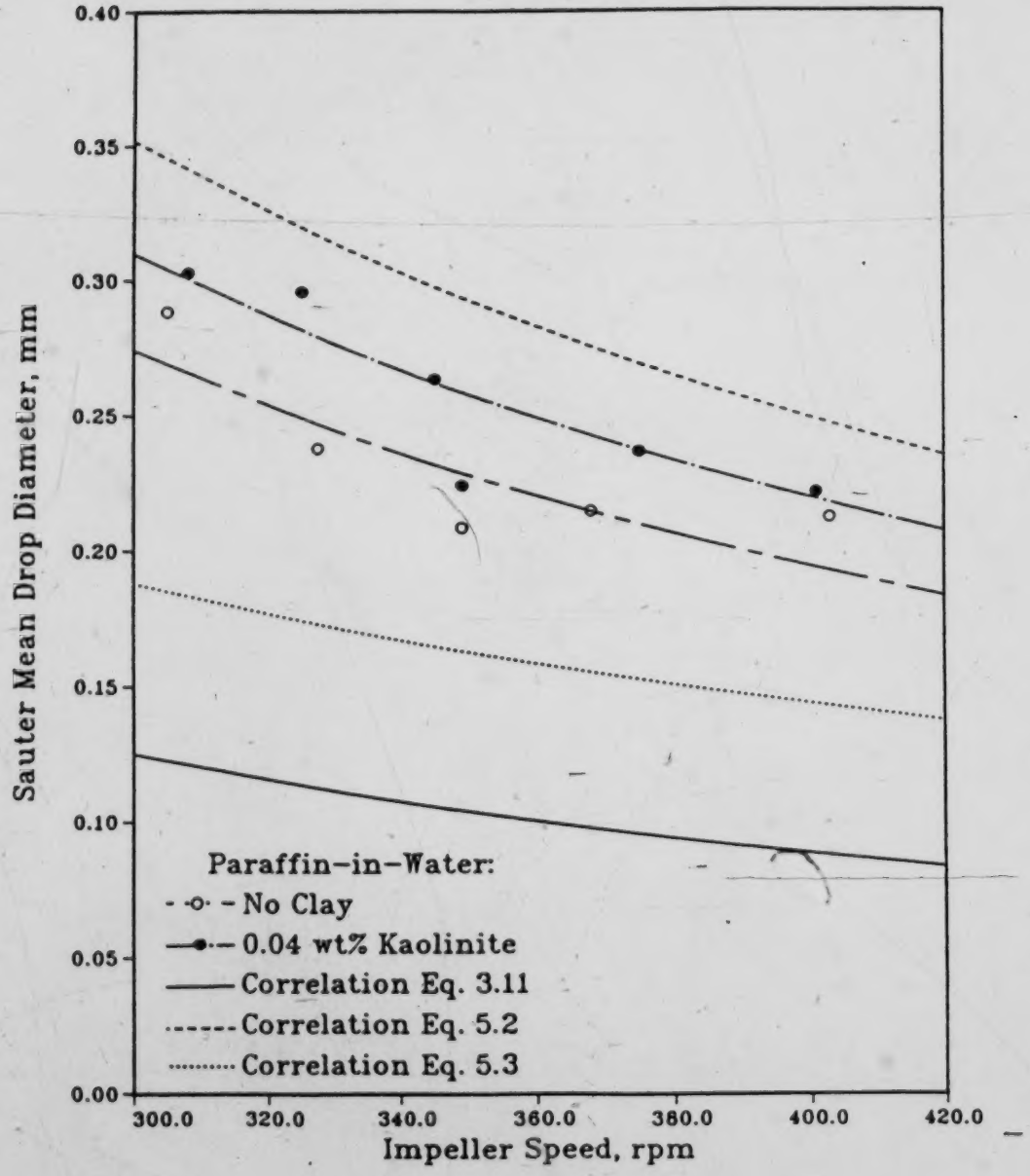

Figure 5.7 : The effect of the addition of 0.04wt% kaolinite to a 5% paraffin oil/water dispersion (0.001M NaCl)

in Equation 3.11 developed by Mlynek and Resnick [25] does not predict the experimental results very well. This is probably because the correlation does not take into account the effect of variations in dispersed phase viscosity. As shown in Table 4.1, the viscosity of paraffin oil is 0.177 kg/m·s, which is much higher than the viscosity of hexane, 0.0003 kg/m·s. A correction factor proposed by Rodger et al. [32] does take into account the effect the continuous and dispersed phase viscosity,

$$d_{32} = 0.058D(1 + 5.4\phi)(We^{-0.6}) \left(\frac{\mu_d}{\mu_c}\right)^{0.2} \qquad (5.2)$$

The viscosity correction factor increases the drop size predicted by the correlation, as shown by the upper line on Figure 5.7. This is closer to the experimental data than those predicted by Equation 3.11, but there is still a gap between predicted and experimental results.

Calabrese et al. [6] have recently proposed an equation which includes a term for dispersed phase viscosity,

$$d_{32}=0.054D(1+3\phi)(We)^{-0.6}\,[1+4.42(1-2.5\phi)Vi(\frac{d_{32}}{D})^{0.333}]^{0.6} \qquad (5.3)$$

where

$$Vi = \left(\frac{\rho_c}{\rho_d}\right)^{0.5} \mu_d \frac{N\,D}{\sigma} \qquad (5.4)$$

For very dilute dispersions with $\phi \simeq 0$, Equation 5.3 reduces

to

$$d_{32} = 0.054D(We)^{-0.6}\ [1+4.42Vi(\ \frac{d_{32}}{D}\ )^{0.333}]^{0.6} \qquad (5.5)$$

Equations 5.3 and 5.5 were developed from experimental studies of silicone oil/water dispersions. Calabrese et al. [5],[6],[43] varied the dispersed phase viscosity from 0.1 to 10 kg/m·s^2, while interfacial tension was varied from 0.001 to 0.045 N/m. The dispersions were created in various baffled cylindrical vessels using flat bladed turbine impellers. A photographic method was used to determine the drop size parameters.

From Figure 5.7 it can be seen that Equation 5.3 provides a better prediction of sauter mean diameter than does Equation 3.11 for paraffin oil/water dispersions. However, the predictions of Equation 5.3 are still slightly farther away from the experimental data than those of Equation 5.2.

The addition of 0.04 wt% kaolinite to the paraffin oil/water dispersion increased the sauter mean drop size, as was the case for hexane. However, the increase was much smaller with the more viscous paraffin oil. This may be due to the higher viscosity of the paraffin oil, or to the lower paraffin oil/water interfacial tension [42].

The results for the bitumen/water dispersions are shown in Figure 5.8 . As with the other hydrocarbons, the amount of bitumen used in the dispersions was 5% by volume. These

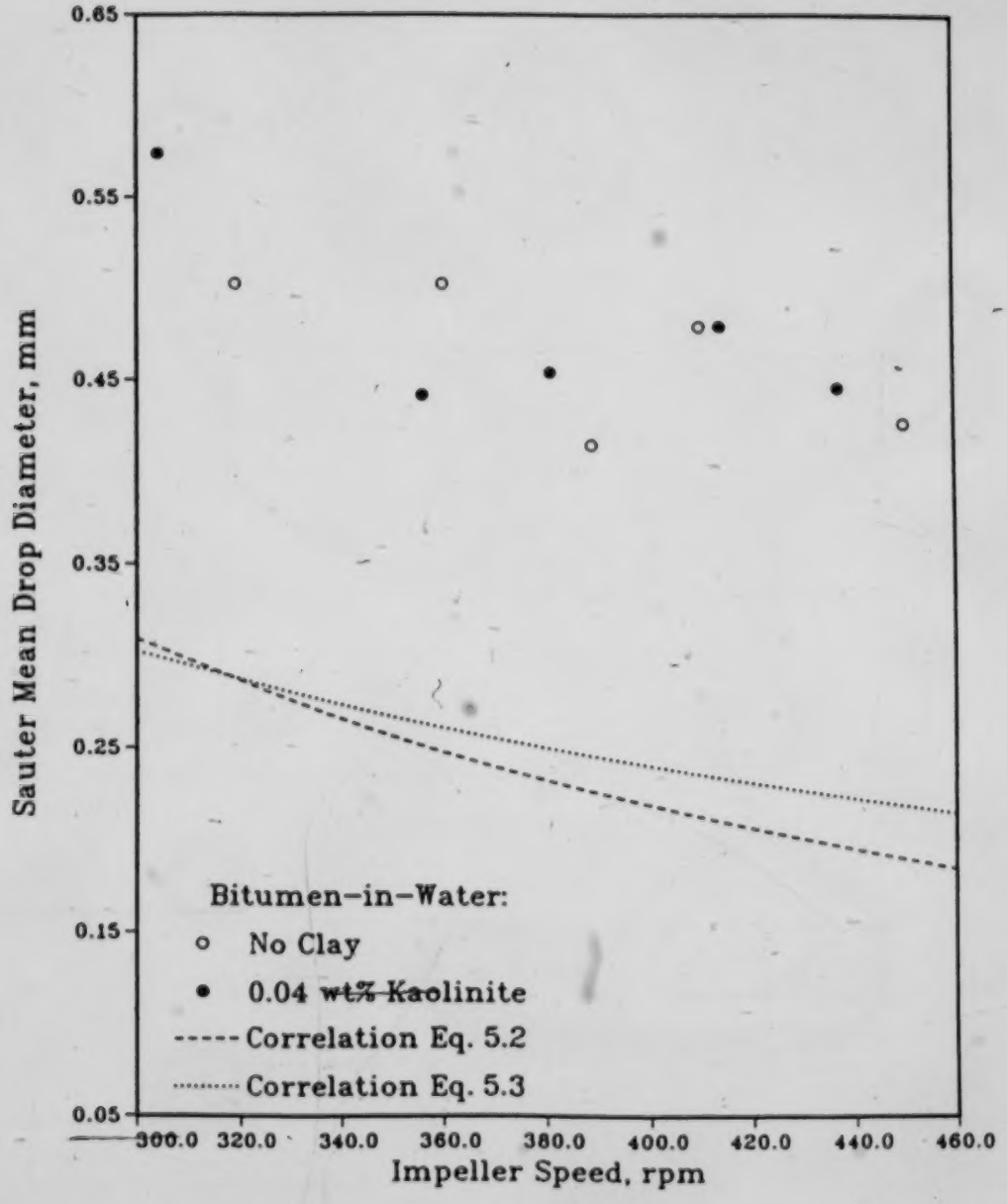

Figure 5.8 : The effect of the addition of 0.04wt% kaolinite to a 5% bitumen/water dispersion (0.001M NaCl, 70°C)

runs were carried out at 70°C, with a NaCl concentration of 0.001M. The bitumen drops were somewhat larger than both those in the hexane/water and paraffin oil/water dispersions. This is in agreement with the increase in sauter mean diameter with increasing dispersed phase viscosity as predicted by Equation 5.3. This effect is partially offset by the decrease in sauter mean diameter as interfacial tension decreases. Equations 5.2 and 5.3 both predict a value for the sauter mean diameter which is much lower than actual experimental data, as shown in Figure 5.8.

As the impeller speed increased, the bitumen drop size decreased. However, the addition of 0.04 wt% kaolinite to the mixture had no discernible effect.

Figure 5.9 compares sauter mean diameters predicted by Equation 5.3 with those determined experimentally for hexane/water, paraffin oil/water and bitumen/water dispersions. Figure 5.10 compares the predictions of Equation 5.5 with the experimental results of several other researchers, [2],[5],[9],[38] and [43]. From Figure 5.9 it can be seen that the experimental data for hexane/water dispersions agree well with the predictions of Equation 5.3. The data fall well within the envelope of other experimental data, shown in Figure 5.10. The results for paraffin oil/water dispersions also fall fairly close to the predictions of Equation 5.3, again within the range of other researchers' experimental data. The results for bitumen/water dispersions are farther away from the

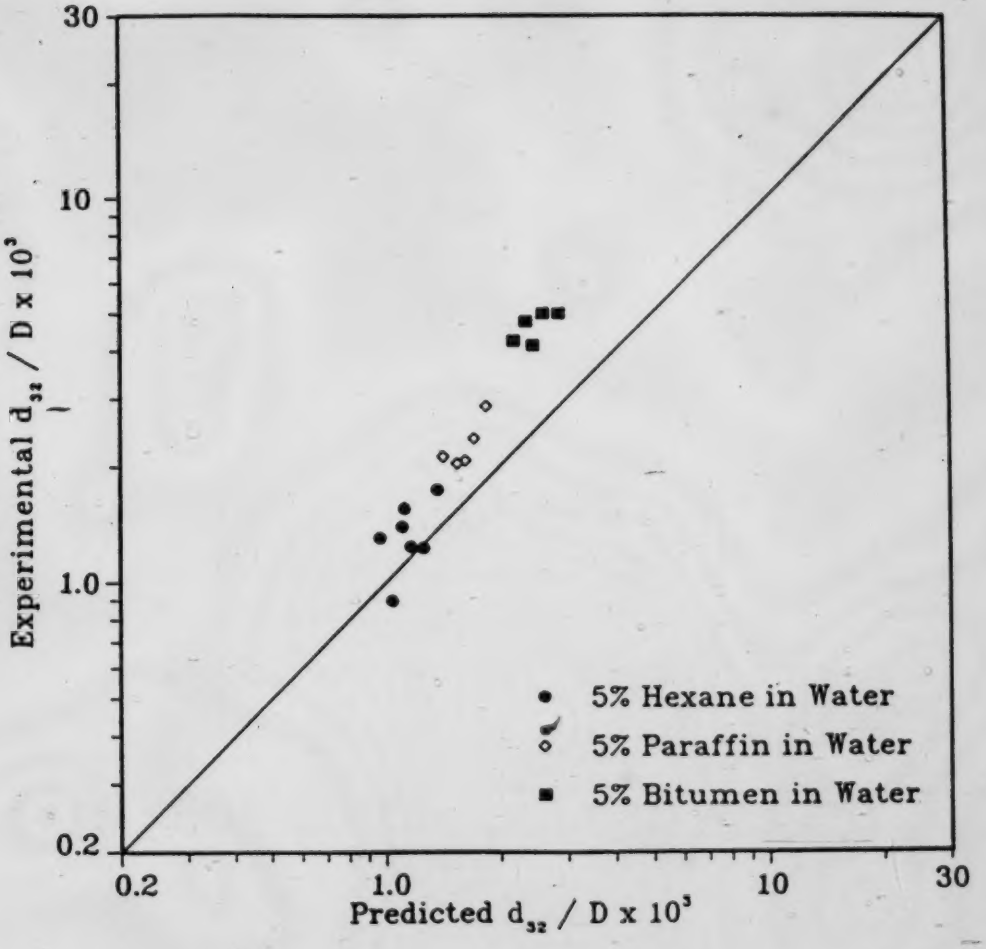

Figure 5.9 : Comparison of experimental data for hexane/ water, paraffin oil/ water and bitumen/ water dispersions to the predictions of Equation 5.3

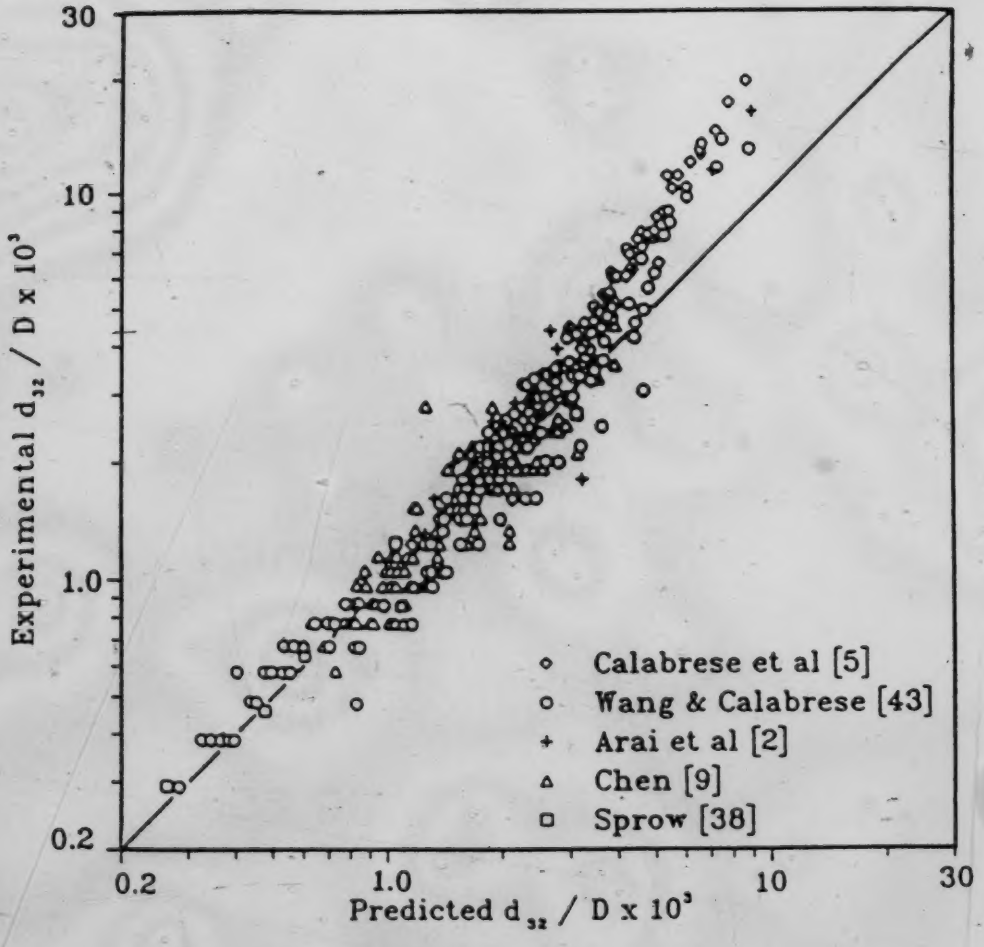

Figure 5.10 : Comparison of the results of other work to the predictions of Equation 5.5, Wang and Calabrese [43], (Information adapted from source)

predictions of Equation 5.3. This is, however, consistent with the results in Figure 5.10 where the deviation increases as the sauter mean diameter increases.

5.1 Average Drop Diameters

The average drop diameters for all of the dispersions studied were less than the sauter mean drop sizes, as shown in Appendix B. This is because the sauter mean diameter (Equation 3.8) is a "volume to surface" mean diameter, and is strongly dependent on the larger drops, as found by Calabrese et al. [5]. In fact, the average drop diameters were approximately the same for hexane/water, paraffin oil/water and bitumen/water dispersions (with no clay added).

The addition of kaolinite to hexane/water and paraffin oil/water dispersions caused a slight increase in average diameter, although the increase was not as large as that found in the sauter mean diameters. A similar trend was found when kaolinite was added to hexane/water dispersions at 0.02M NaCl. No change was found in the average drop diameter when kaolinite was added to the bitumen/water dispersions, which agrees with the results for sauter mean diameters.

5.2 Drop Size Distributions

Drop size distributions were plotted for each of the experimental runs performed. Examples for each of the general systems studied are shown in Figures 5.11 to 5.16. The distributions for all of the remaining runs are given in Appendix C. Standard deviations for all runs are given in Appendix B. For each plot, the overall range of drop sizes studied was divided into 20 equal size partitions. A typical drop size distribution for a hexane/water dispersion is shown in Figure 5.11. The drops for this run follow a fairly typical distribution. The addition of kaolinite broadens the drop size distribution, producing quite a few more larger drops, as shown in Figure 5.12. The addition of Athabasca fines has a similar effect on the hexane/water drop size distribution, although not as pronounced. Increasing the NaCl concentration also tends to broaden the drop size distribution by producing more of the larger drops.

The drop size distribution for a typical paraffin oil/water dispersion is shown in Figure 5.13. There is a greater proportion of smaller drops compared to the total number of drops for the paraffin oil/water system than there is for the hexane/water system. There are also more of the larger drops. The broadening of the drop size distribution with increasing dispersed phase viscosity is in agreement with the results found by Calabrese et al. [5]. As with the hexane runs, the addition of kaolinite tends to broaden the drop size distribution for the paraffin oil/water system, as

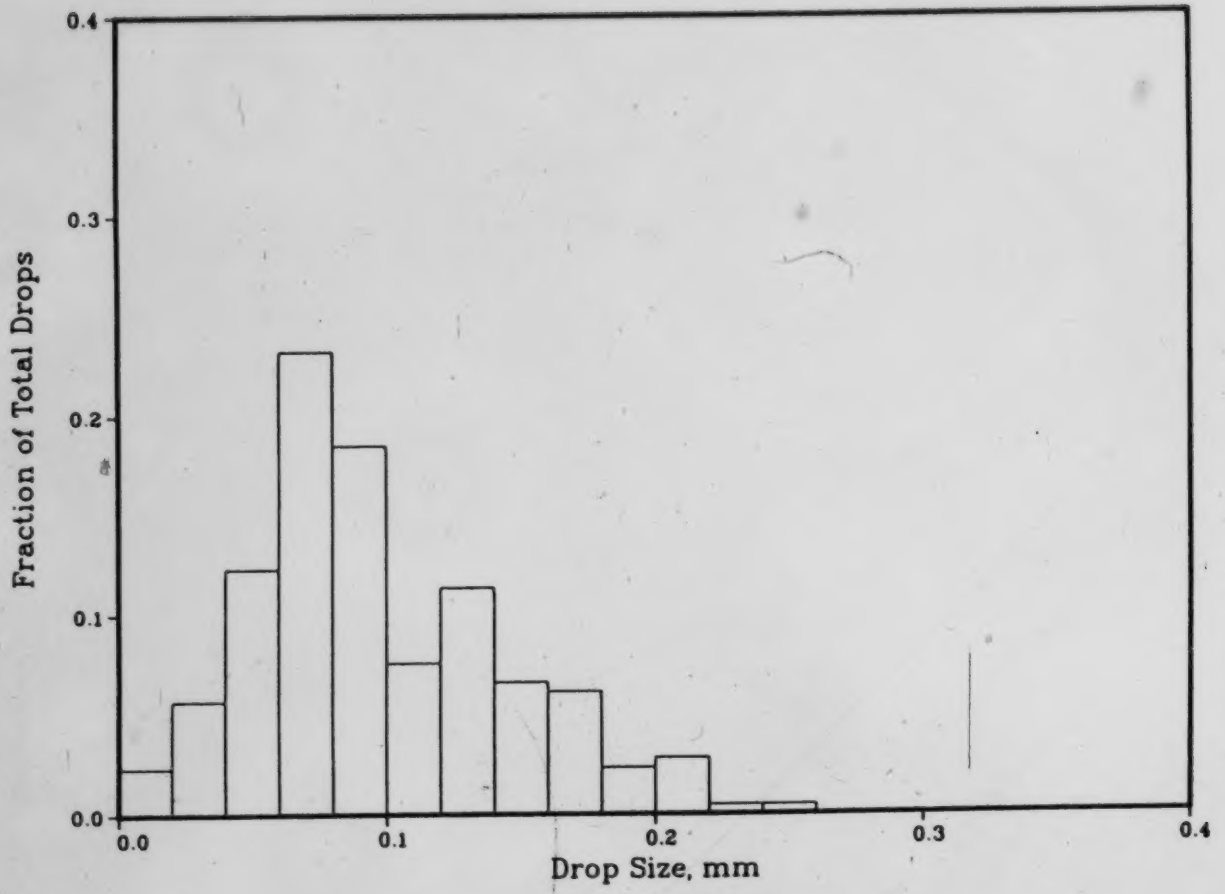

Figure 5.11 : Drop size distribution for a 5% hexane, 95% water dispersion, 0.001M NaCl, 389 rpm

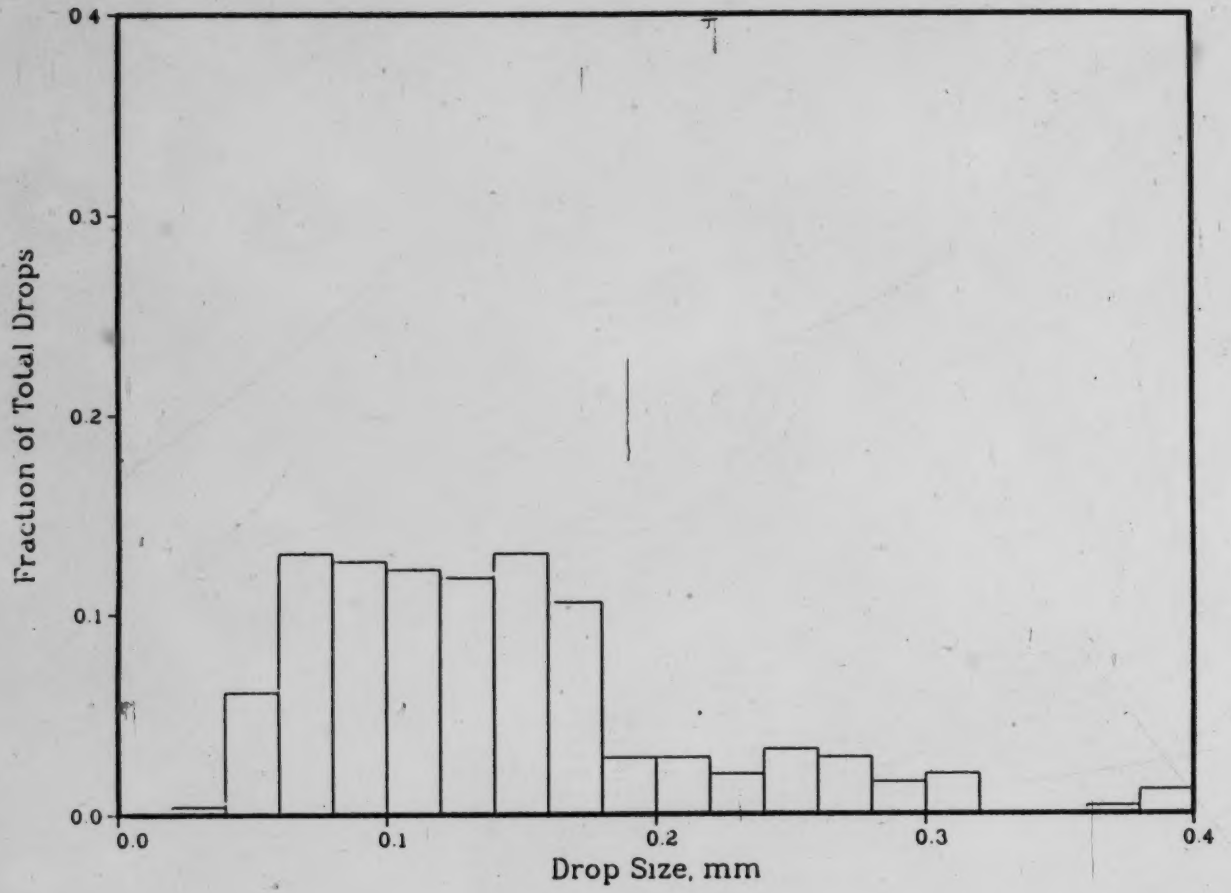

Figure 5.12 : Drop size distribution for a 5% hexane, 95% water dispersion, 0.04 wt% kaolinite, 0.001M NaCl, 384 rpm

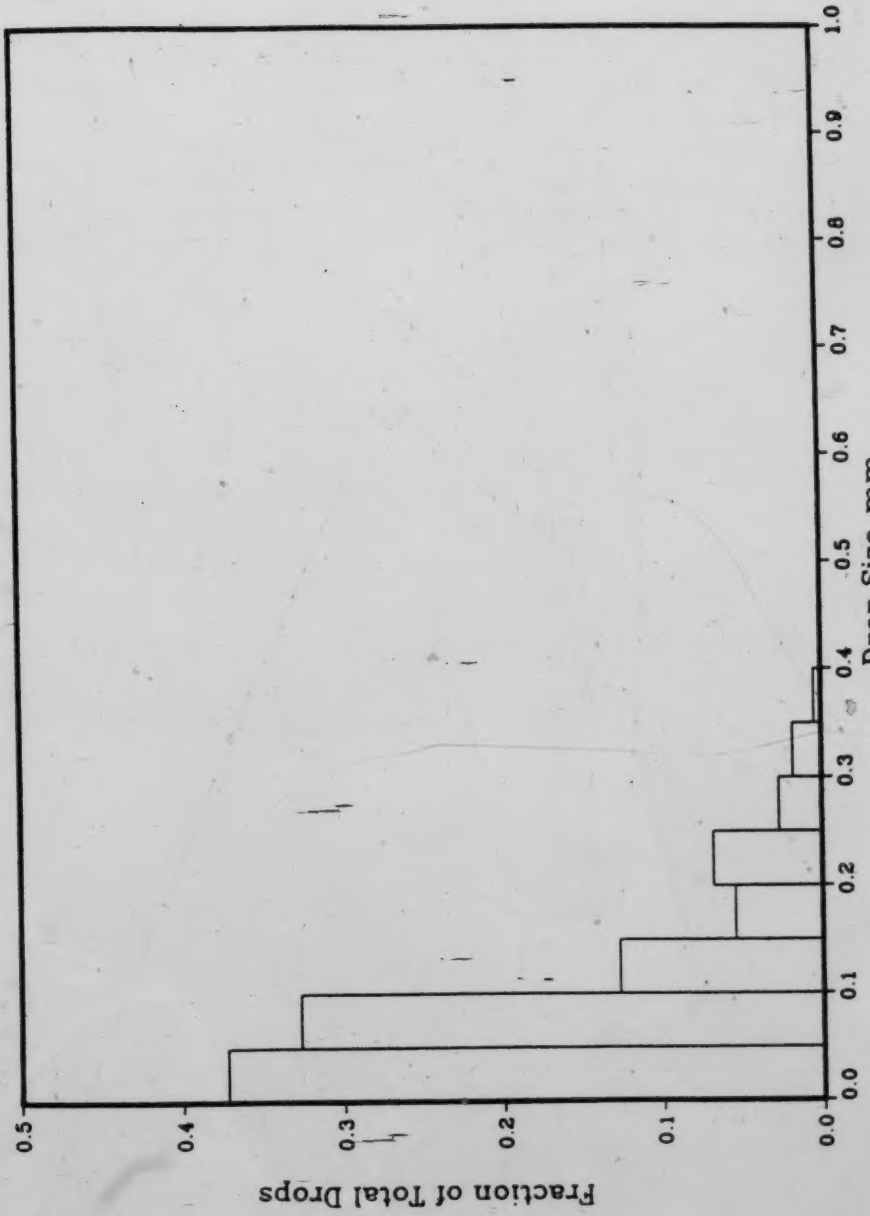

Figure 5.13 : Drop size distribution for a 5% paraffin oil, 95% water dispersion, 0.001M NaCl, 368 rpm

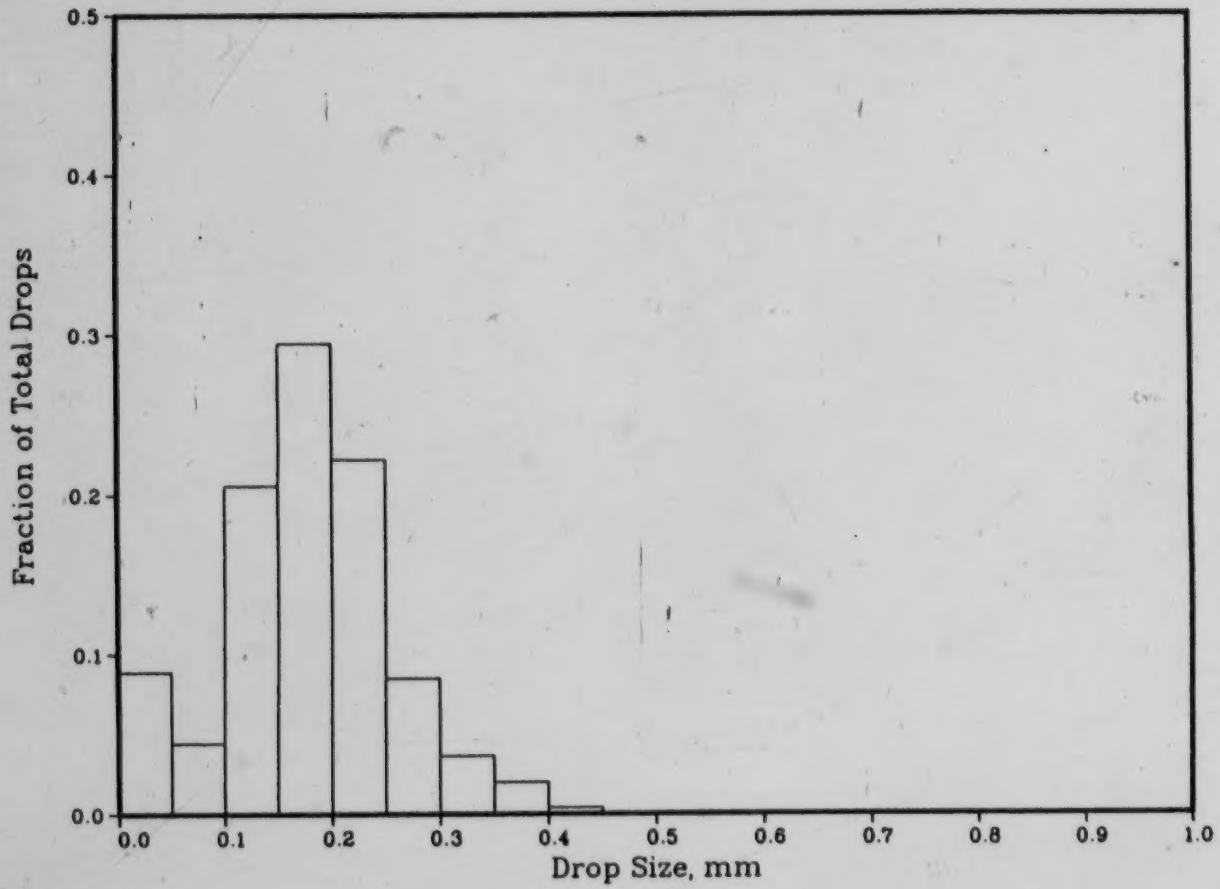

Figure 5.14 : Drop size distribution for a 5% paraffin oil, 95% water dispersion, 0.04 wt% kaolinite, 0.001M NaCl, 375 rpm

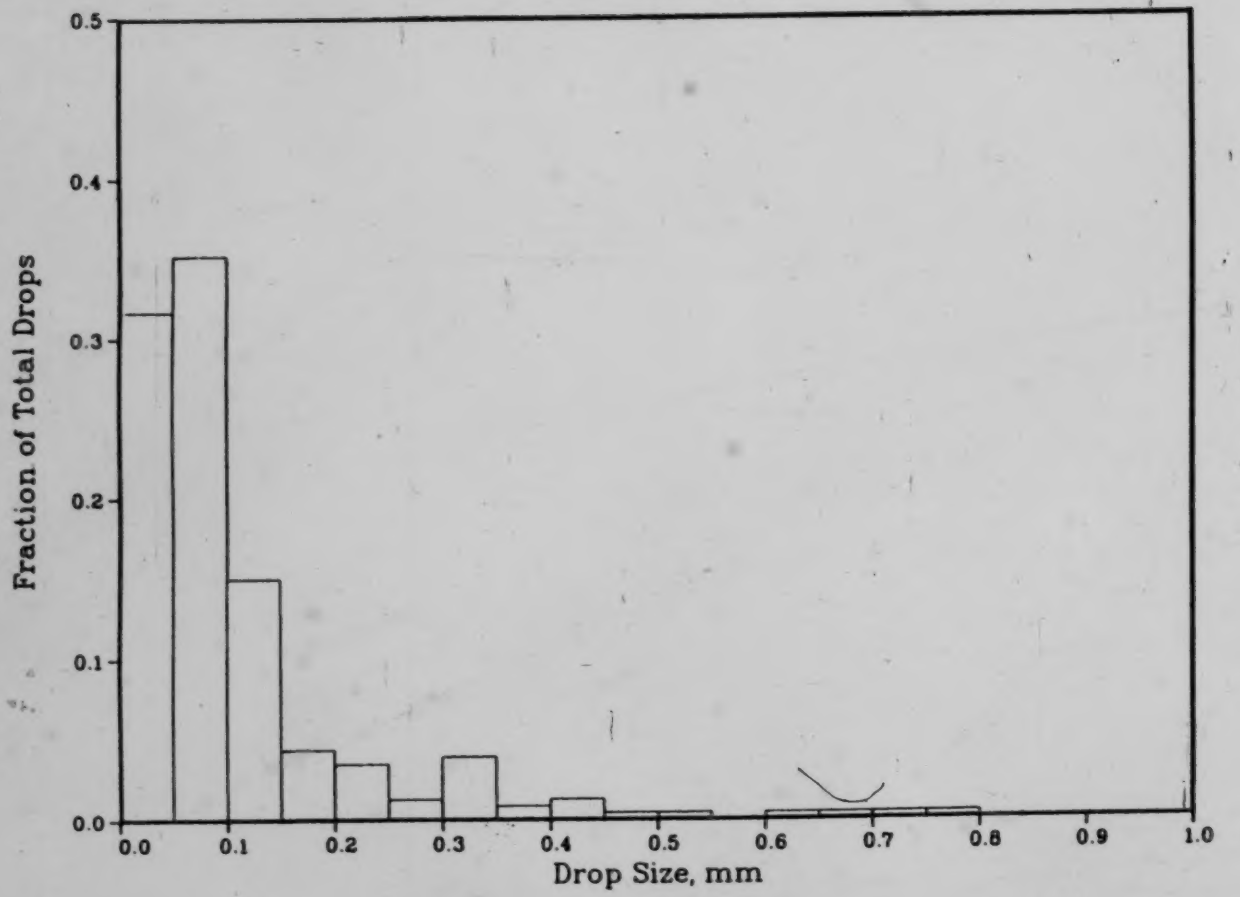

Figure 5.15 : Drop size distribution for a 5% bitumen, 95% water dispersion, 0.001M NaCl, 389 rpm

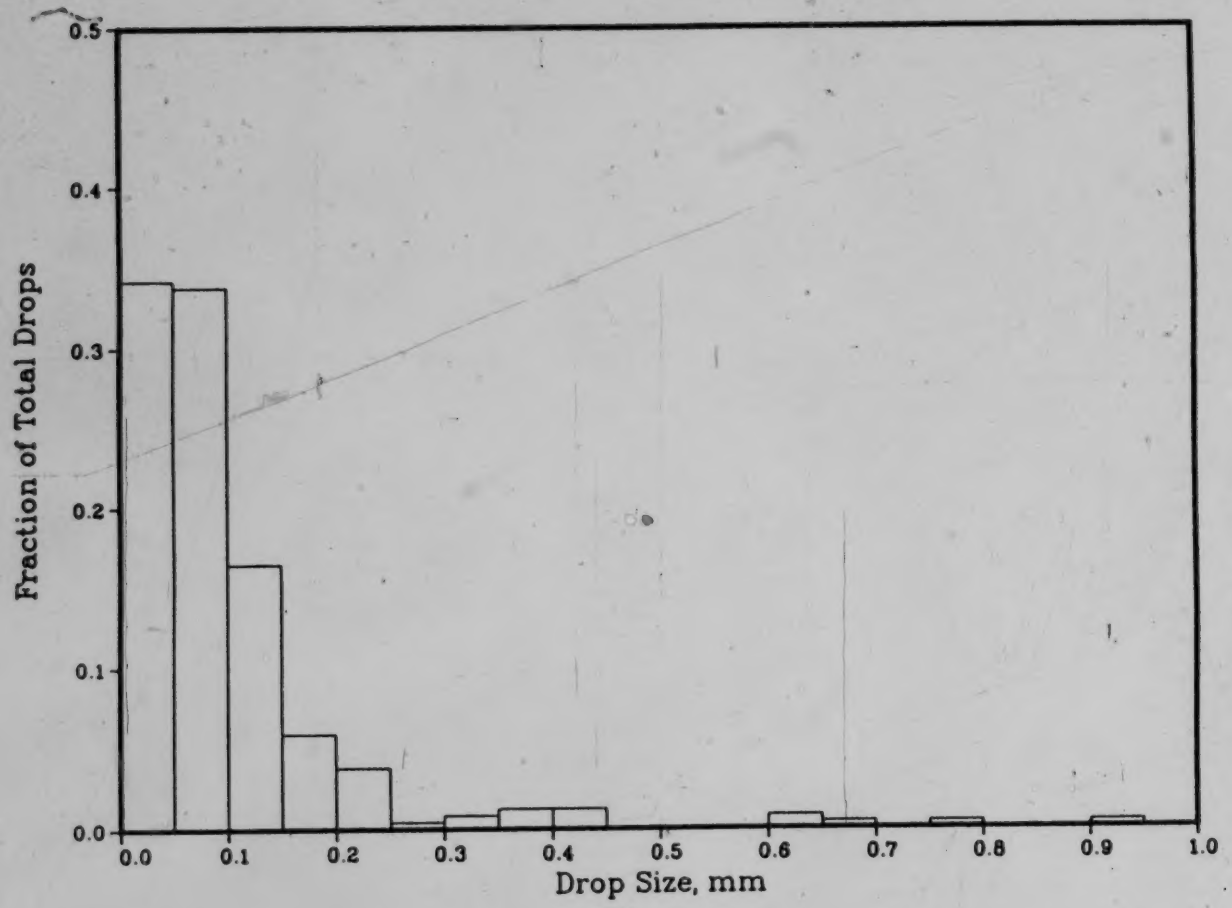

Figure 5.16 : Drop size distribution for a 5% bitumen, 95% water dispersion, 0.04 wt% kaolinite, 0.001M NaCl, 381 rpm

shown in Figure 5.14.

The bitumen/water drop size distributions again have a greater proportion of smaller drops, as shown in Figure 5.15. There are also a few very large drops present, up to 1.0 millimeter in diameter. The presence of larger drops is also consistent with the results of Calabrese et al. [5]. The addition of kaolinite has little noticeable effect on the drop size distributions for the bitumen/water system, Figure 5.16. This corresponds to the lack of change found in the sauter mean diameters when kaolinite was added.

Figure 5.17 shows the drop size distribution for a hexane/water dispersion plotted on log-probability axes. The data points lie in a straight line, which indicates that the distribution is a log-normal distribution. The addition of kaolinite to the hexane/water system produced a distribution with the same slope as without the clay, but with larger drop sizes, as shown in Figure 5.17.

The drop size distribution for a paraffin/water distribution plotted on log-probability axes is shown in Figure 5.18. The data follow a fairly straight line, which indicates a log-normal distribution. When kaolinite is added, the data exhibit two distinct regions, each with a different slope. This may indicate that there are two separate populations in the system.

The log-probability curves for the bitumen/water system, both with and without kaolinite addition, follow a log-normal distribution, as shown in Figure 5.19. The two

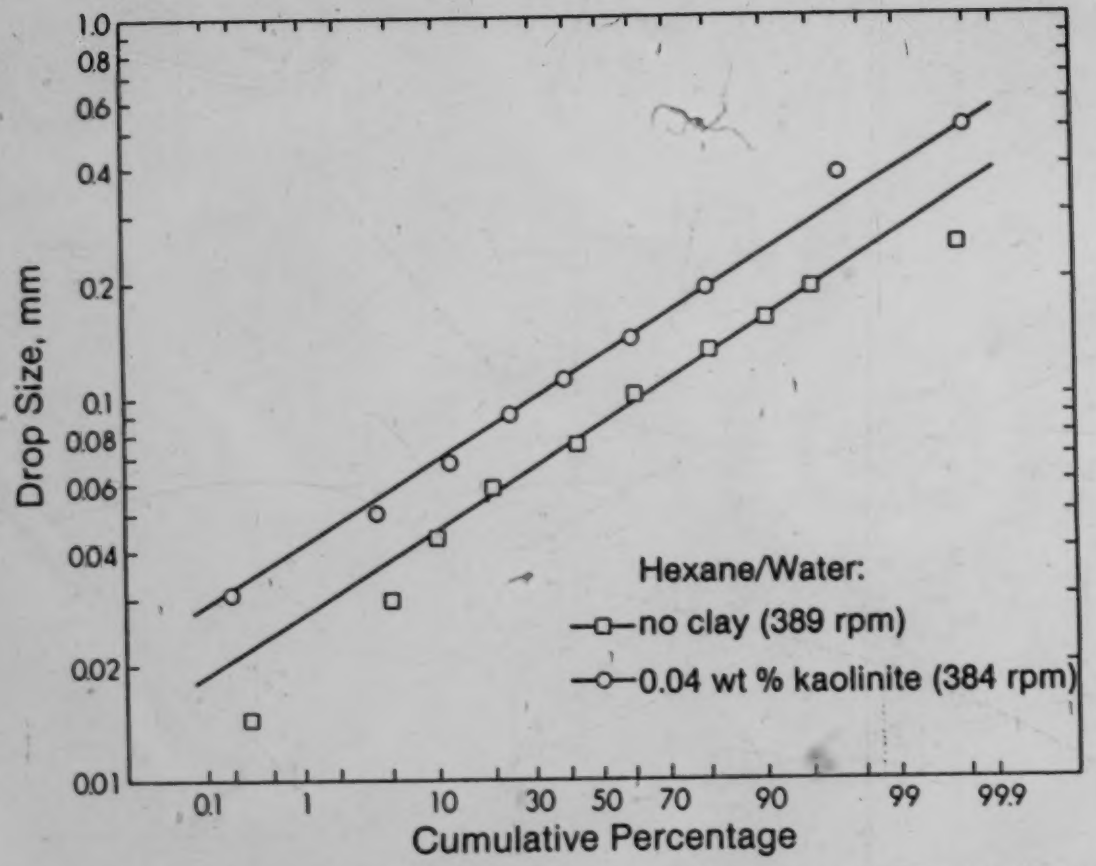

Figure 5.17 : Log-normal probability plot showing the effect of kaolinite addition to a 5% hexane/water dispersion at 0.001M NaCl (not all points shown)

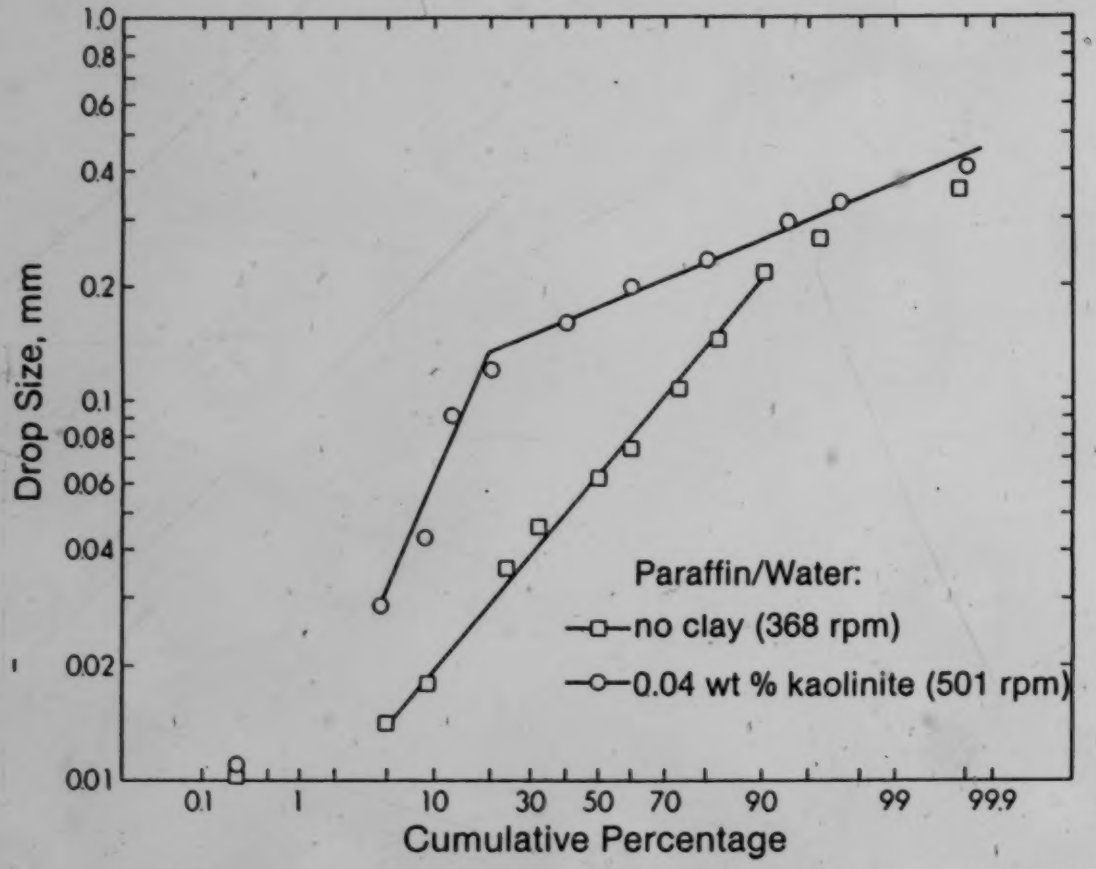

Figure 5.18 : Log-normal probability plot showing the effect of kaolinite addition to a 5% paraffin/water dispersion at 0.001M NaCl (not all points shown)

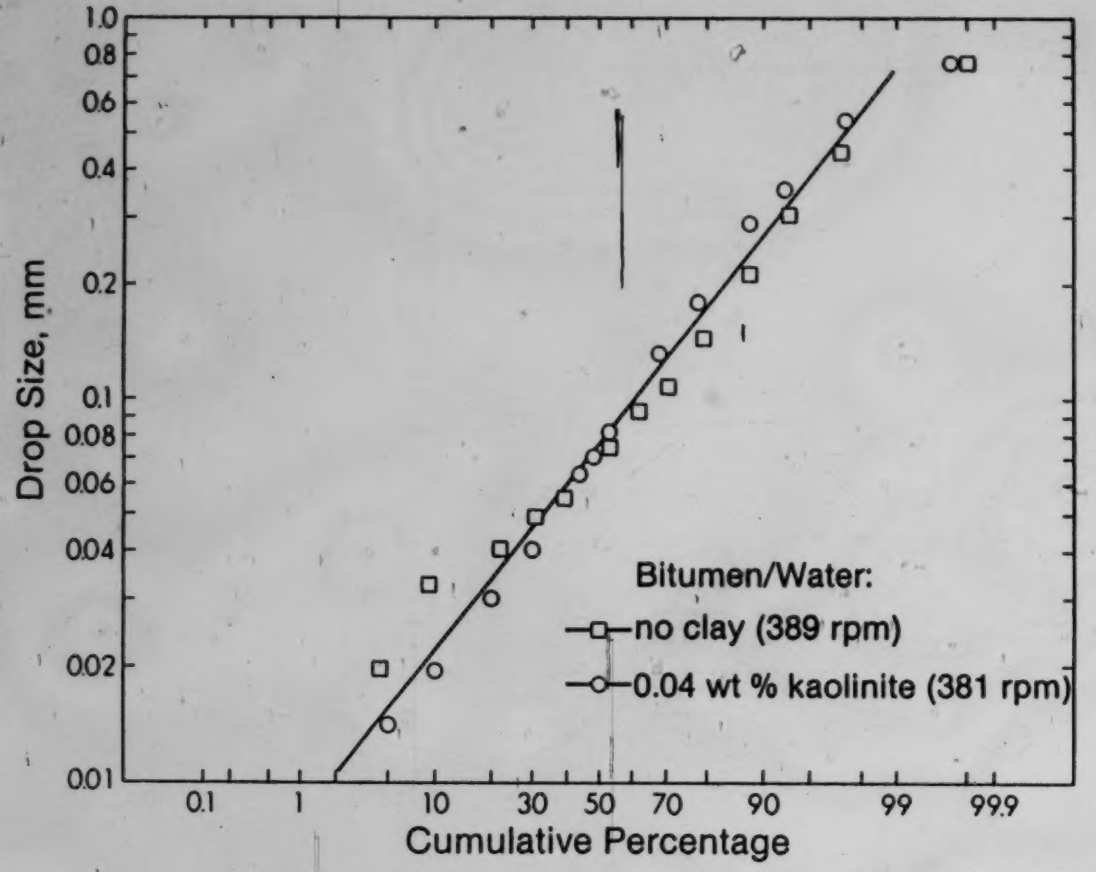

Figure 5.19 : Log-normal probability plot showing the effect of kaolinite addition to a 5% bitumen/water dispersion at 0.001M NaCl (not all points shown)

curves overlap, which indicates that the addition of kaolinite to this system had no effect on the drop size distribution.

5.3 Maximum Drop Sizes

Dispersions can be characterized in terms of maximum drop size. The results of this work, in terms of maximum drop size for a given dispersion, are shown in Table 10.1 in Appendix B. As expected from the trends in sauter mean drop size, the bitumen/water dispersions have the largest maximum diameters. There is a good deal of scatter between maximum drop sizes for similar dispersions. One of the reasons for this is that only 200 to 300 drops were measured for each dispersion. There are actually several thousand drops in each of the dispersions studied in this work, and therefore it is unlikely that the largest drops would consistently be found in a sample of only 200 to 300 drops. However, the primary focus of this work was to determine sauter mean drop sizes, and not the maximum diameters. Therefore, the sample size chosen is acceptable for the main focus of this work.

One trend which is shown in the maximum drop sizes is that as the dispersed phase viscosity increases, the maximum drop size also increases (Table 10.1). This is consistent with Equation 5.6 developed theoretically by Arai et al. [2],

$$d_{max} = 0.367D \left(\frac{\rho_c N D^2}{\mu_d}\right)^{-0.75} \qquad (5.6)$$

This equation was proven experimentally by Arai et al. over a wide range of experimental conditions. Polystyrene -o-xylene/water dispersions were studied in a baffled cylindrical vessel. Drop sizes were determined from photographs taken through the wall of the vessel. The polystyrene concentration was varied from 0 to 25wt%, which changed the dispersed phase viscosity from 0.00078 to 1.500 kg/m·s.

When Equation 5.6 is applied to the systems being studied in this work, the results calculated are shown in Table 5.1. The actual experimental maximum drop diameters are also shown in this table.

Hydrocarbon Type	d_{max} (mm) Equation 5.6	d_{max} (mm) Experimental, no clay	d_{max} (mm) Experimental, +kaolinite
Hexane	0.0035	0.1438	0.3300
Paraffin Oil	0.4238	0.3125	0.3496
Bitumen	0.9510	0.8747	0.9265

Table 5.1 : Theoretical and experimental maximum drop diameters (at a nominal agitation speed of 408 rpm)

Figure 5.20 shows the experimental and theoretical results presented in graphical form. From Table 5.1 and Figure 5.20 it can be seen that the experimental results of this work agree reasonably well with the predictions of Equation 5.6. However, the predicted maximum drop size for the hexane/water dispersion does not agree very well with

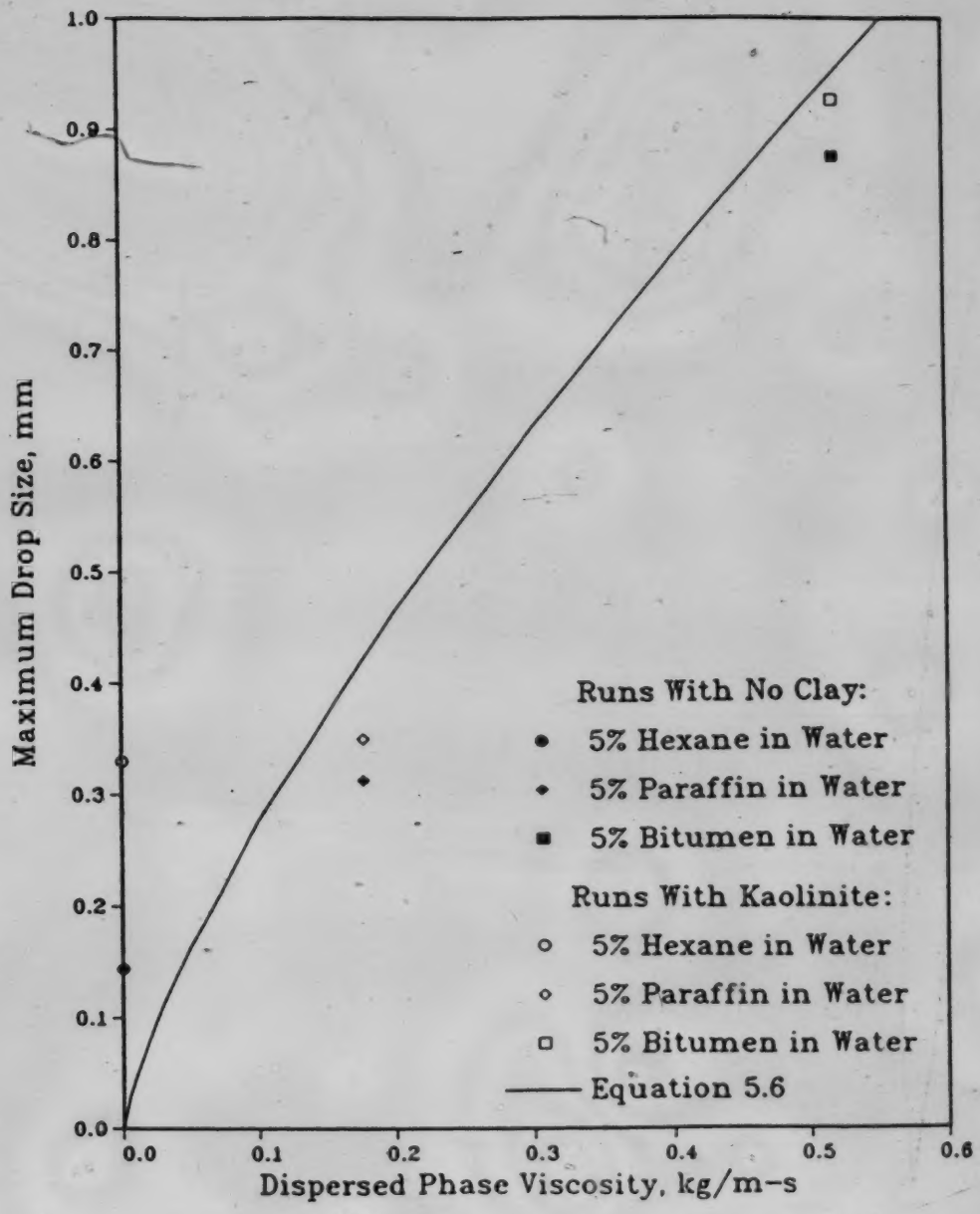

Figure 5.20 : Experimental and theoretical maximum drop sizes at 408 rpm

that determined experimentally. The addition of 0.04wt% kaolinite to a hexane/water dispersion greatly increases the maximum drop diameter, as shown in Table 5.1 and Figure 5.20. The paraffin oil/water and bitumen/water dispersions show only a slight increase in maximum drop diameter when kaolinite is added.

The average values of the ratio d_{32}/d_{max} for the three different types of dispersions studied are shown in Table 5.2. Appendix B contains data for d_{32}/d_{max} for all of the different experimental runs.

Hydrocarbon Type	Average d_{32}/d_{max}, no clay	Average d_{32}/d_{max}, +kaolinite
Hexane	0.5374	0.5069
Paraffin Oil	0.5905	0.6337
Bitumen	0.5453	0.5647

Table 5.2 : Comparison of average values of d_{32}/d_{max}

Calabrese et al. [5] found d_{32}/d_{max} to be 0.6 for moderate viscosity oils, and 0.5 for high viscosity oils. From Table 5.2 it can be seen that the values of the ratio d_{32}/d_{max} found in this work agree well with those found by Calabrese et al. [5]. The results of this work, however, show no real trend of decreasing d_{32}/d_{max} with increasing dispersed phase viscosity.

From Table 5.2 it can be seen that the values of d_{32}/d_{max} are approximately the same for hexane/water dispersions with and without added kaolinite. A similar trend is found for the paraffin oil/water and the bitumen/water dispersions. It is interesting to note that values of d_{32}/d_{max} are similar for the hexane, paraffin oil and bitumen dispersions, with and without the addition of kaolinite. The average value of d_{32}/d_{max} for the six tabulated d_{32}/d_{max} values of Table 5.2 is 0.56.

5.4 Experimental Errors

The repeatibility of results in this work was found by repeating several runs and determining the percent difference between the largest and the smallest sauter mean drop sizes. The error was estimated to be ±15%. This error is of the same order of magnitude as that found by other researchers using similar optical methods [16], [44].

By definition, the sauter mean drop size is weighted more towards the very large drops in comparison to the very small drops. As a result of the magnification used for most of this work, (56X), some of the very small drops may not have been visible, and therefore would not have been measured. This would therefore have little effect on the sauter mean drop size, but it would skew the drop size distributions.

The field of focus for the objective lens used in the photomicrographic probe was chosen so as to be wide enough

to allow even the largest drops to be seen. However, there could be some problems with drops which were just on the edge of the field of focus, because the inner part of the drop would be visible, but the edges might be indistinct. The gap between the optical probe and the light probe was varied from 1 to 3 centimeters, but no effect was found on the measured sauter mean drop size. The gap used for all of the resulting runs was 2.0 centimeters. Other researchers have determined the variation of sauter mean drop size at different points in the vessel, such as in the work of Park and Blair [28],[29] and others [40]. It was found that the drops are smaller in the region of the impeller than at the top of the vessel. In the present work, the optical probe was kept at the same position for all runs, which was 15 centimeters from the top of the vessel.

The level of illumination used in the experiments was found to be important because if it was too bright some of the drops, especially the smaller ones, may not have been visible. Alternatively, if there was not enough illumination, it was also difficult to see the drops because of the reduced contrast levels. The hexane and paraffin oil drops were essentially clear (transparent), and were only visible as a dark outer circle with a transparent center. The lighting was less critical with the bitumen/water system because the bitumen drops showed as solid black circles. However, overlapping bitumen drops would tend to obscure each other causing some analysis problems. Occasionally a

large bitumen drop would attach itself to the glass cover of the optical probe, making it impossible to see a portion of the dispersion.

One area where some error may have been introduced is in the analysis procedure where the drops in focus have to be circled prior to bleaching. This procedure was a subjective one, because the drops appearing in the photographs ranged from sharp images to very unclear ones, with most falling somewhere in between. An effort was made to be consistent in the choice of drops which were sufficiently in focus to be circled, and therefore recorded. However, it is possible that some error was introduced with the smaller drops which often were the most difficult to see.

Almost all of the drops studied for the different oil/water dispersions were essentially spherical in shape. For those few that were not, an average was taken of the drop's length and width. Even the non-spherical drops were only partially elongated, and there were no drops that could be called "cigar shaped".

The minimum number of drops required for each separate experimental run was approximately 200. This number was chosen as a compromise between getting enough drops to make the run statistically meaningful, but not trying to analyze too many drops, which would decrease the amount of different experimental runs which could be performed. The circling of the drops was the most time consuming step of the analysis

procedure.

The experimental work done by Park and Blair [29] and others suggests that one hour was sufficient to allow the mixed dispersion to reach equilibrium (ie. for the drop coalescence and breakup rates to stabilize). To avoid any possible problems, the dispersions in the present work were stirred for at least two hours.

Another possible source of error was loss of hexane due to evaporation. From Equation 5.1 it can be seen that the term which describes the effect of dispersed phase concentration on sauter mean drop size only has a small effect. This means that even if there were a small loss of hexane it would have little effect on the sauter mean drop size. Therefore, evaporation was not an important factor. The paraffin oil and the bitumen are even less volatile, and so would have little evaporation. The bitumen, however, tended to stick to the baffles, shaft, probe and vessel walls, so there may have been some small errors caused by the decrease in bitumen concentration.

6. Conclusions

1. The addition of pure kaolinite to a hexane/water and to a paraffin oil/water dispersion increases the sauter mean drop size. This may be caused by the clay particles acting as nucleate sites aiding in coalescence. Alternatively, the kaolinite particles may stabilize the drops during breakup.
2. The addition of an unpurified mixture of Athabasca fines to a hexane/water dispersion increases the sauter mean drop size by only a small amount. The decreased effect in comparison with pure kaolinite is possibly caused by the presence of organics in the unpurified Athabasca fines, or by the larger size of the Athabasca fines.
3. Increasing the sodium chloride concentration increases the sauter mean drop size for hexane/water dispersions. This is because the sodium chloride decreases the strength of the electrical double layer surrounding the drops, thus aiding coalescence.
4. The addition of kaolinite has less effect on sauter mean drop size at higher sodium chloride concentrations. This may be due to the sodium chloride causing the clay particles to form aggregates, which would decrease the net clay concentration, and therefore its effect on the hexane/water dispersion.

7. Recommendations

1. Further work should be done with bitumen/water dispersions, studying the effects of NaCl and NaOH.
2. The effect of using a pure oil-wet clay in the dispersions should be studied, as well as the results of using pure illite or silica fines.
3. The consequences of adding various surfactants to oil/water/clay dispersions should be studied.
4. To allow more work in a shorter period of time, a more versatile image analyzer should be used in future studies.

8. References

1. Akida, K. and Yoshida, F., "Bubble Size, Interfacial Area and Liquid Phase Mass Transfer Coefficient in Bubble Columns", Ind. Eng. Chem. Process Design Development, 13, #1, pp 84-91 (1974)

2. Arai, K., Konno, M., Matunaga, Y., and Saito, S., "Effect of Dispersed Phase Viscosity On The Maximum Stable Drop Size For Breakup In Turbulent Flow", J. Chem. Eng. Japan, 10, #4, pp 325-330 (1977)

3. Brown, D.E. and Pitt, K., "Drop Breakup In a Stirred Liquid - Liquid Contactor", Proc. Chemeca 1970, Melbourne and Sidney, p 83-97 (1970)

4. Brown, D.E. and Pitt, K. "Effect of Impeller Geometry on Drop Break-Up in a Stirred Liquid - Liquid Contactor", Chem. Eng. Sci., 29, pp 345-348 (1974)

5. Calabrese, R.V., Chang, T.P.K., and Dang, P.T., "Drop Breakup in Turbulent Stirred-Tank Contactors, Part I: Effect of Dispersed Phase Viscosity" A.I.Ch.E.J., 32, #4, pp 657-666 (1986)

6. Calabrese, R.V., Wang, C.Y., and Bryner, N.P., "Drop Breakup in Turbulent Stirred-Tank Contactors, Part III: Correlations for Mean Size and Drop Size Distribution", A.I.Ch.E.J., 32, #4, pp 677-681 (1986)

7. Calderbank, P.H., "Physical Rate Processes in Industrial Fermentation Part I: The Interfacial Area in Gas - Liquid Contacting with Mechanical Agitation", Trans. Instn. Chem. Engrs., 36 , pp 443-459 (1958)

8. Calderbank, P.H., Evans, F., and Rennie, J., "The Mass-Transfer Efficiency of Distillation and Gas-Absorption Plate Columns. Part I: Techniques For Measuring Gas - Liquid Interfacial Areas and Foam Densities In Plate Columns", International Symposium on Distillation, Instn. Chem. Engrs. , pp 51-58 (1960)

9. Chen, H. T., "Drop Size Distribution in Agitated Tanks", Ph.D. Thesis, The University of Rochester (1966)

10. Collopy, I.J. and Mueller, J.H., "Role of Inorganic Surfactants in Liquid - Liquid Extraction Systems", NL CO-867 (1963)

11. Coulaloglou, C.A, "Dispersed Phase Interactions in an Agitated Flow Vessel", Ph.D. Thesis, Illinois Institute of Technology (1975)

12. Coulaloglou, C.A. and Tavlarides, L.L., "Drop Size Distributions and Coalescence Frequencies of Liquid - Liquid Dispersions in Flow Vessels", A.I.Ch.E.J., 22 , #2, pp 289-297 (1976)

13. Dippenar, A., "The Destabilization of Froth by Solids I , The Mechanism of Film Rupture", Inter.J.Miner.Proc. 9, pp 1-14 (1982)

14. Dippenar, A., "The Destabilization of Froth by Solids II, The Rate Determining Step", Inter. J. Miner. Proc., 9, pp 15-23 (1982)

15. Gelot, A., Friesen, W. and Hamza, H.A., "Emulsification of Oil and Water in the Presence of Finely Divided Solids and Surface Active Agents", Colloids and Surfaces, 12, pp 271-303 (1984)

16. Gnanasundaram, S., Degaleesan, T.E., and Laddha, G.S., "Prediction of Mean Drop Size in Batch Stirred Agitated Vessels", Can. J. Chem. Eng., 57, pp 141-144 (1979)

17. Hillestad, J.G., "Coalescence Rates in Mixing Tanks", Ph.D. Thesis, Purdue University, West Lafayette, Indiana (1965)

18. Hinze, J.O., "Fundamentals of the Hydrodynamic Mechanism of Splitting in Dispersion Processes", A.I.Ch.E.J., 1, #3, pp 289-295 (1955)

19. Hsia, M.A., and Tavlarides, L.L., "Simulation Analysis of Drop Breakage, Coalescence and Micromixing in Liquid-Liquid Stirred Tanks", Chem. Eng. Journal, 26, pp 189-199 (1983)

20. Kolmogoroff, A., "The Local Structure of Turbulence in Incompressible Viscous Fluid for Very Large Reynolds Number", C.R. Acad. Sci. USSR, 30, #4, pp 301-305 (1941)

21. Landau, J., Gomaa, H.G. and Al Taweel, A.M., "Measurement of Large Interfacial Areas by Light Attenuation", Trans. I. Chem. E., 55, pp 212-215 (1977)

22. Levine, S., and Sanford, E., "Clay-Bitumen Interactions and Their Relevance to Tar Sand Processing", Proc 30th, Can. Chem. Eng. Conf., Edmonton, pp 1112-1124 (1980)

23. Levine, S. and Sanford, E., "Stabilization of Emulsion Droplets by Fine Powders", C.J.Ch.E., 63, #2, pp 258-268 (1985)

24. Mizrahi, J. and Barnea, E., "The Effects of Solid Additives on the Formation and Separation of Emulsions", Brit. Chem. Eng.,15, #4, pp 497-503 (1970)

25. Mlynek, Y., and Resnick, W., "Drop Sizes in an Agitated Liquid - Liquid System", A.I.Ch.E.J., 18, #1, pp 122-127 (1972)

26. Nagata, S., "Mixing Principles and Applications", Halstead, New York (1975)

27. Oldshoue, J.Y., "Fluid Mixing Technology", McGraw-Hill, New York (1975)

28. Park, J.Y., "The Effect of Coalescence on Drop Size Distribution In An Agitated Liquid-Liquid Dispersion", M.S. Thesis, University of Idaho, 1973

29. Park, J.Y. and Blair, L.M., "The Effect of Coalescence on Drop Size Distribution in an Agitated Liquid - Liquid Dispersion", Chem. Eng. Sci., 30, pp 1057-1064 (1975)

30. Pickering, S.U., "Remarks On Direct Separation Of Emulsions By Filtration", J.Soc.Chem.Ind., 29, pp 129-[illegible]00 (1910)

31. Reith, T., "Interfacial Area and Scaling-Up of Gas - Liquid Contactors", Brit. Chem. Eng., 15 , #12 , pp 1559-1563 (1970)

32. Rodger, W.A., Trice, V.G. and Rushton, J.H., "Effect of Fluid Motion on Interfacial Area of Dispersions", Chem. Eng. Prog., 52, #12, pp 515-520 (1956)

33. Sanford, E.C., "Processibility of Athabasca Oil Sand", Can. J. Chem. Eng., 61, pp 554-567 (1983)

34. Sharma, M.M., and Danckwerts, P.V., "Chemical Methods of Measuring Interfacial Area and Mass Transfer Coefficients in Two Fluid Systems", Brit. Chem. Eng., 15, #4, pp 522-528 (1970)

35. Shaw, D.J., "Introduction to Colloid and Surface Chemistry", Butterworths, London (1975)

36. Shinnar, R. "On the Behavior of Liquid Dispersions in Mixing Vessels", J. Fluid Mech., 10, pp 259-275 (1961)

37. Shinnar, R. and Church, J.M., "Predicting Particle Size in Agitated Dispersions", Ind. Eng. Chem., 52, #3, pp 253-256 (1960)

38. Sprow, F.B., "Drop Size Distributions in Strongly Coalescing Agitated Liquid - Liquid Systems", A.I.Ch.E.J., 13, #5, pp 995-998 (1967)

39. Stokes, V.K. and Harvey, A.C., "Drop Size Distributions in Oil Water Mixtures", Control Technology R & D, Conference on Prevention and Control of Oil Spills, Am. Petrol. Inst., pp 457-65 (1973)

40. Tanaka, M., "Local Droplet Diameter Variation in a Stirred Tank", C.J.Ch.E., 63, pp 723-727 (1985)

41. Tavlarides, L.L. and Stamatoudis, M., "The Analysis of Interphase Reactions and Mass Transfer in Liquid - Liquid Dispersions", Advances In Chemical Engineering, V. 11 , pp 199-273 (1981)

42. Vermeulen, T., Williams, G.M. and Langlois, G.E., "Interfacial Area in Liquid - Liquid and Gas - Liquid Agitation", Chem. Eng. Prog., 51, #2, pp 85-94 (1955)

43. Wang, C.Y., and Calabrese, R.V., "Drop Breakup in Turbulent Stirred-Tank Contactors, Part II: Relative Influence of Viscosity and Interfacial Tension" A.I.Ch.E.J., 32, #4, pp 667-676 (1986)

44. Ward, J.P., and Knudsen, J.G., "Turbulent Flow of Unstable Liquid - Liquid Dispersions: Drop Sizes and Velocity Distributions", A.I.Ch.E.J., 13, #2, pp 356-365 (1967)

45. Watanabe, A., "Electrochemistry of Oil - Water Interfaces", Surface and Colloid Science, 13, Plenum Press, New York (1984)

46. Weinstein, B. and Treybal, R.E., "Liquid - Liquid Contacting in Unbaffled, Agitated Vessels", A.I.Ch.E.J., 19, #2, pp 304-312 (1973)

9. Appendix A : Material Properties

9.1 Properties of Kaolinite used in this work

Name: Kaolinite

Type: Hydrite UF

Supplier: Georgia Kaolin

Chemical Properties

Chemical Analysis (%):

Aluminum Oxide	38.38
Silicon Dioxide(combined)	45.30
Ignition Loss at 950C (combined water)	13.97
Iron Oxide	0.30
Titanium Dioxide	1.44
Calcium Oxide	0.05
Magnesium Oxide	0.25
Sodium Oxide	0.27
Potassium Oxide	0.04

Chemical Reactivity: Kaolinites are chemically inert and react with acids and bases only under extreme conditions. This kaolinite was water processed to reduce soluble salt content to extremely low levels.

Physical Properties

Kaolinite particles finer than 2 microns are thin, flat hexagonal plates.

Particles larger than 2 microns are stacks of these plates, and are bound together as a single particle.

Physical Constants:

Refractive Index: 1.56

Weight per solid gallon: 21.66 pounds

Moisture: 1% Maximum

Specific Gravity: 2.58

Physical Test Results:

Median Particle size: 0.2 microns

Maximum Particle size: 1.0 microns

Brightness (G.E. % of MgO): 82.0 - 85.0

pH of a 20% aqueous slurry: 4.2 - 5.2

325-Mesh Residue Max. (%): 0.03

Oil Adsorption (%): 47

Surface Area B.E.T. Nitrogen Adsorption (m^2/gm): 21

Typical Aqueous Viscosity (centipoise): 400
(58% solids, 0.5% sodium hexametaphosphate on weight of kaolinite. Measured at 10 rpm on a Brookfield Viscometer.)

9.2 Properties of Athabasca Fines

ORIGINAL WEIGHT(gms)

96.80

PHI	SIZE IN MICROMETRES	WEIGHT IN GRAMS	WEIGHT PERCENT	CUMULATIVE WEIGHT %	100 MINUS CUMWT %
-1.00	2000.00	0.47	0.49	0.49	99.51
-0.50	1414.21	0.17	0.18	0.67	99.33
0.00	1000.00	0.38	0.40	1.07	98.93
0.50	707.11	0.80	0.84	1.90	98.10
1.00	500.00	0.97	1.01	2.92	97.08
1.50	353.55	0.82	0.86	3.78	96.22
2.00	250.00	0.93	0.97	4.75	95.25
2.50	176.78	0.80	0.84	5.59	94.41
3.00	125.00	1.36	1.42	7.01	92.99
3.50	88.39	2.17	2.27	9.28	90.72
4.00	62.50	4.09	4.28	13.56	86.44
4.50	44.19	3.72	3.89	17.45	82.55
5.00	31.25	7.44	7.78	25.23	74.77
5.50	22.10	8.26	8.64	33.87	66.13
6.00	15.63	8.68	9.08	42.95	57.05
6.50	11.05	6.61	6.91	49.86	50.14
7.00	7.81	5.79	6.06	55.91	44.09
7.50	5.52	7.02	7.34	63.26	36.74
8.00	3.91	4.96	5.19	68.44	31.56
8.50	2.76	4.55	4.76	73.20	26.80
9.00	1.95	4.96	5.19	78.39	21.61
9.50	1.38	3.72	3.89	82.28	17.72
10.00	0.98	3.31	3.46	85.74	14.26
10.50	0.69	1.65	1.73	87.47	12.53
11.00	0.49	1.24	1.30	88.77	11.23
<11.00	<0.49	10.74	11.23	100.00	0.00

STATISTICS

WEIGHT RECOVERED (GRAMS)	SAND PERCENT	SILT PERCENT	CLAY PERCENT
95.61	13.56	64.35	22.10

CLAY CUTOFF=2.0 MICROMETRES

PHI MEDIAN	PHI MEAN	STANDARD DEVIATION
6.52	6.79	2.81

9.3 Properties of Cold Lake Bitumen used in this work

Oil Sands Physical Properties Data Base

Sample Identification

Sample I.D. No.: 82-01
Country: Canada
Stratographic Unit: Clearwater
Location: LSD SEC 4 TWP 65 RGE 3 W 4M
Classification: Bitumen
Field (pool): Cold Lake
Method of Production: Steam-stimulation
Source of Sample: ESSO Resources
Date Sampled: January/82
Other Sample Description: 82-01: sample had 8.62% water which was extracted

Simulated Distillation

Cut Temp. 0 deg. C	Vol. %	Sum Vol.%
197	IBP	0.50
225	1.75	2.25
250	1.56	3.81
275	1.85	5.66
300	3.48	9.14
325	3.61	12.75
343	2.60	15.35
375	4.74	20.09
400	4.05	24.14
425	4.00	28.14
450	4.01	32.15
475	4.00	36.15
500	4.01	40.16
524	3.72	43.88
residue	56.12	100.00

Hydrocarbon Characteristics

Gravity		9.999
Relative Density	15/15 deg.C	0.9994
Viscosity (cps.)	15 deg.C	410,233
	25 deg.C	86,943
	60 deg.C	2,751
	100 deg.C	220
Molecular Weight		552
Carbon Residue R	wt.%	12.0
Ash	wt.%	0.05
Carbon	wt.%	83.91
Hydrogen	wt.%	10.46
Nitrogen	wt.%	0.60
Sulphur	wt.%	4.50
Oxygen	wt.%	1.26
Vanadium	ppm wt.	155
Nickel	ppm wt.	67
Saturates	wt.%	17.34
Aromatics	wt.%	12.49
Polar I	wt.%	21.45
Polar II	wt.%	13.18
Polar III	wt.%	17.94
Asphaltenes	wt.%	16.61
Acid Number		0.88
Heat of Combustion	J/g	42.041

10. Appendix B : Experimental Data

Table 10.1 : Drop size parameters

Hydrocarbon and Clay Types	[NaCl] (M)	Impeller Speed (rpm)	Number of Drops	d_{max} (mm)	d_{32} (mm)	$\bar{d}$ (mm)	s	d_{32}/d_{max}
Hexane-5 vol% No Clay	0.001	325	335	0.4262	0.1747	0.1193	0.0566	0.4099
		349	258	0.2872	0.1233	0.1011	0.0327	0.4293
		372	196	0.2002	0.1243	0.1105	0.0276	0.6209
		385	210	0.2962	0.1560	0.1238	0.0445	0.5267
		389	211	0.2403	0.1400	0.0966	0.0477	0.5826
		410	252	0.1438	0.0899	0.0816	0.0186	0.6252
		436	406	0.2305	0.1307	0.1073	0.0362	0.5670
Hexane-5 vol% Kaolinite-0.04 wt%	0.001	325	201	0.5405	0.2734	0.1453	0.0937	0.5058
		329	228	0.5048	0.2316	0.1230	0.0764	0.4588
		347	220	0.4258	0.2289	0.1286	0.0777	0.5376
		352	226	0.4566	0.2402	0.1231	0.0828	0.5261
		383	224	0.3829	0.1864	0.1295	0.0607	0.4868
		384	246	0.5073	0.2456	0.1445	0.0807	0.4841
		385	162	0.6150	0.2897	0.1224	0.0944	0.4711
		420	224	0.3300	0.1926	0.1272	0.0658	0.5836
		423	251	0.5053	0.2801	0.1139	0.0929	0.5543
		440	208	0.3646	0.1739	0.1250	0.0559	0.4770
		450	224	0.5475	0.2689	0.1080	0.0882	0.4911
Hexane-5 vol% Athabasca fines-0.04 wt%	0.001	344	223	0.3077	0.1670	0.1117	0.0569	0.5427
		374	251	0.6396	0.2029	0.1088	0.0590	0.3172
		393	218	0.2773	0.1394	0.1026	0.0449	0.5027
		417	223	0.3224	0.1639	0.1007	0.0554	0.5084
		435	227	0.3081	0.1570	0.0983	0.0523	0.5096

Hydrocarbon and Clay Types	[NaCl] (M)	Impeller Speed (rpm)	Number of Drops	d_{max} (mm)	d_{32} (mm)	$\bar{d}$ (mm)	s	d_{32}/d_{max}
Hexane-5 vol% Kaolinite-0.04 wt% (added to oil phase)	0.001	327	246	0.8286	0.3048	0.1474	0.0864	0.3678
		365	247	0.5327	0.2151	0.1097	0.0662	0.4038
		369	202	0.3717	0.2058	0.1283	0.0680	0.5537
		410	243	0.3303	0.1950	0.1007	0.0675	0.5904
		434	199	0.3506	0.2107	0.1388	0.0719	0.6010
Hexane-5 vol% No Clay	0.02	346	219	0.3627	0.1884	0.1267	0.0643	0.5194
		371	235	0.3376	0.1958	0.1261	0.0717	0,5800
		372	224	0.3256	0.2034	0.1432	0.0666	0.6247
		377	214	0.3044	0.1675	0.1220	0.0530	0.5503
		407	225	0.3227	0.1777	0.1259	0.0572	0.5507
		435	234	0.2870	0.1573	0.1139	0.0502	0.5481
		457	262	0.3102	0.1690	0.1170	0.0555	0.5448
Hexane-5 vol% Kaolinite-0.04 wt%	0.02	350	228	0.3752	0.2054	0.1273	0.0716	0.5474
		374	238	0.4326	0.2305	0.1296	0.0787	0.5328
		377	231	0.4038	0.2043	0.1459	0.0643	0.5059
		400	234	0.3813	0.2022	0.1292	0.0687	0.5303
		420	211	0.3336	0.1974	0.1377	0.0651	0.5917

Hydrocarbon and Clay Types	[NaCl] (M)	Impeller Speed (rpm)	Number of Drops	d_{max} (mm)	d_{32} (mm)	$\bar{d}$ (mm)	s	d_{32}/d_{max}
Paraffin Oil-5 vol% No Clay	0.001	305	236	0.6322	0.2884	0.1047	0.1050	0.4562
		327.5	229	0.3340	0.2378	0.1022	0.0914	0.7120
		349	248	0.4000	0.2085	0.0935	0.0746	0.5213
		368	220	0.3528	0.2047	0.0880	0.0743	0.5802
		403	253	0.3125	0.2133	0.1586	0.0727	0.6826
Paraffin Oil-5 vol% Kaolinite-0.04 wt%	0.001	308	158	0.4690	0.3028	0.1940	0.1155	0.6456
		325	222	0.5149	0.2958	0.2038	0.1107	0.5745
		345	210	0.3628	0.2634	0.1888	0.0946	0.7260
		349	223	0.3436	0.2241	0.1371	0.0855	0.6522
		375	248	0.4154	0.2366	0.1772	0.0783	0.5696
		401	224	0.3496	0.2217	0.1520	0.0806	0.6342
Bitumen-5 vol% No Clay	0.001	319	218	0.8663	0.5025	0.1046	0.1385	0.5801
		360	235	0.8723	0.5028	0.1266	0.1443	0.5764
		389	227	0.7687	0.4148	0.1110	0.1203	0.5396
		410	208	0.8747	0.4794	0.1320	0.1560	0.5481
		450	274	0.8846	0.4268	0.1284	0.1371	0.4825

Hydrocarbon and Clay Types	[NaCl] (M)	Impeller Speed (rpm)	Number of Drops	d_{max} (mm)	d_{32} (mm)	$\bar{d}$ (mm)	s	d_{32}/d_{max}
Bitumen-5 vol% Kaolinite-0.04 wt%	0.001	304	222	0.8524	0.5743	0.0944	0.1341	0.6737
		356	213	0.7962	0.4420	0.1179	0.1350	0.5551
		380	210	0.6967	0.3325	0.1026	0.1025	0.4772
		381	206	0.7727	0.4544	0.1315	0.1481	0.5881
		414	237	0.9265	0.4796	0.1039	0.1209	0.5176
		437	206	0.7738	0.4462	0.1140	0.1282	0.5766

11. Appendix C : Experimental Drop Size Distributions

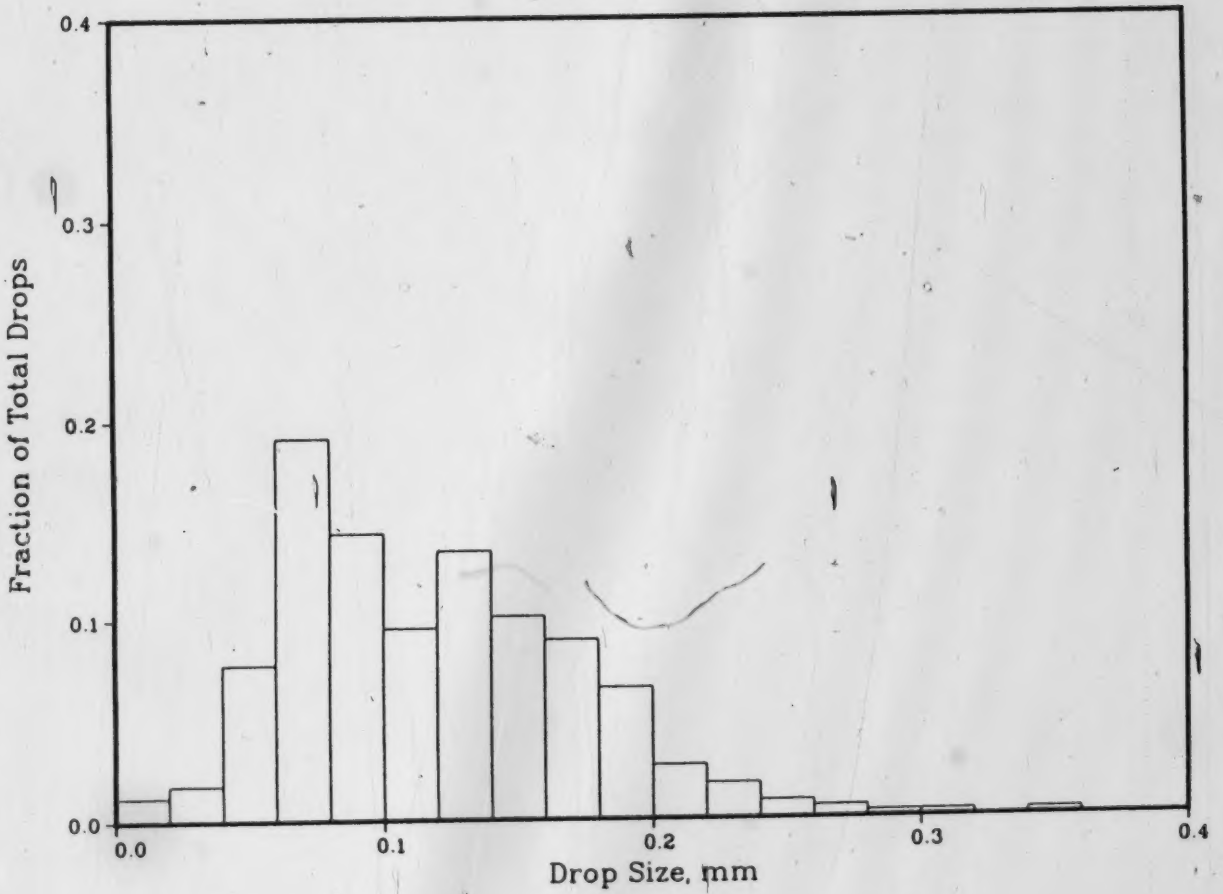

Figure 11.1.1 : Drop size distribution for a 5% hexane, 95% water dispersion, 0.001M NaCl, 325 rpm

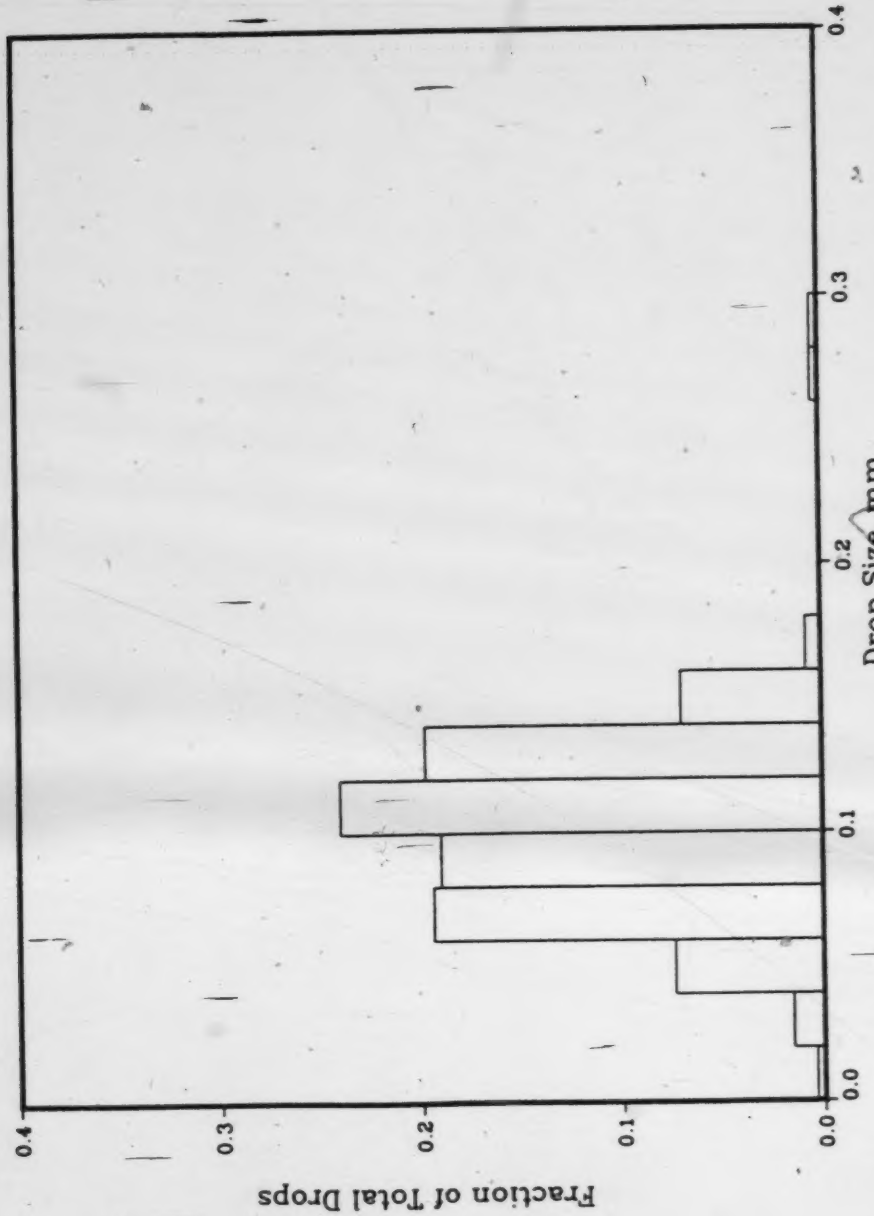

Figure 11.1.2 : Drop size distribution for a 5% hexane, 95% water dispersion, 0.001M NaCl, 349 rpm

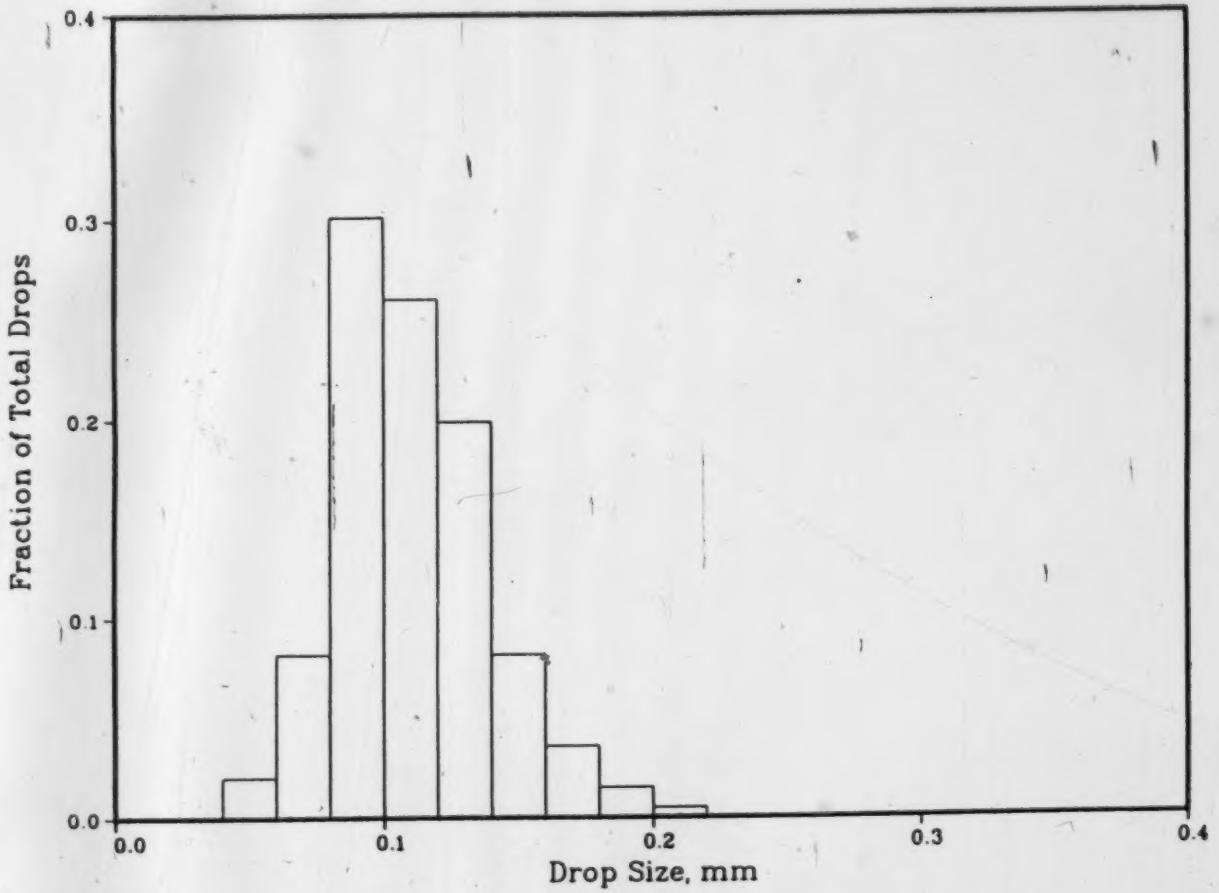

Figure 11.1.3 : Drop size distribution for a 5% hexane, 95% water dispersion, 0.001M NaCl, 372 rpm

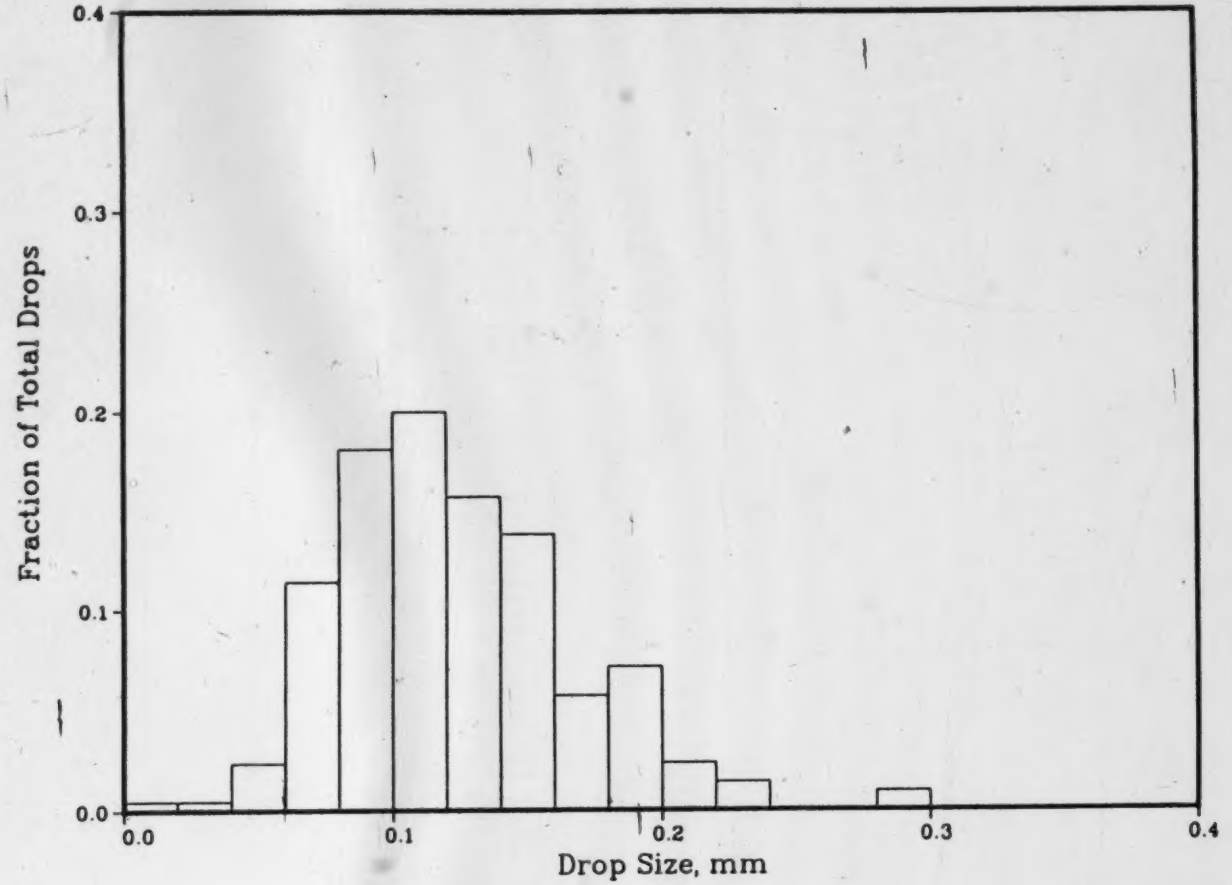

Figure 11.1.4 : Drop size distribution for a 5% hexane, 95% water dispersion, 0.001M NaCl, 385 rpm

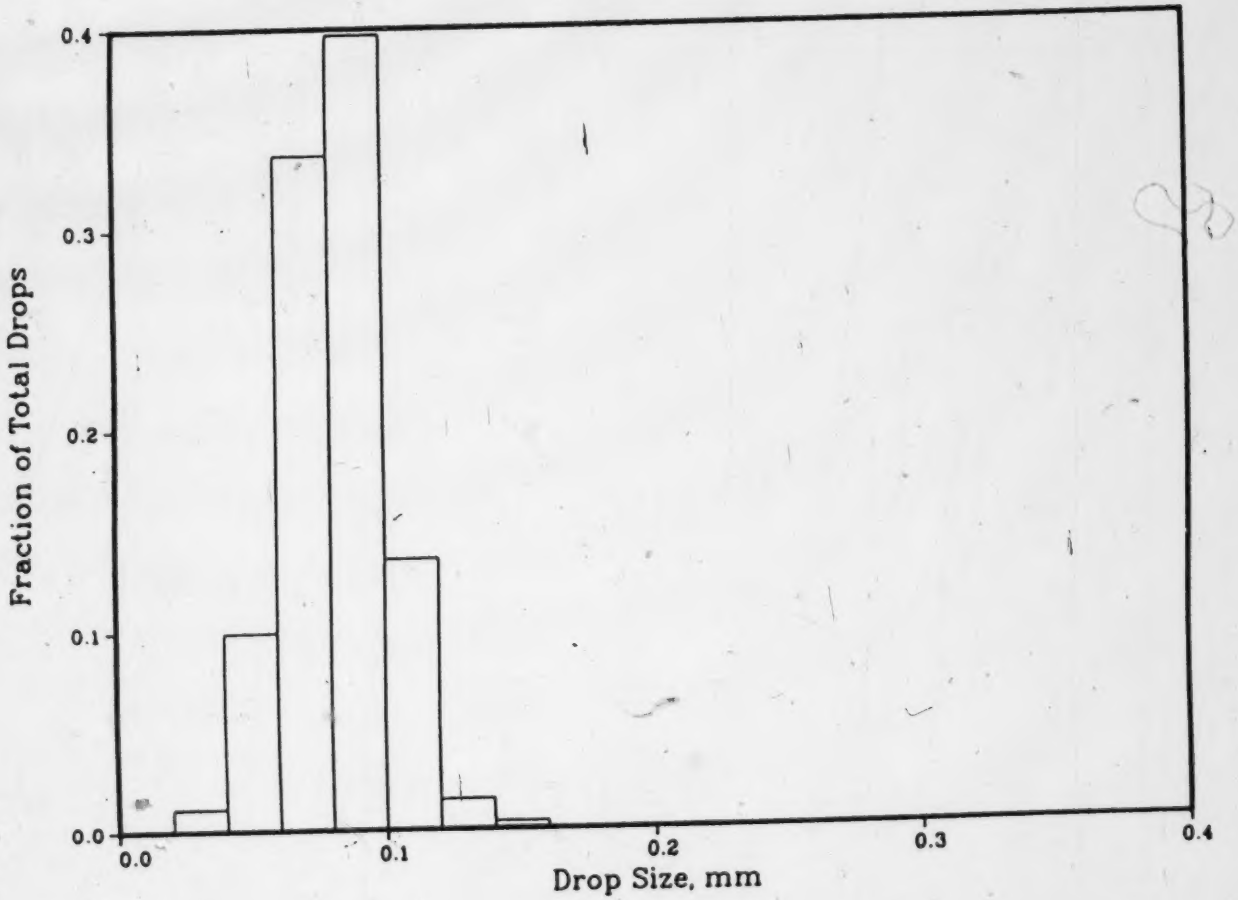

Figure 11.1.5 : Drop size distribution for a 5% hexane, 95% water dispersion, 0.001M NaCl, 410 rpm

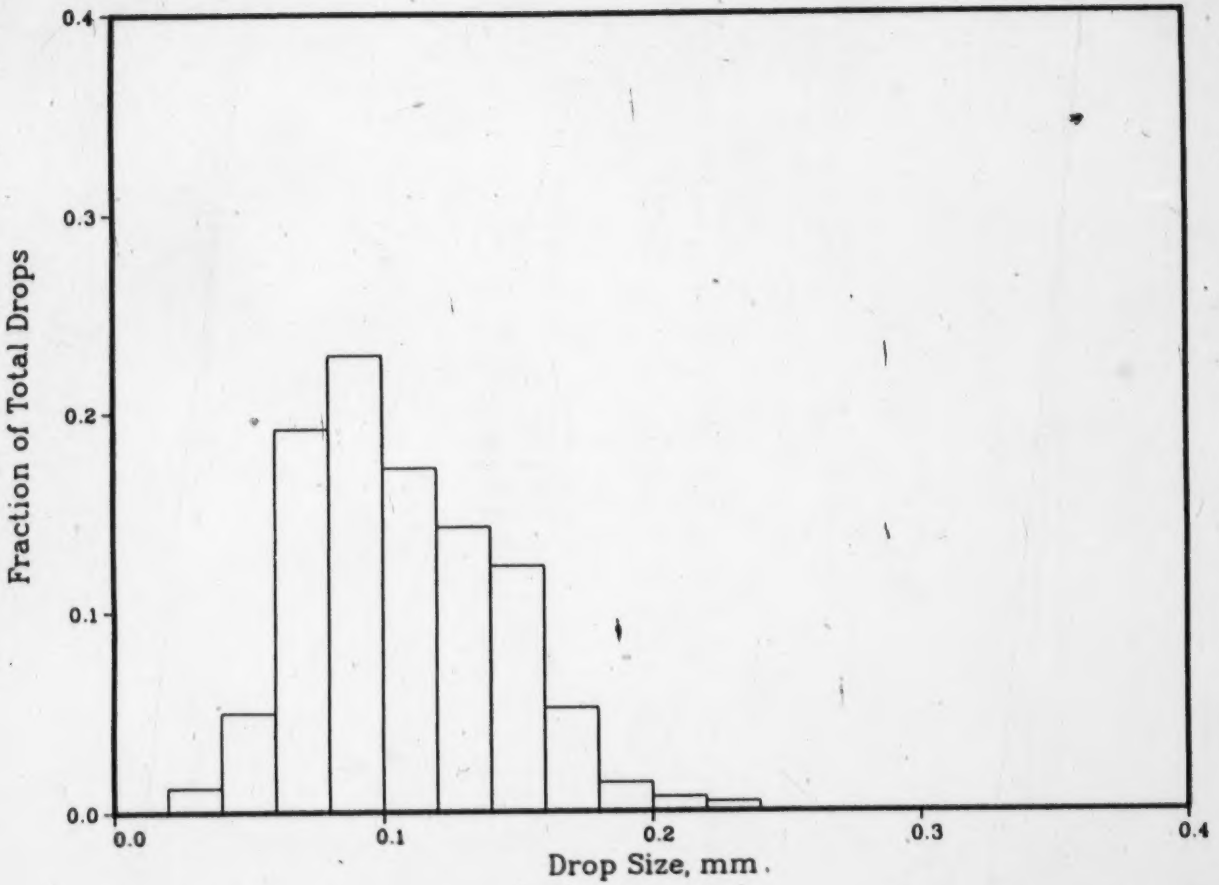

Figure 11.1.6 : Drop size distribution for a 5% hexane, 95% water dispersion, 0.001M NaCl, 436 rpm

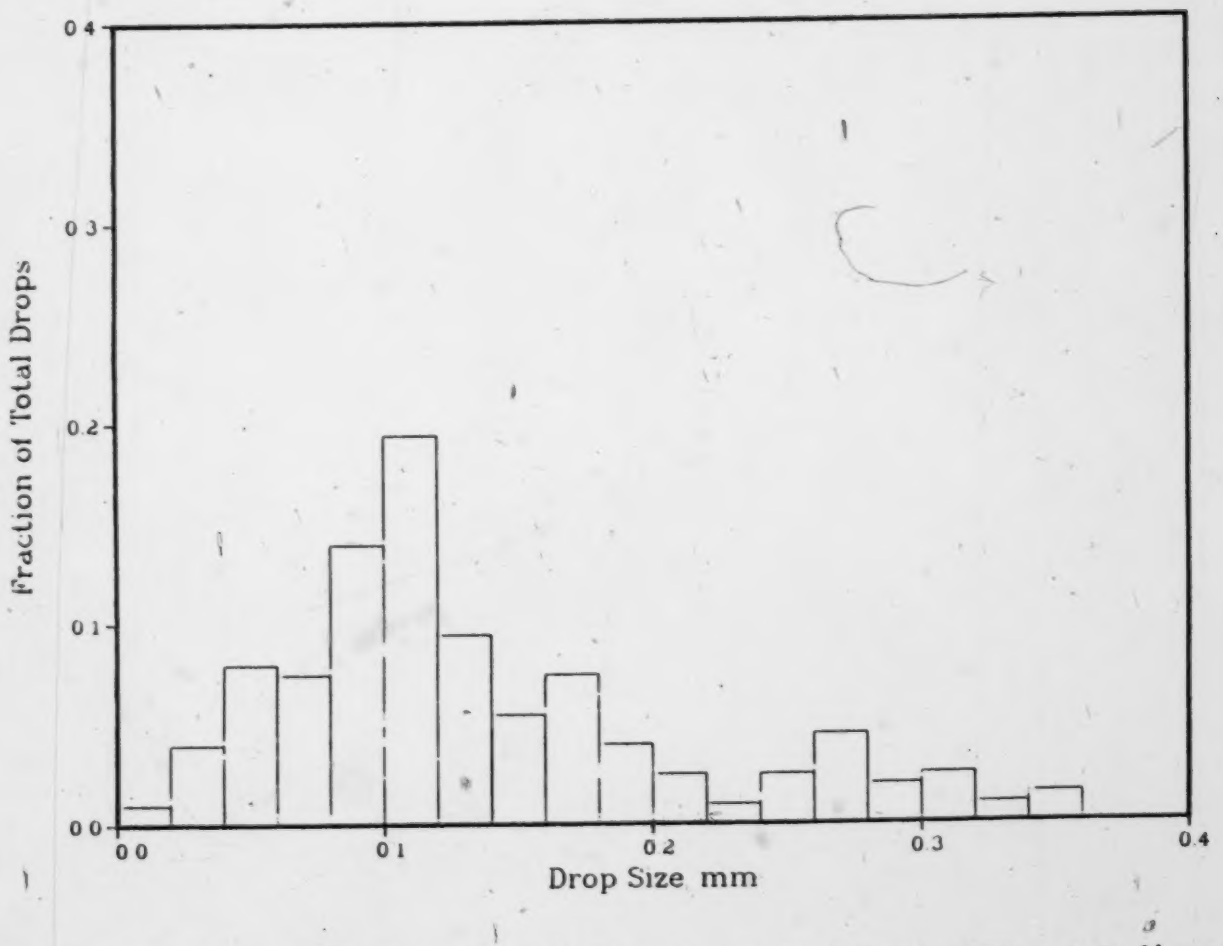

Figure 11.1.7 : Drop size distribution for a 5% hexane, 95% water dispersion, 0.04 wt% kaolinite, 0.001M NaCl, 325 rpm

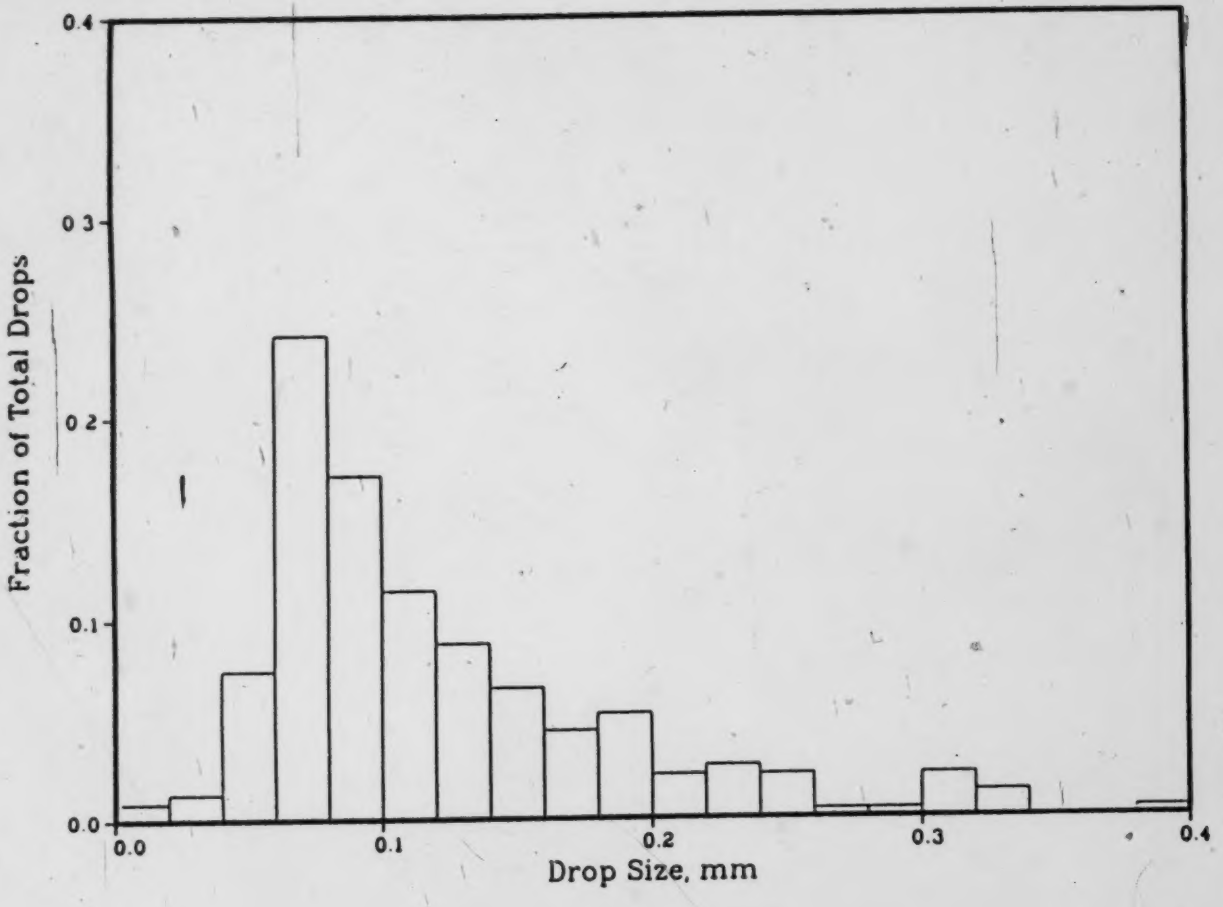

Figure 11.1.8 : Drop size distribution for a 5% hexane, 95% water dispersion, 0.04 wt% kaolinite, 0.001M NaCl, 329 rpm

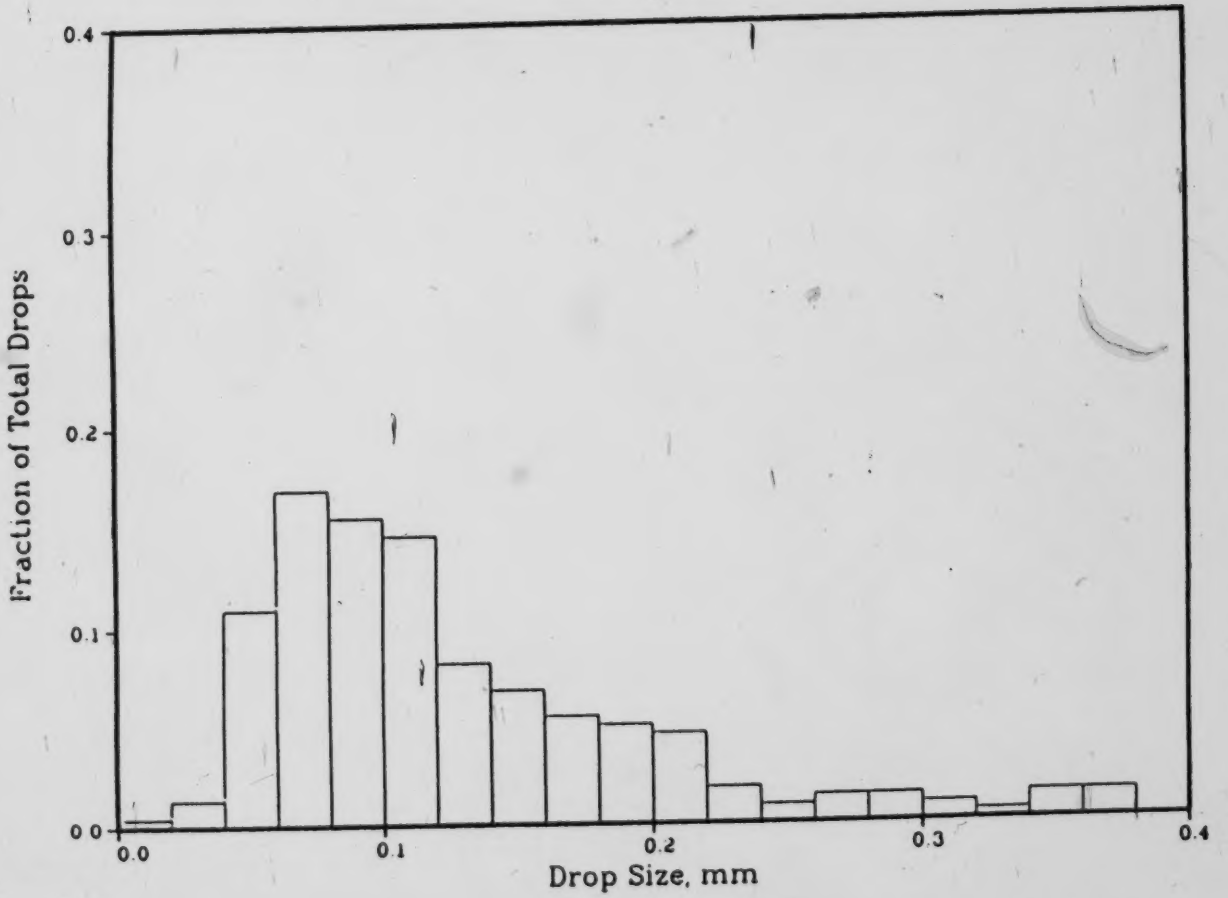

Figure 11.1.9 : Drop size distribution for a 5% hexane, 95% water dispersion, 0.04 wt% kaolinite, 0.001M NaCl, 347 rpm

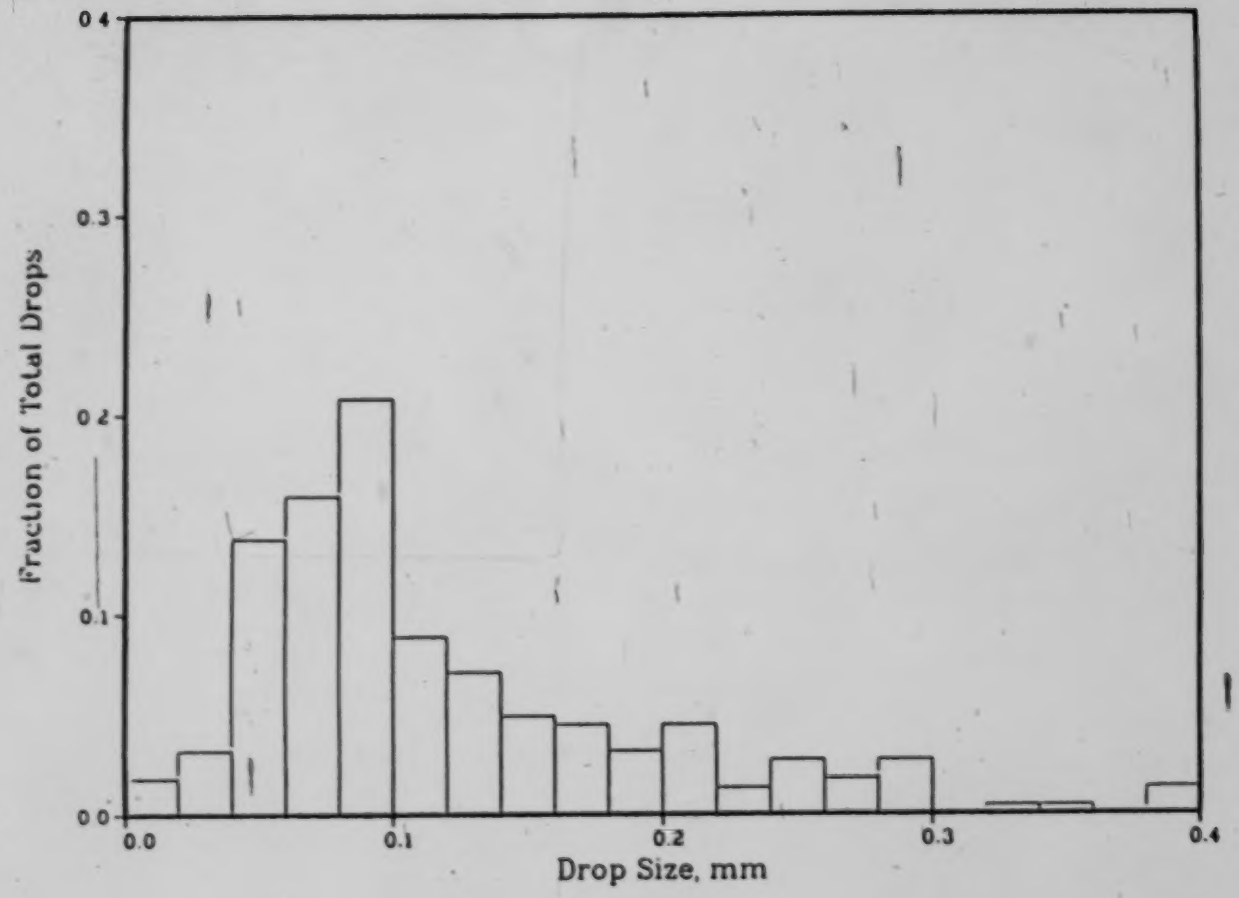

Figure 11.1.10: Drop size distribution for a 5% hexane, 95% water dispersion, 0.04 wt% kaolinite, 0.001M NaCl, 352 rpm

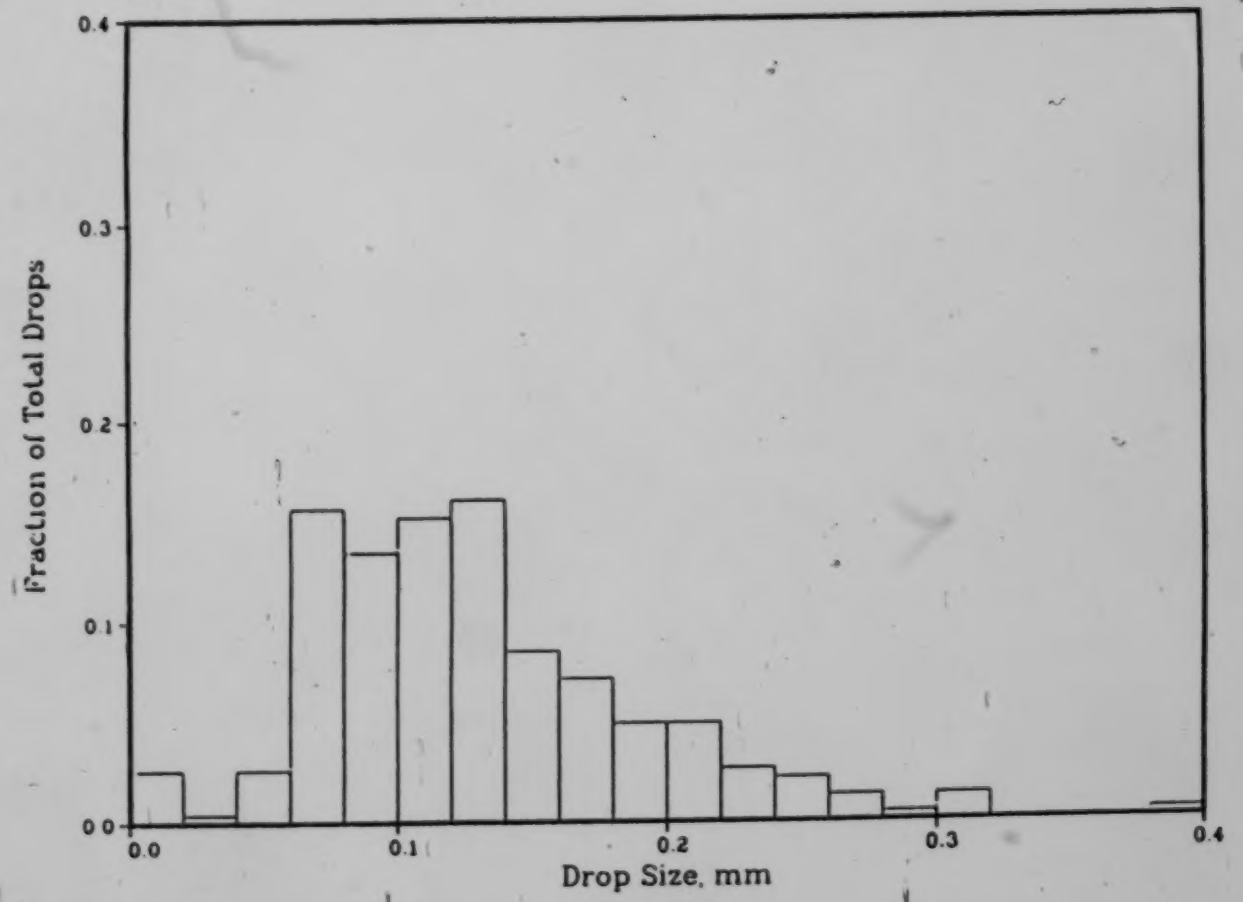

Figure 11.1.11: Drop size distribution for a 5% hexane, 95% water dispersion, 0.04 wt% kaolinite, 0.001M NaCl, 383 rpm

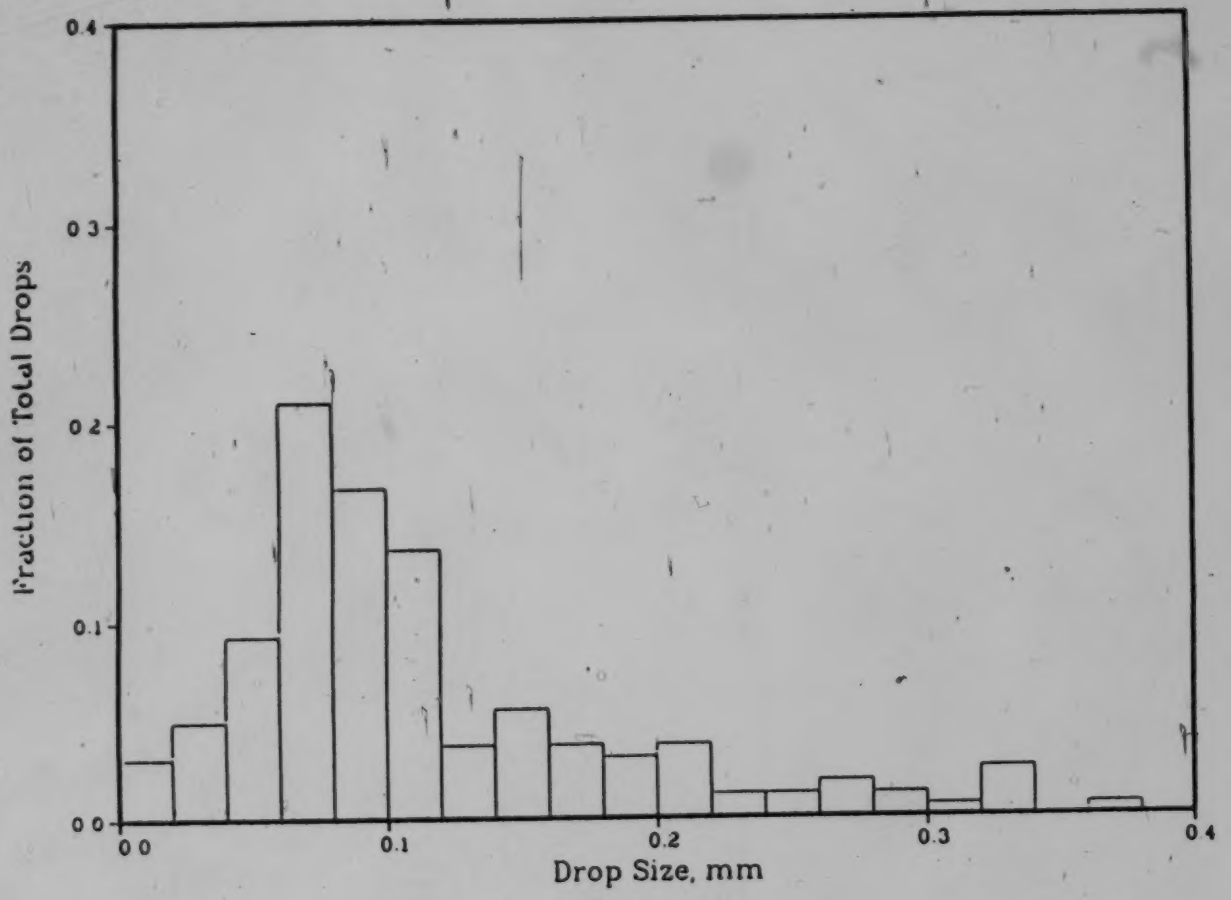

Figure 11.1.12: Drop size distribution for a 5% hexane, 95% water dispersion, 0.04 wt% kaolinite, 0.001M NaCl, 385 rpm

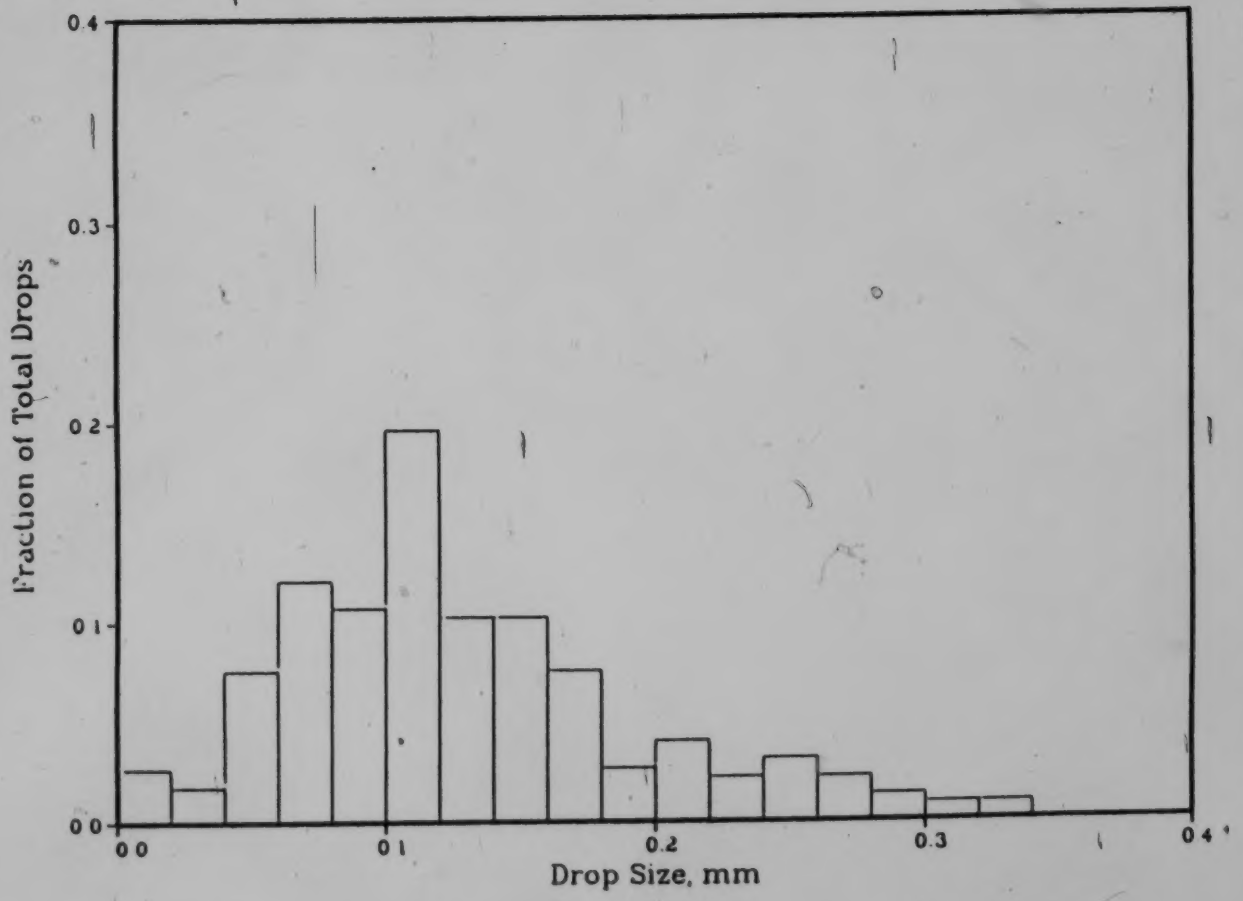

Figure 11.1.13: Drop size distribution for a 5% hexane, 95% water dispersion, 0.04 wt% kaolinite, 0.001M NaCl, 420 rpm

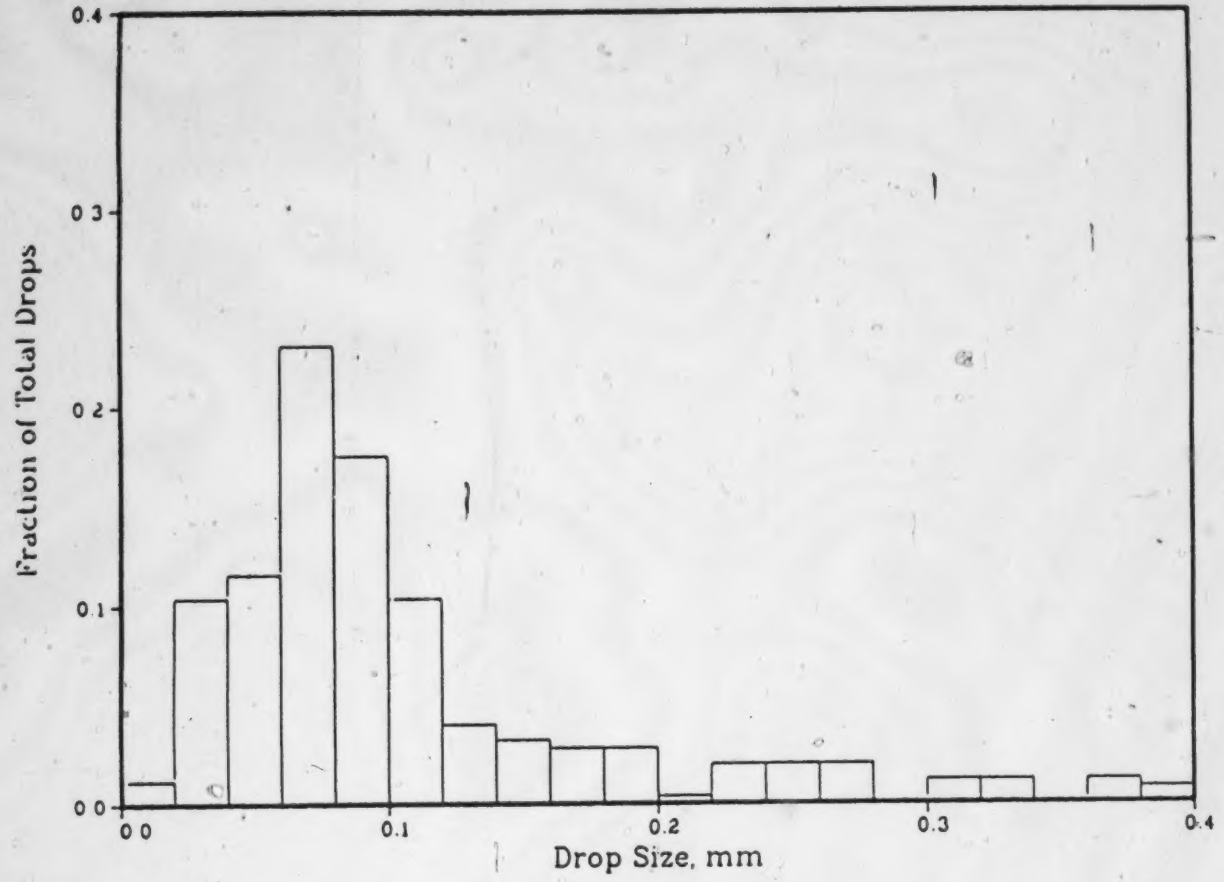

Figure 11.1.14: Drop size distribution for a 5% hexane, 95% water dispersion, 0.04 wt% kaolinite, 0.001M NaCl, 423 rpm

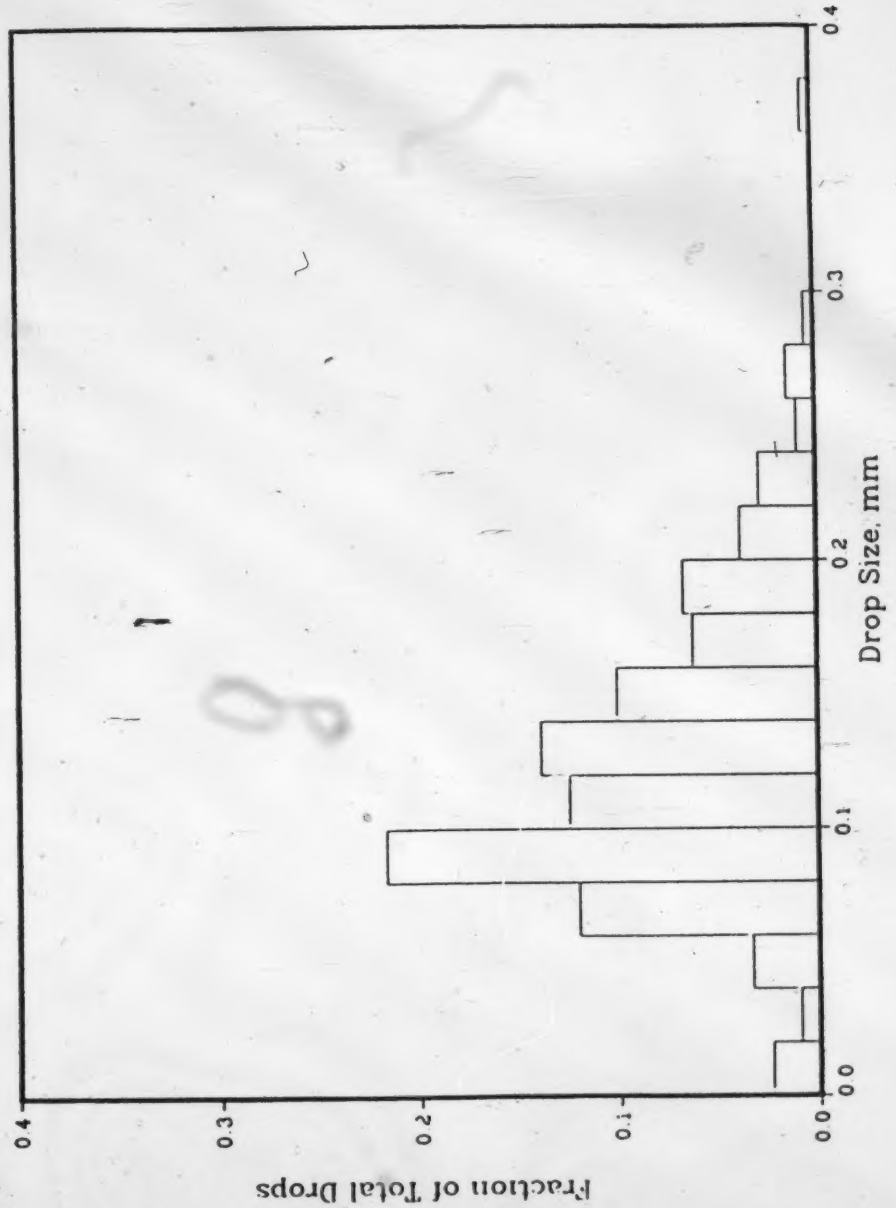

Figure 11.1.15: Drop size distribution for a 5% hexane, 95% water dispersion, 0.04 wt% kaolinite, 0.001M NaCl, 440 rpm

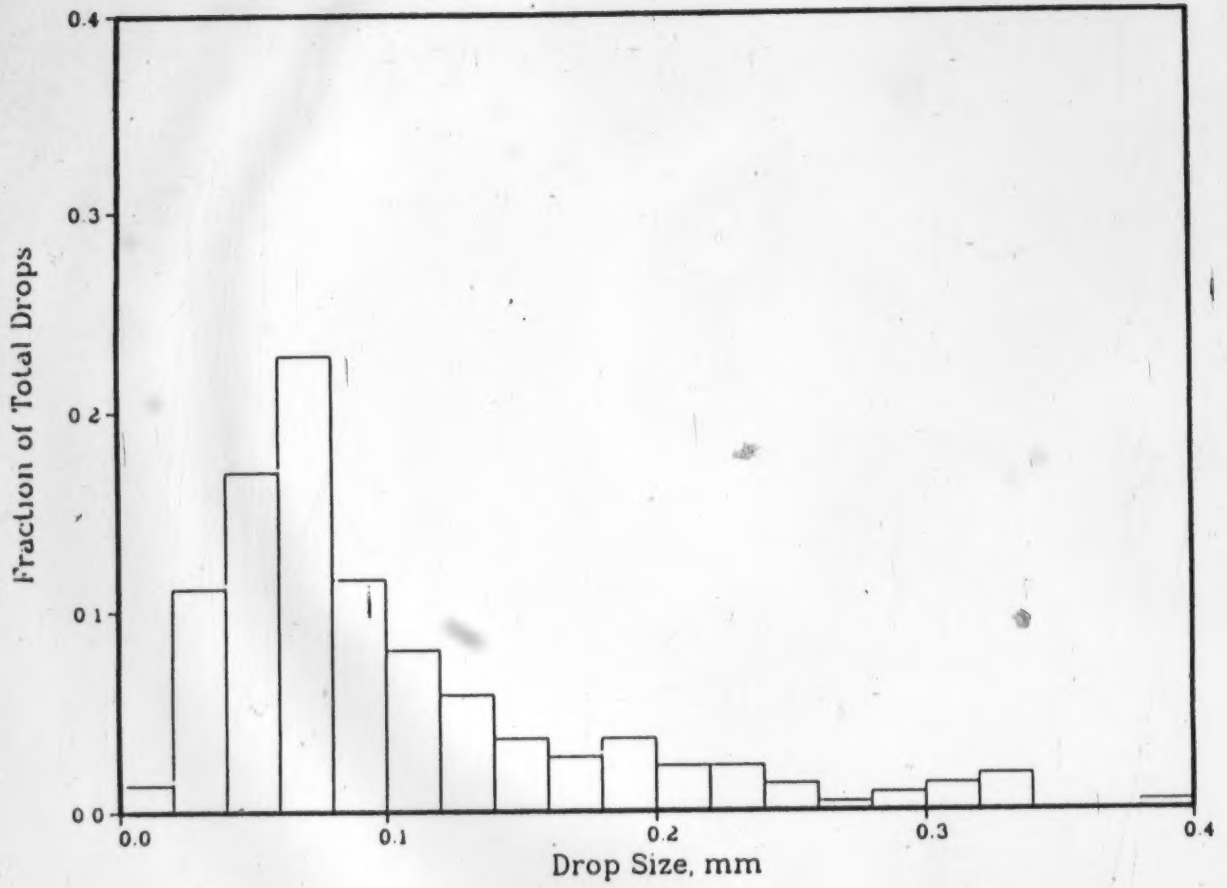

Figure 11.1.16: Drop size distribution for a 5% hexane, 95% water dispersion, 0.04 wt% kaolinite, 0.001M NaCl, 450 rpm

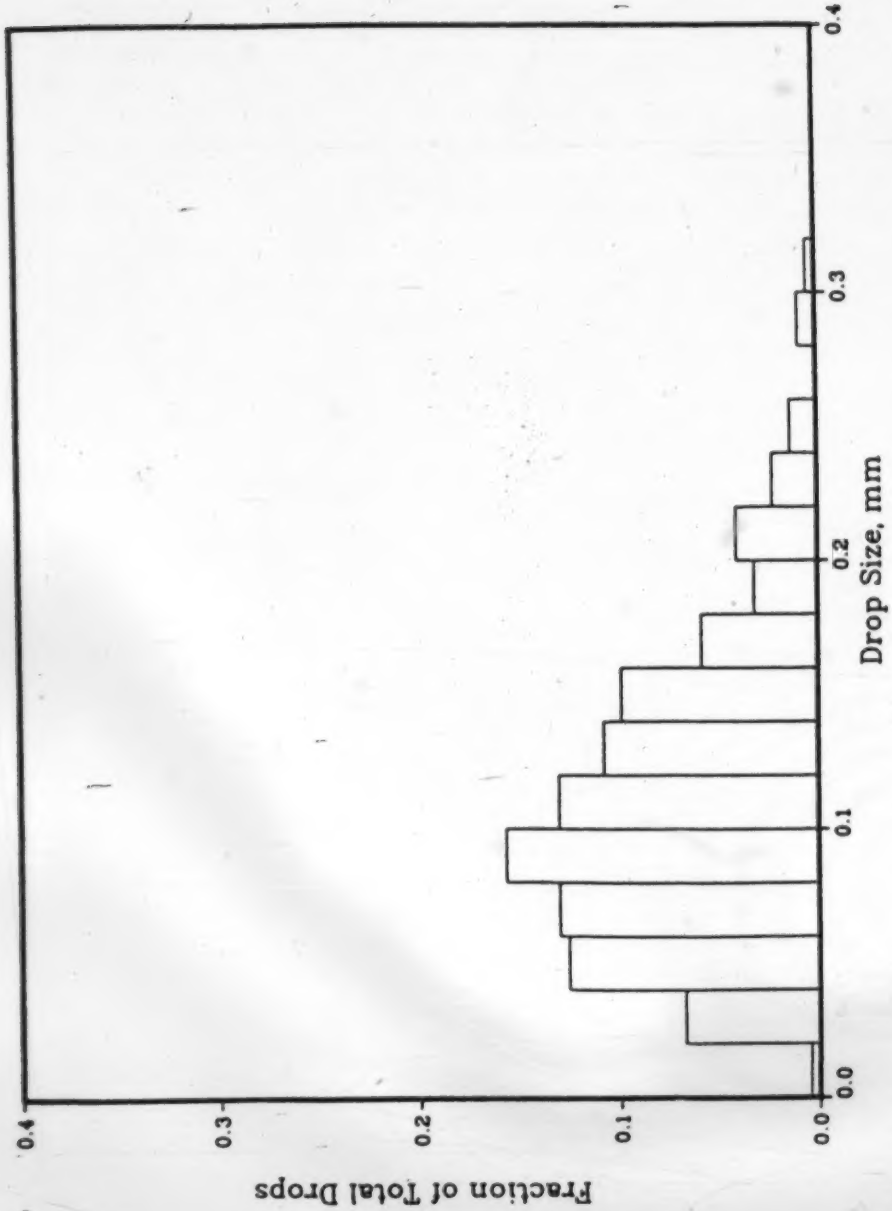

Figure 11.1.17: Drop size distribution for a 5% hexane, 95% water dispersion, 0.04 wt% Athabasca fines, 0.001M NaCl, 344 rpm

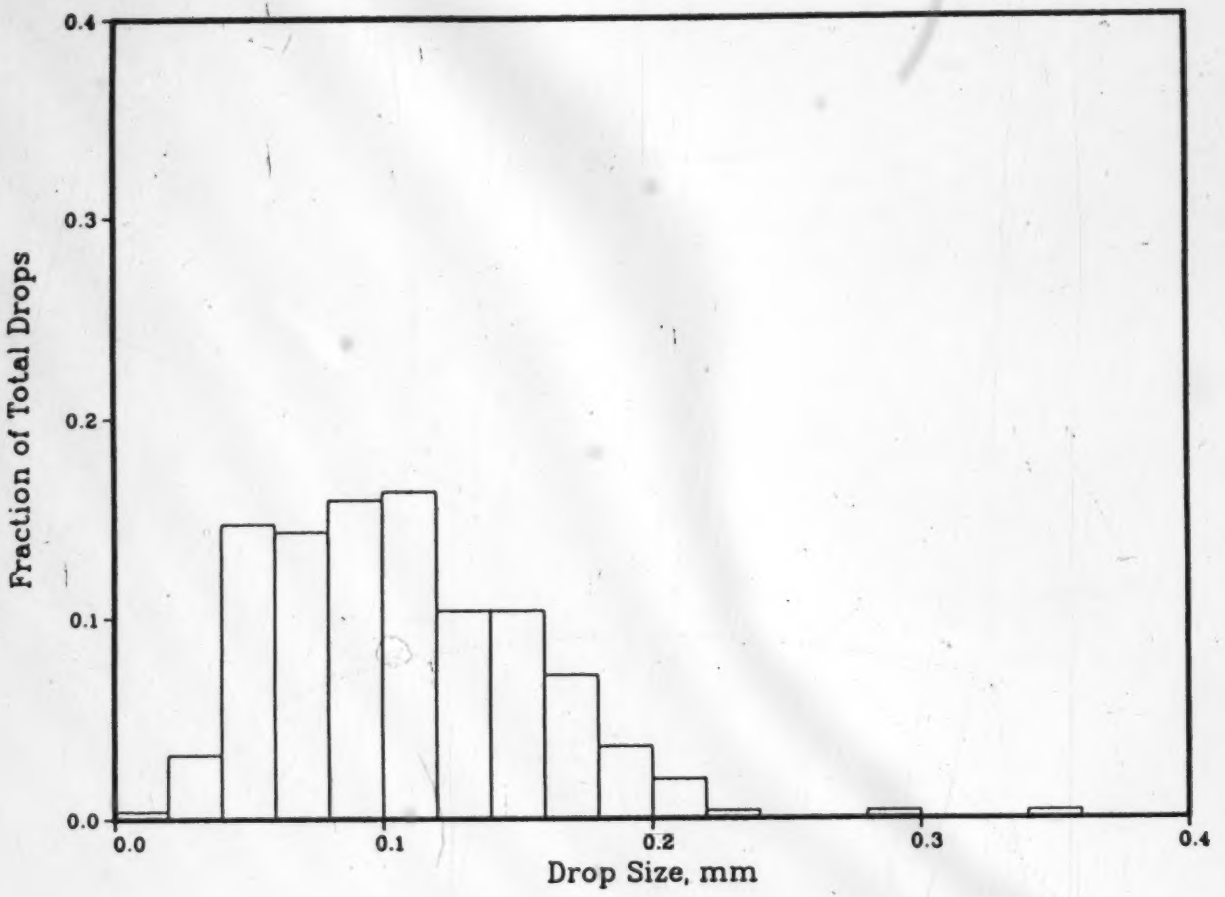

Figure 11.1.18: Drop size distribution for a 5% hexane, 95% water dispersion, 0.04 wt% Athabasca fines, 0.001M NaCl, 374 rpm

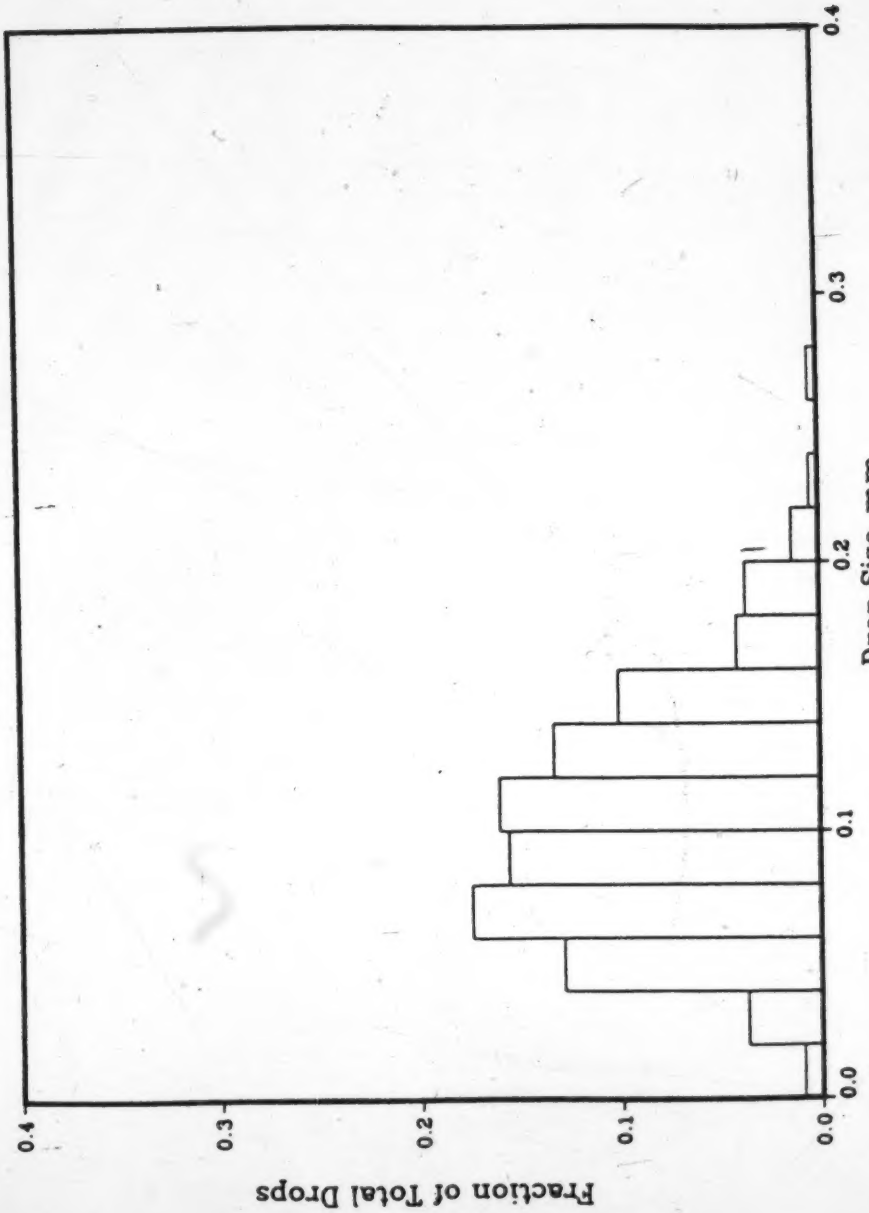

Figure 11.1.19: Drop size distribution for a 5% hexane, 95% water dispersion, 0.04 wt% Athabasca fines, 0.001M NaCl, 393 rpm

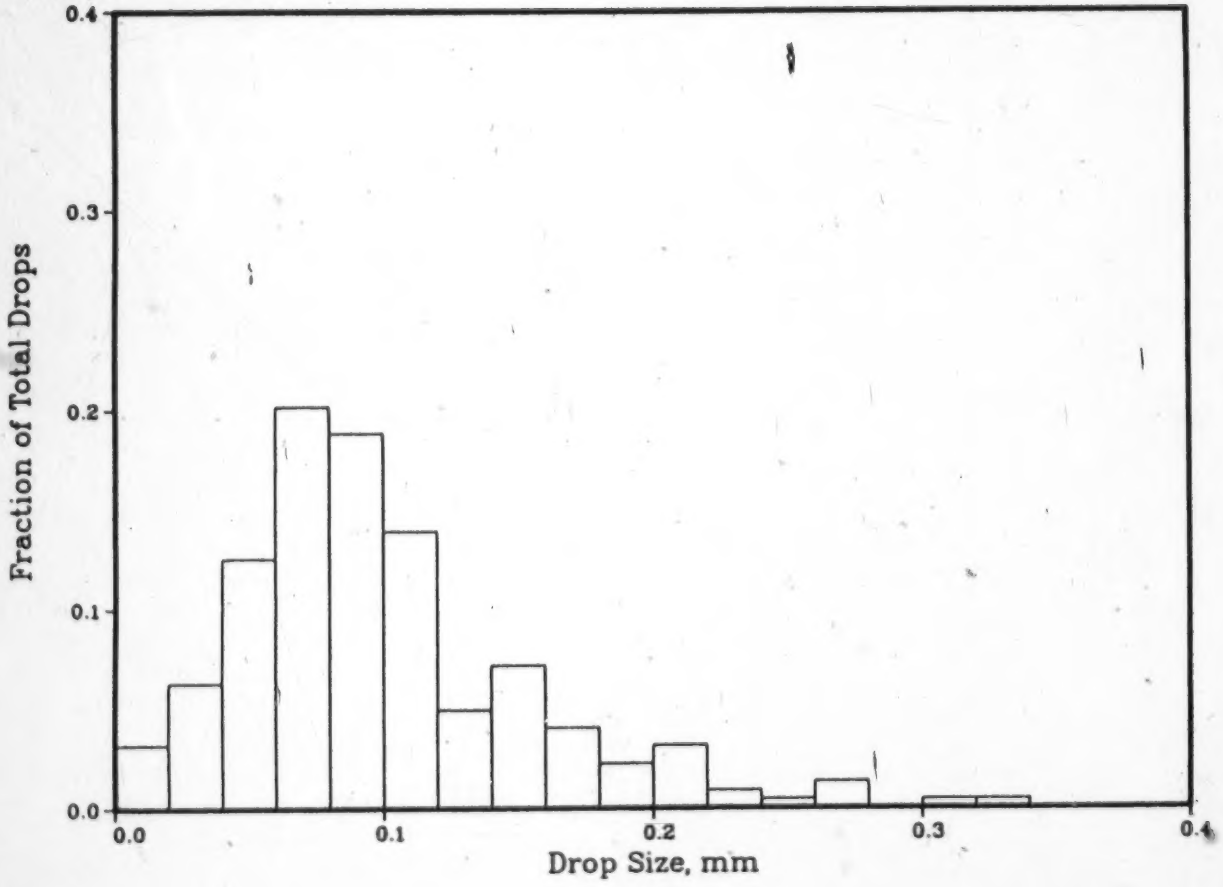

Figure 11.1.20: Drop size distribution for a 5% hexane, 95% water dispersion, 0.04 wt% Athabasca fines, 0.001M NaCl, 417 rpm

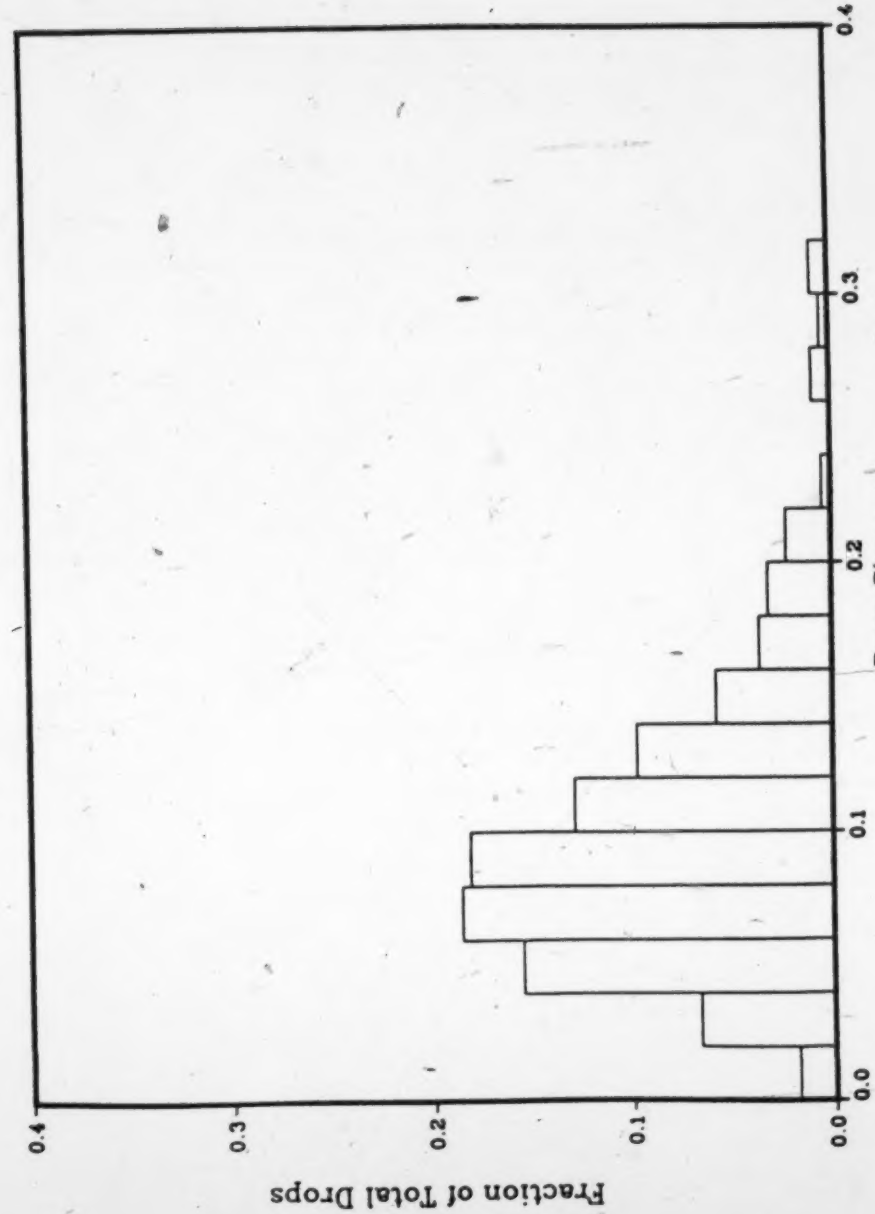

Figure 11.1.21: Drop size distribution for a 5% hexane, 95% water dispersion, 0.04 wt% Athabasca fines, 0.001M NaCl, 435 rpm

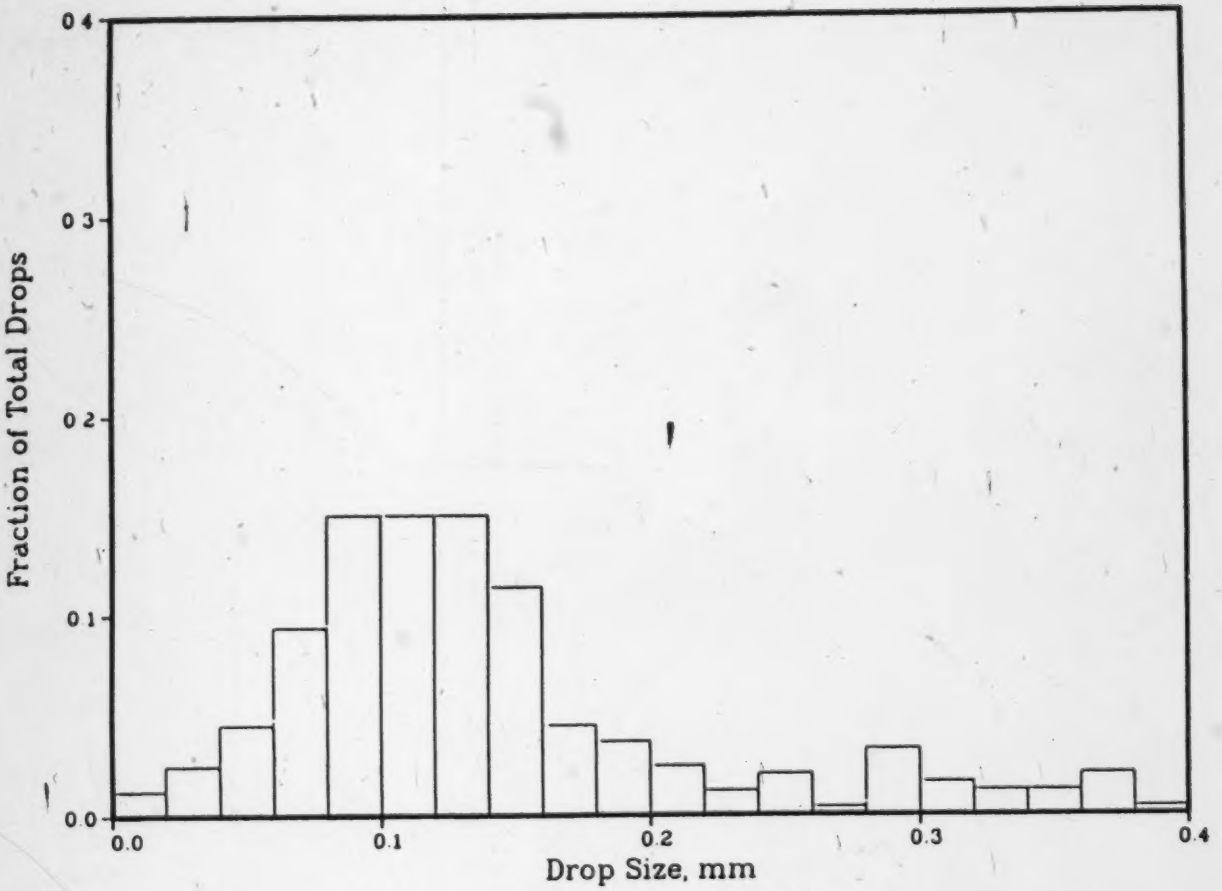

Figure 11.1.22: Drop size distribution for a 5% hexane, 95% water dispersion, 0.04 wt% kaolinite (added to the oil phase), 0.001M NaCl, 327 rpm

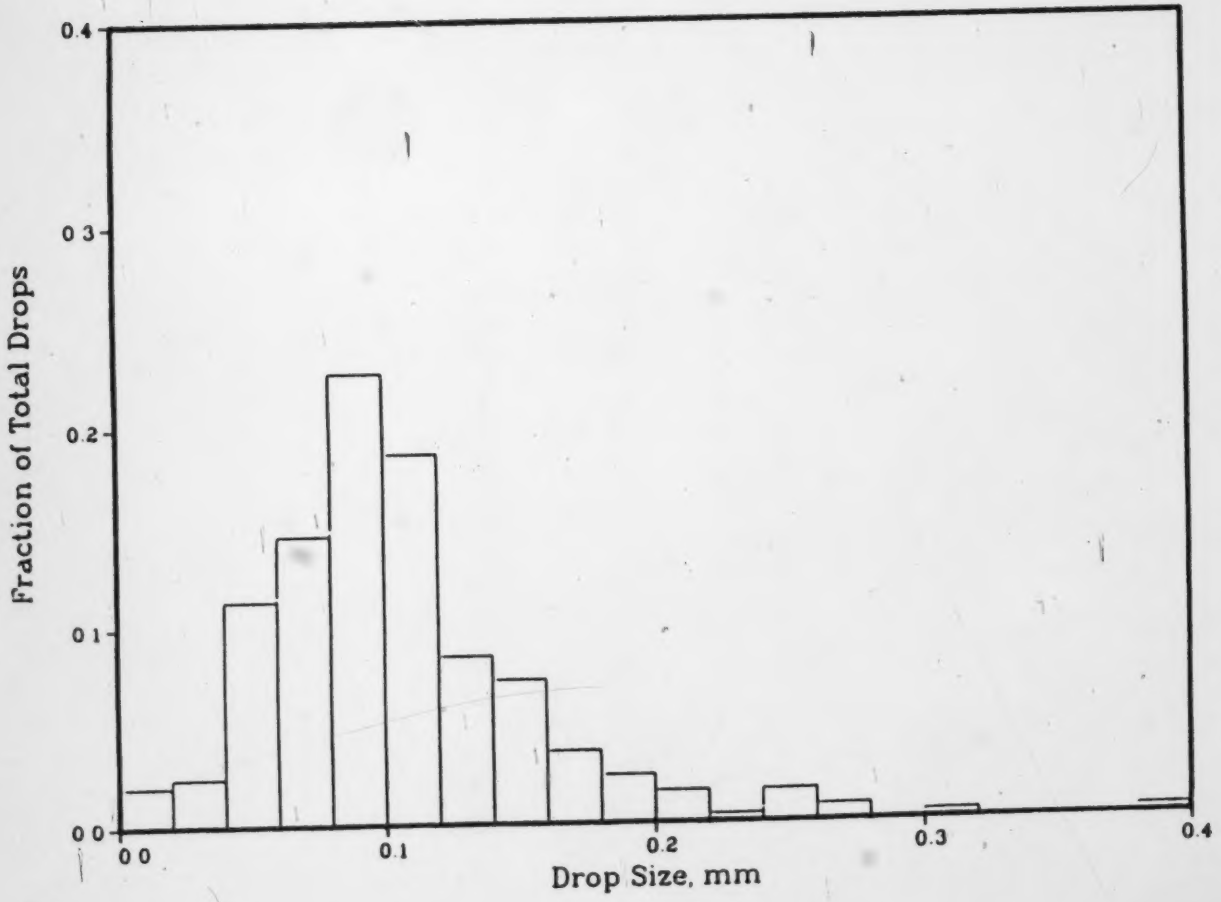

Figure 11.1.23: Drop size distribution for a 5% hexane, 95% water dispersion, 0.04 wt% kaolinite (added to the oil phase), 0.001M NaCl, 365 rpm

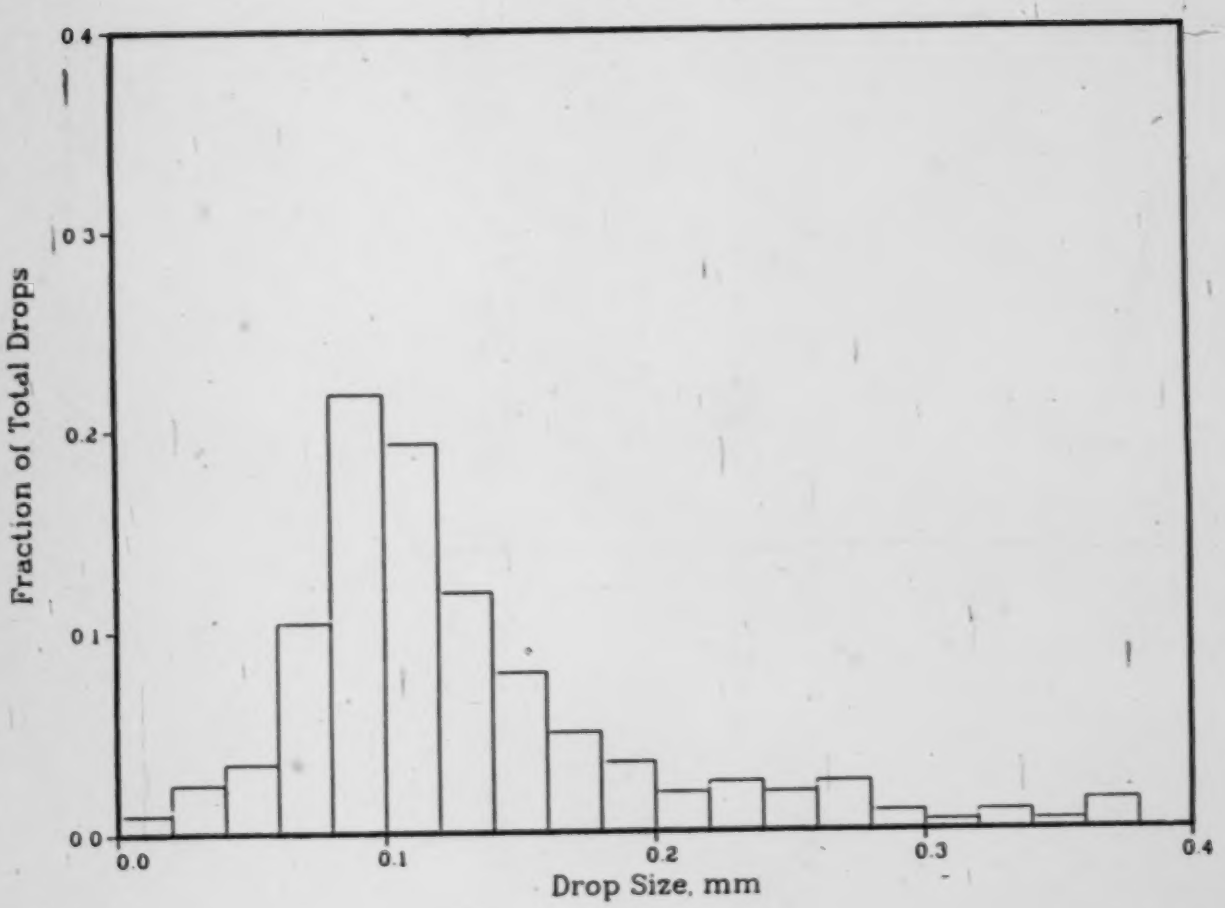

Figure 11.1.24: Drop size distribution for a 5% hexane, 95% water dispersion, 0.04 wt% kaolinite (added to the oil phase), 0.001M NaCl, 369 rpm

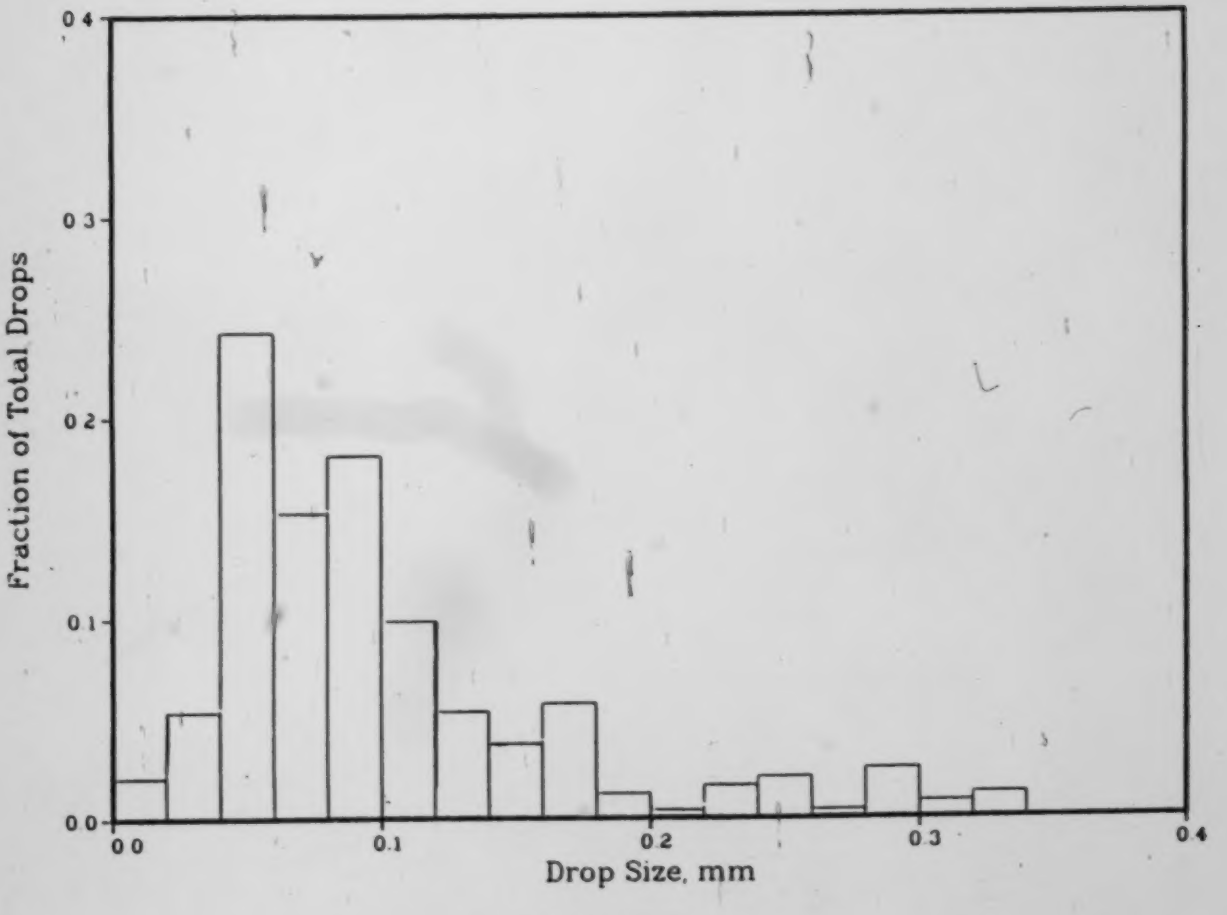

Figure 11.1.25: Drop size distribution for a 5% hexane, 95% water dispersion, 0.04 wt% kaolinite (added to the oil phase), 0.001M NaCl, 410 rpm

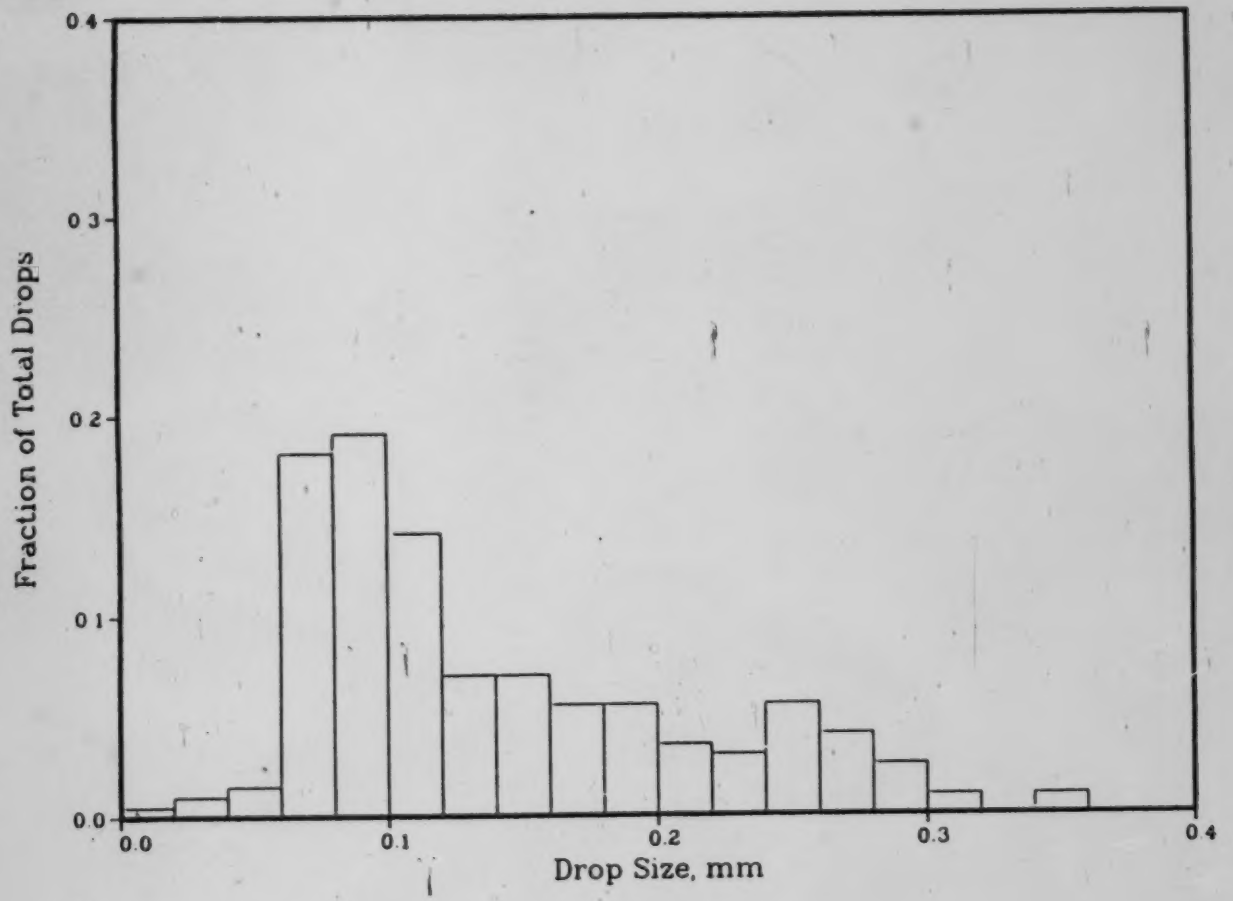

Figure 11.1.26: Drop size distribution for a 5% hexane, 95% water dispersion, 0.04 wt% kaolinite (added to the oil phase), 0.001M NaCl, 434 rpm

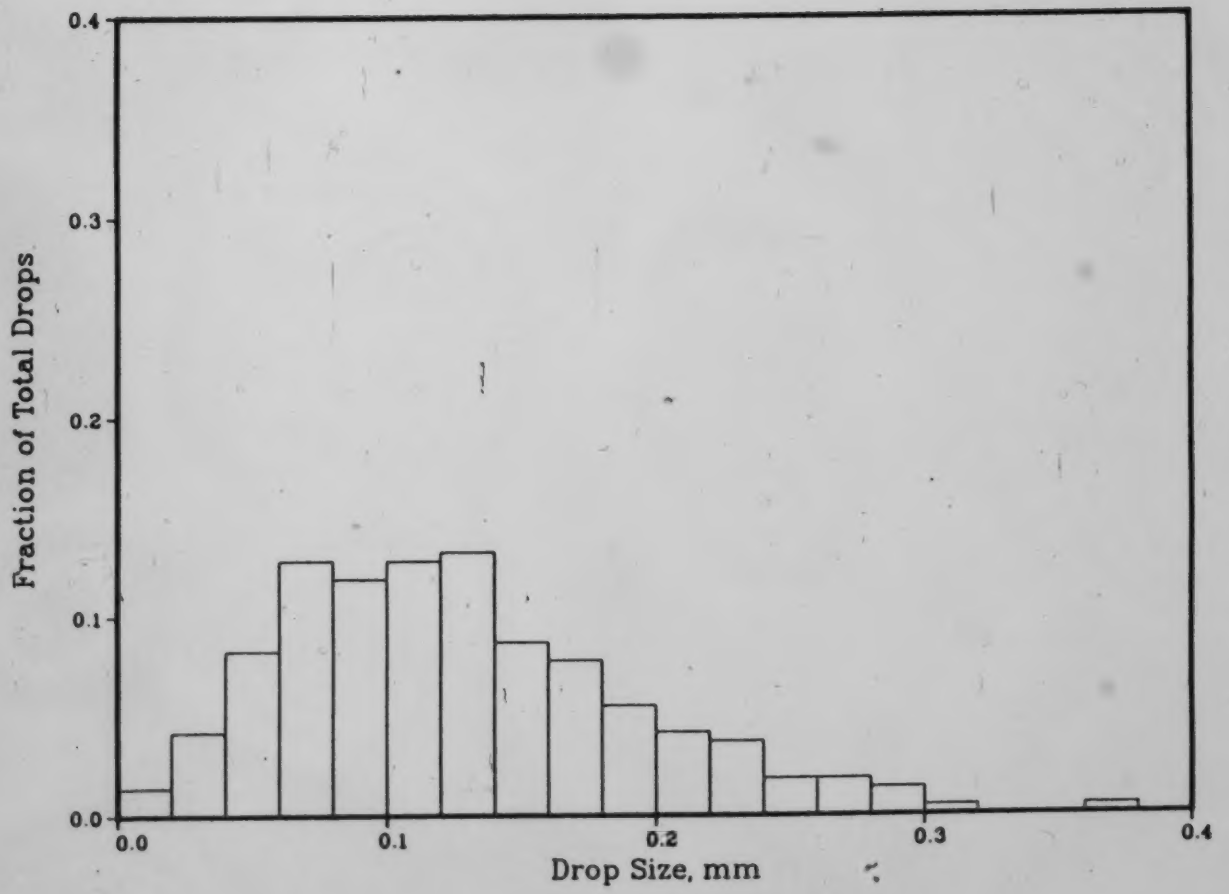

Figure 11.1.27: Drop size distribution for a 5% hexane, 95% water dispersion, 0.02M NaCl, 346 rpm

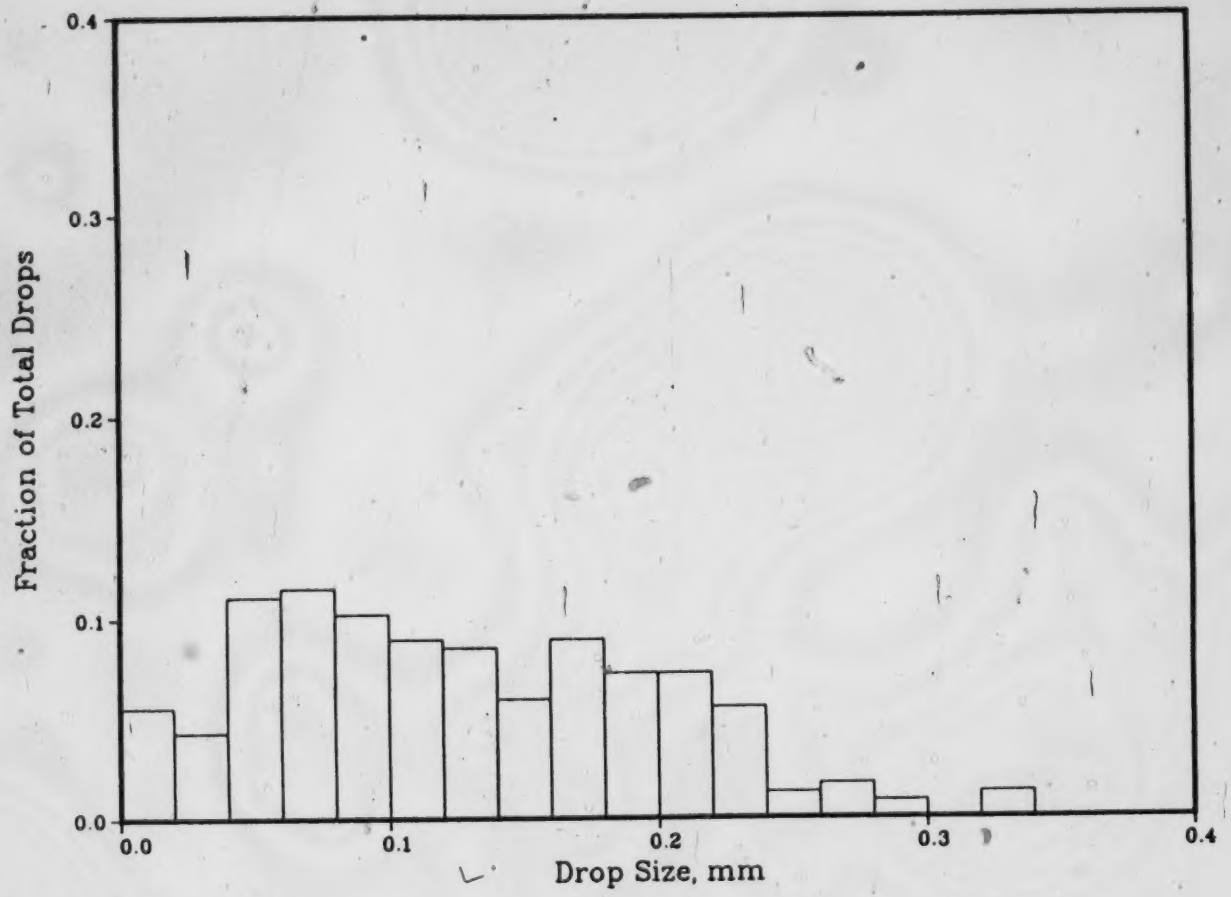

Figure 11.1.28: Drop size distribution for a 5% hexane, 95% water dispersion, 0.02M NaCl, 371 rpm

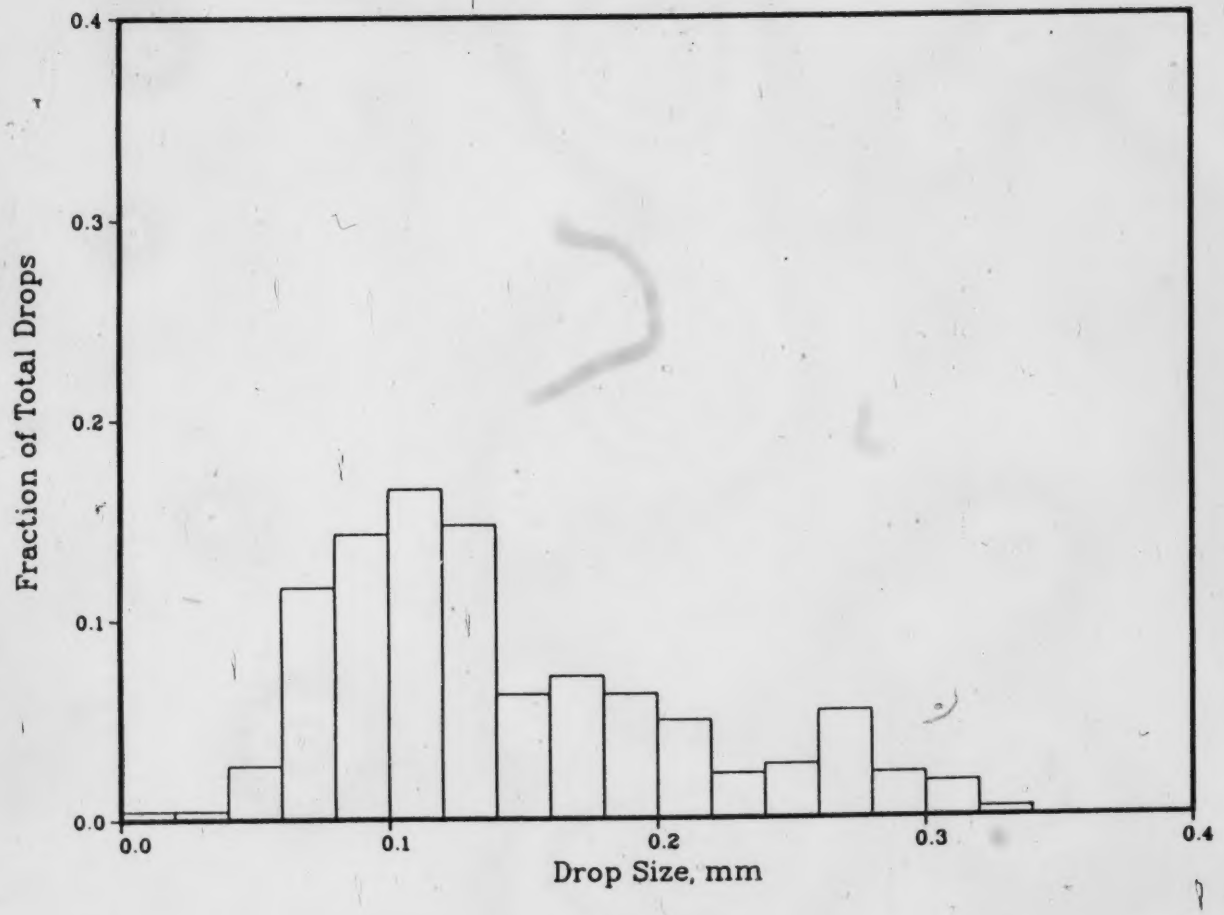

Figure 11.1.29: Drop size distribution for a 5% hexane, 95% water dispersion, 0.02M NaCl, 372 rpm

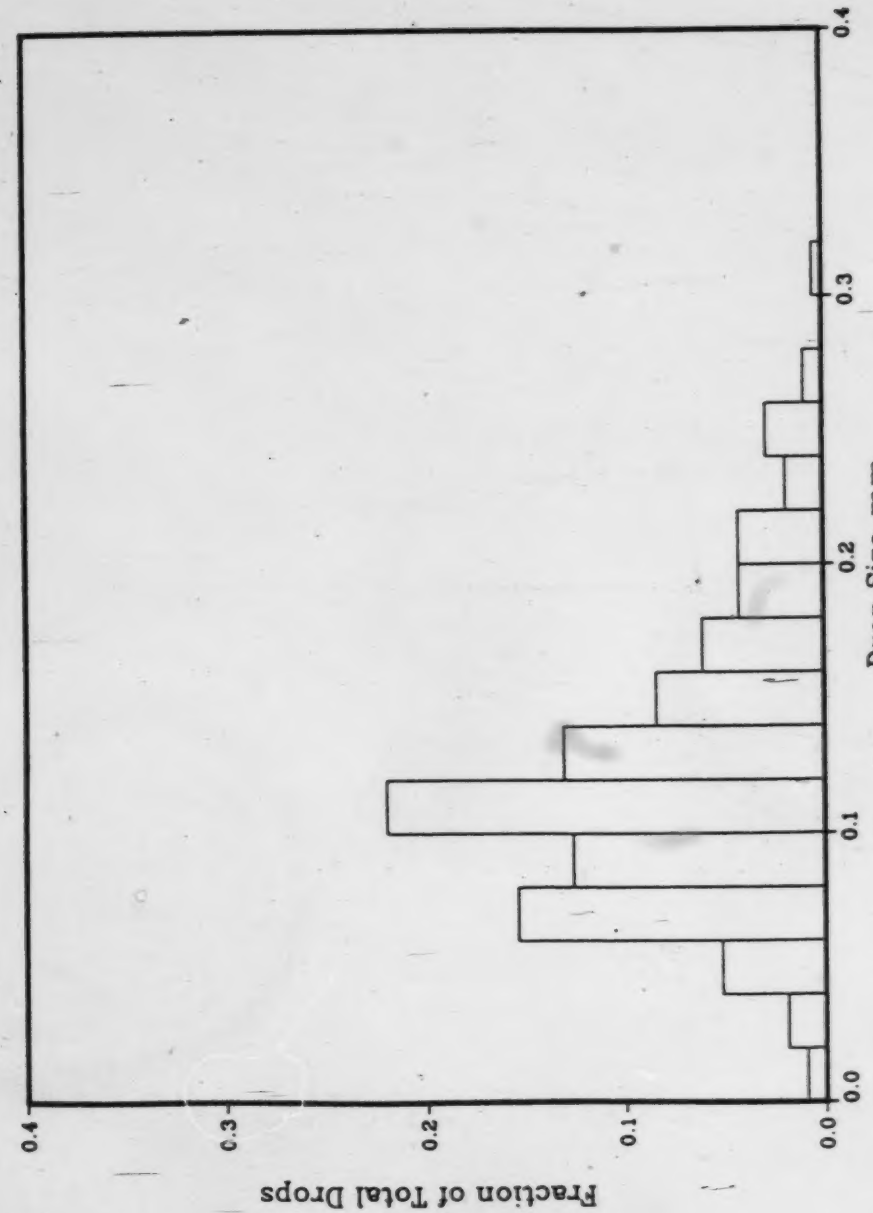

Figure 11.1.30: Drop size distribution for a 5% hexane, 95% water dispersion, 0.02M NaCl, 377 rpm

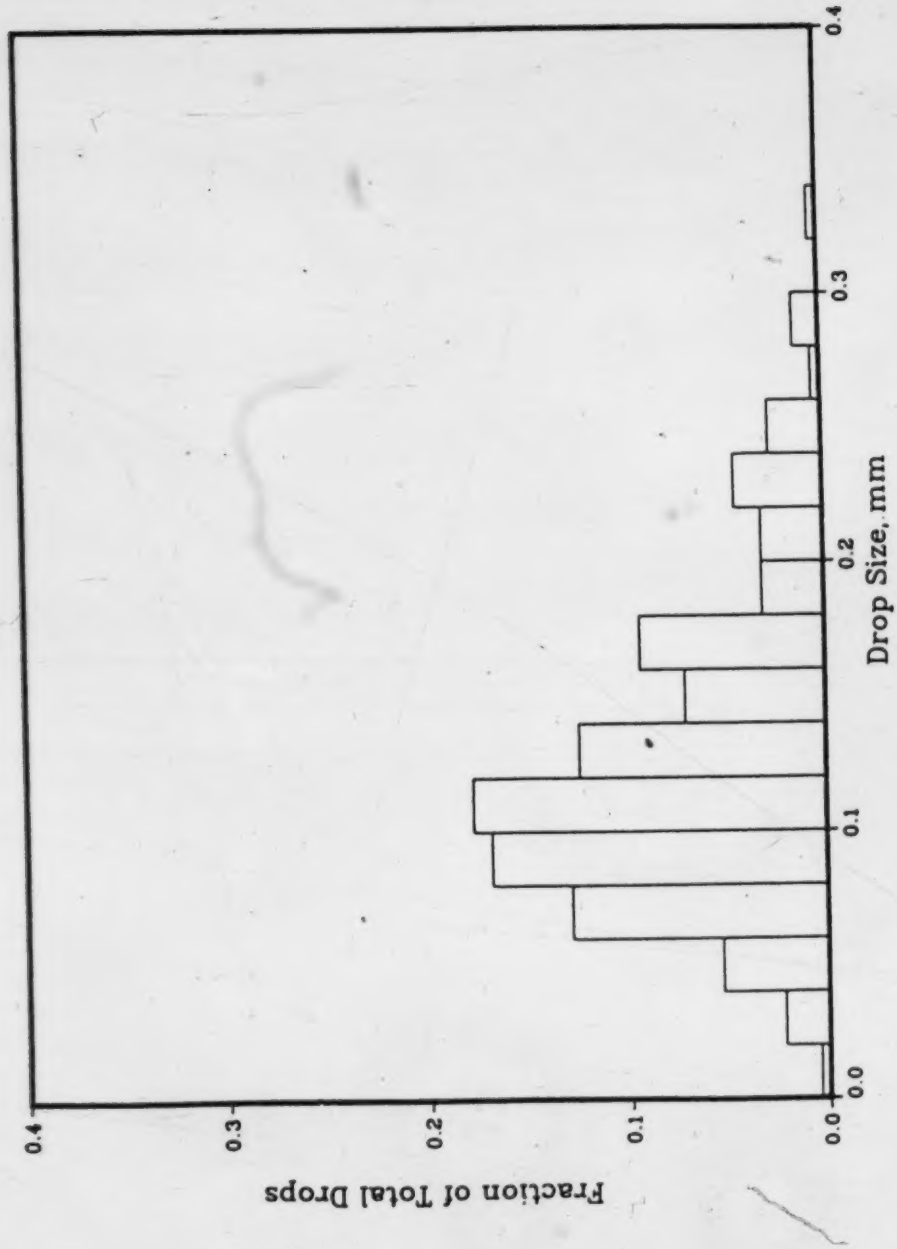

Figure 11.1.31: Drop size distribution for a 5% hexane, 95% water dispersion, 0.02M NaCl, 407 rpm

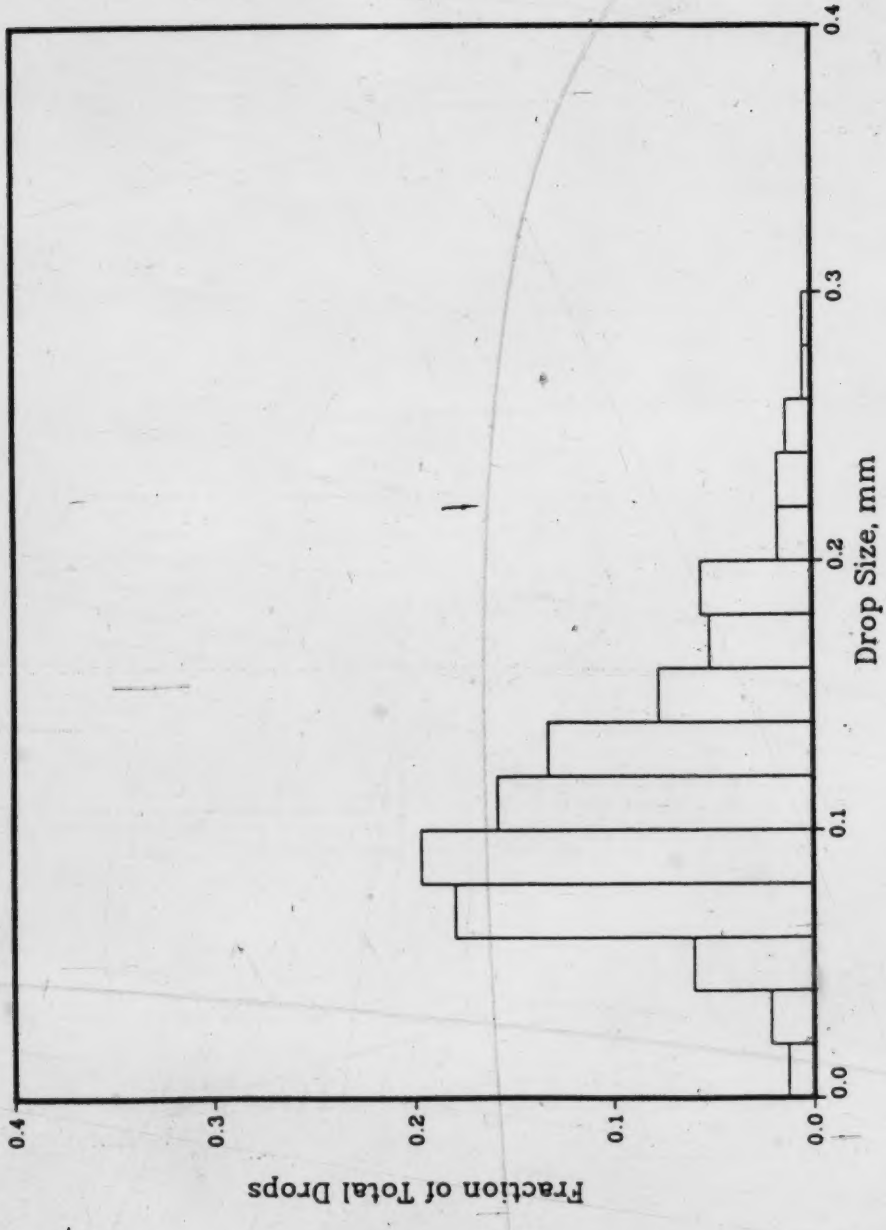

Figure 11.1.32: Drop size distribution for a 5% hexane, 95% water dispersion, 0.02M NaCl, 435 rpm

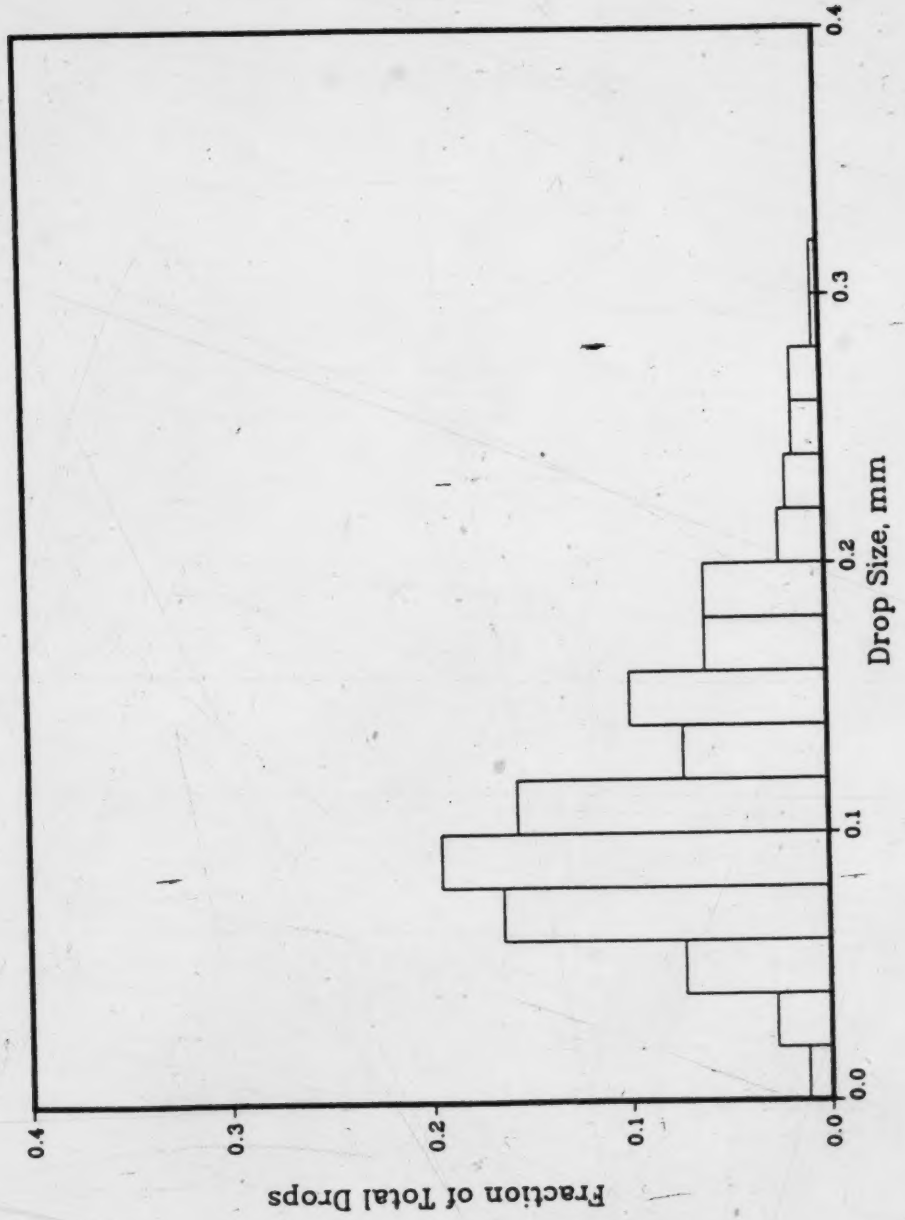

Figure 11.1.33: Drop size distribution for a 5% hexane, 95% water dispersion, 0.02M NaCl, 457 rpm

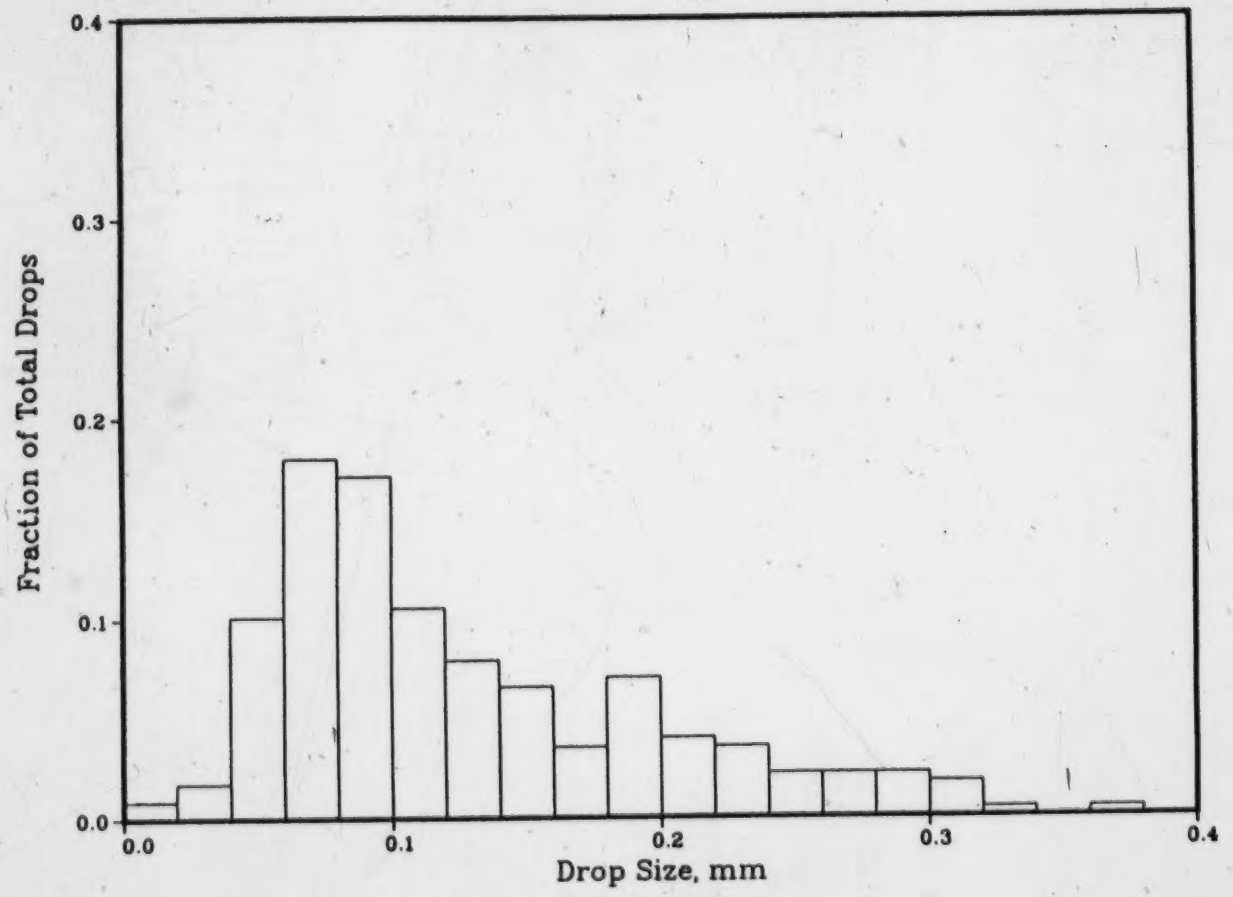

Figure 11.1.34: Drop size distribution for a 5% hexane, 95% water dispersion, 0.04 wt% kaolinite, 0.02M NaCl, 350 rpm

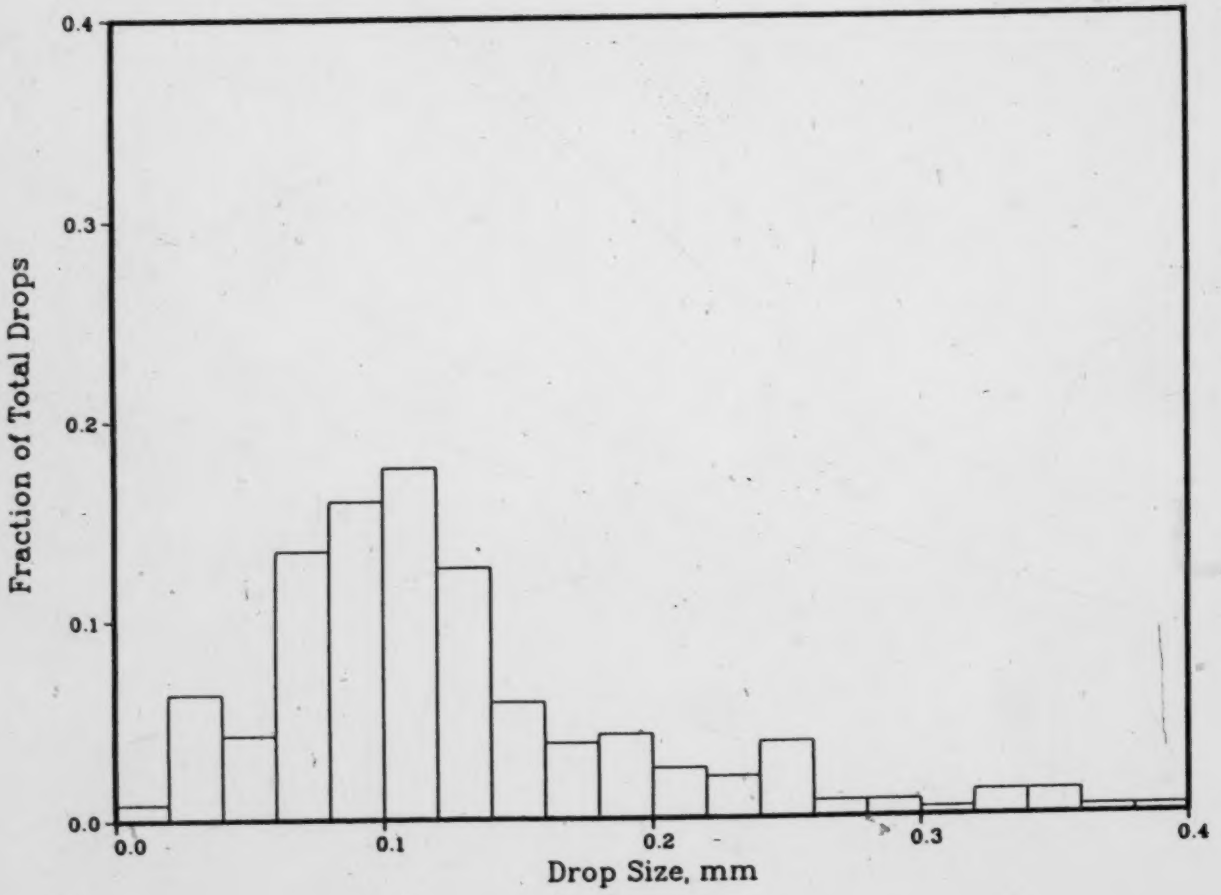

Figure 11.1.35: Drop size distribution for a 5% hexane, 95% water dispersion, 0.04 wt% kaolinite, 0.02M NaCl, 374 rpm

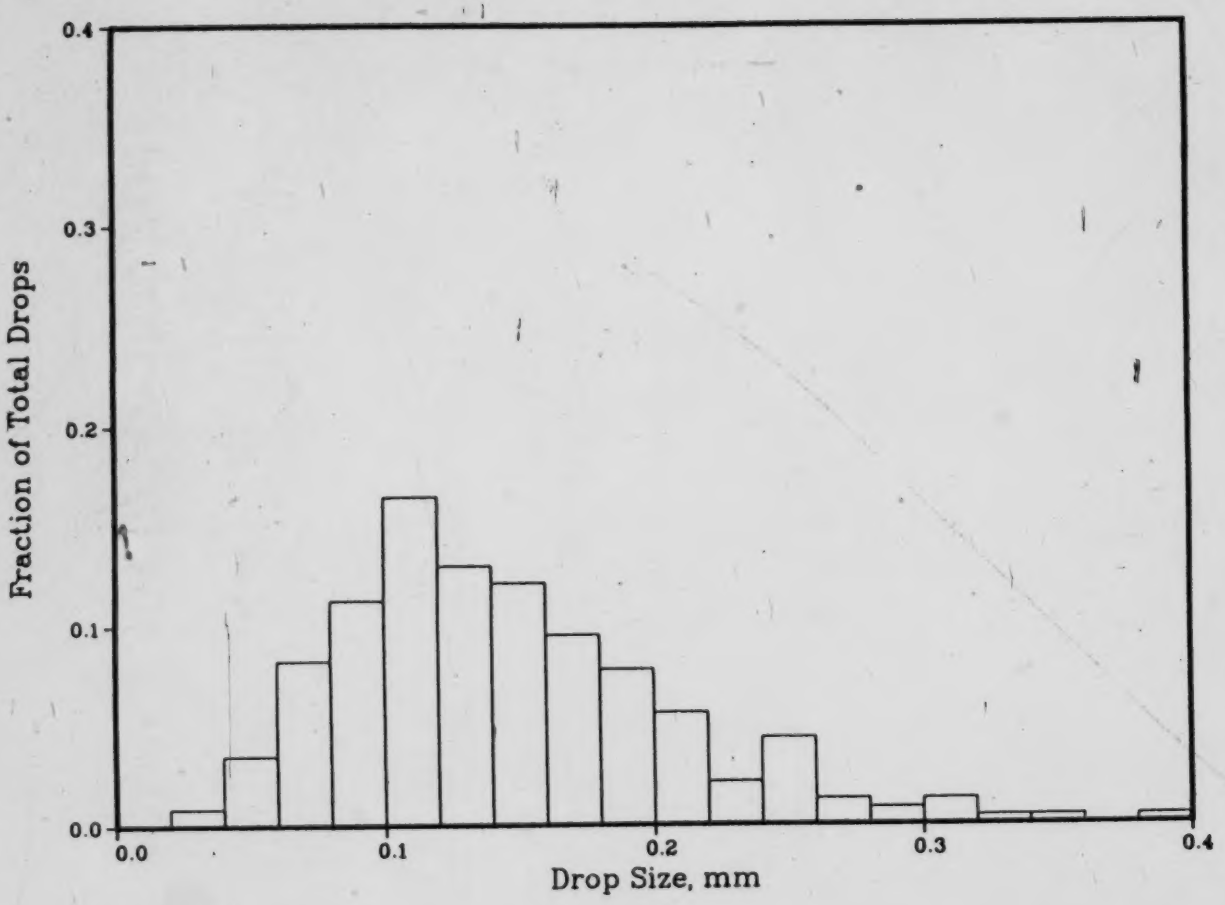

Figure 11.1.36: Drop size distribution for a 5% hexane, 95% water dispersion, 0.04 wt% kaolinite, 0.02M NaCl, 377 rpm

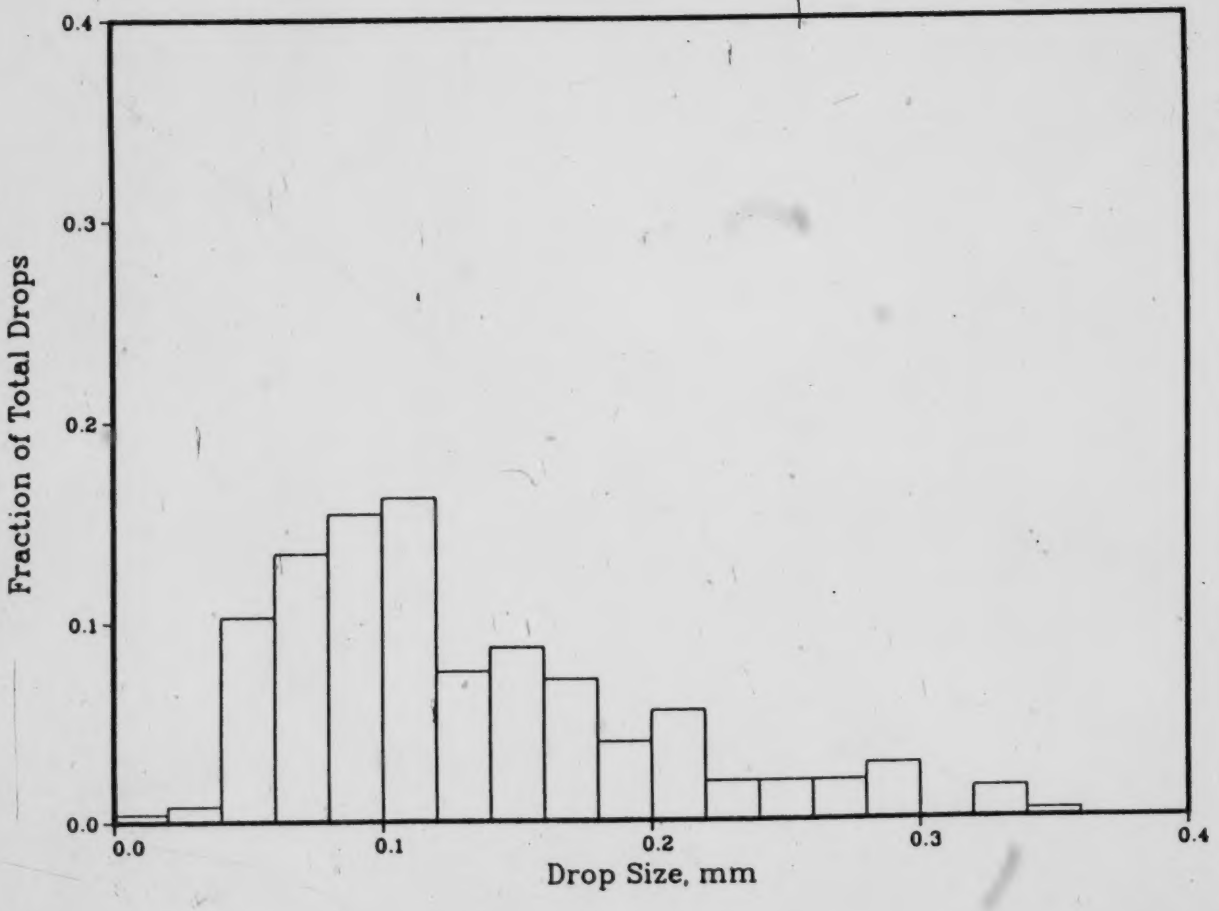

Figure 11.1.37: Drop size distribution for a 5% hexane, 95% water dispersion, 0.04 wt% kaolinite, 0.02M NaCl, 400 rpm

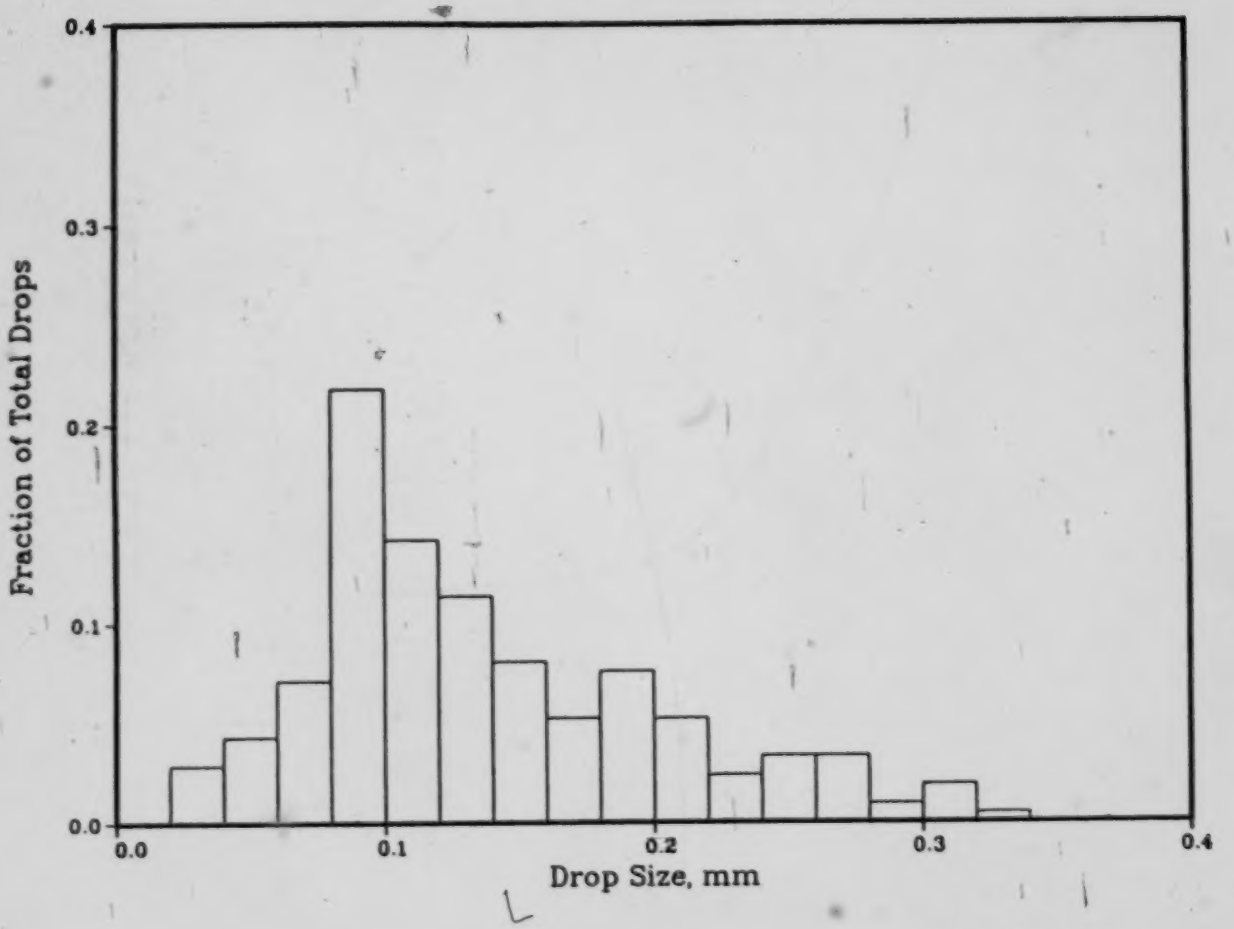

Figure 11.1.38: Drop size distribution for a 5% hexane, 95% water dispersion, 0.04 wt% kaolinite, 0.02M NaCl, 420 rpm

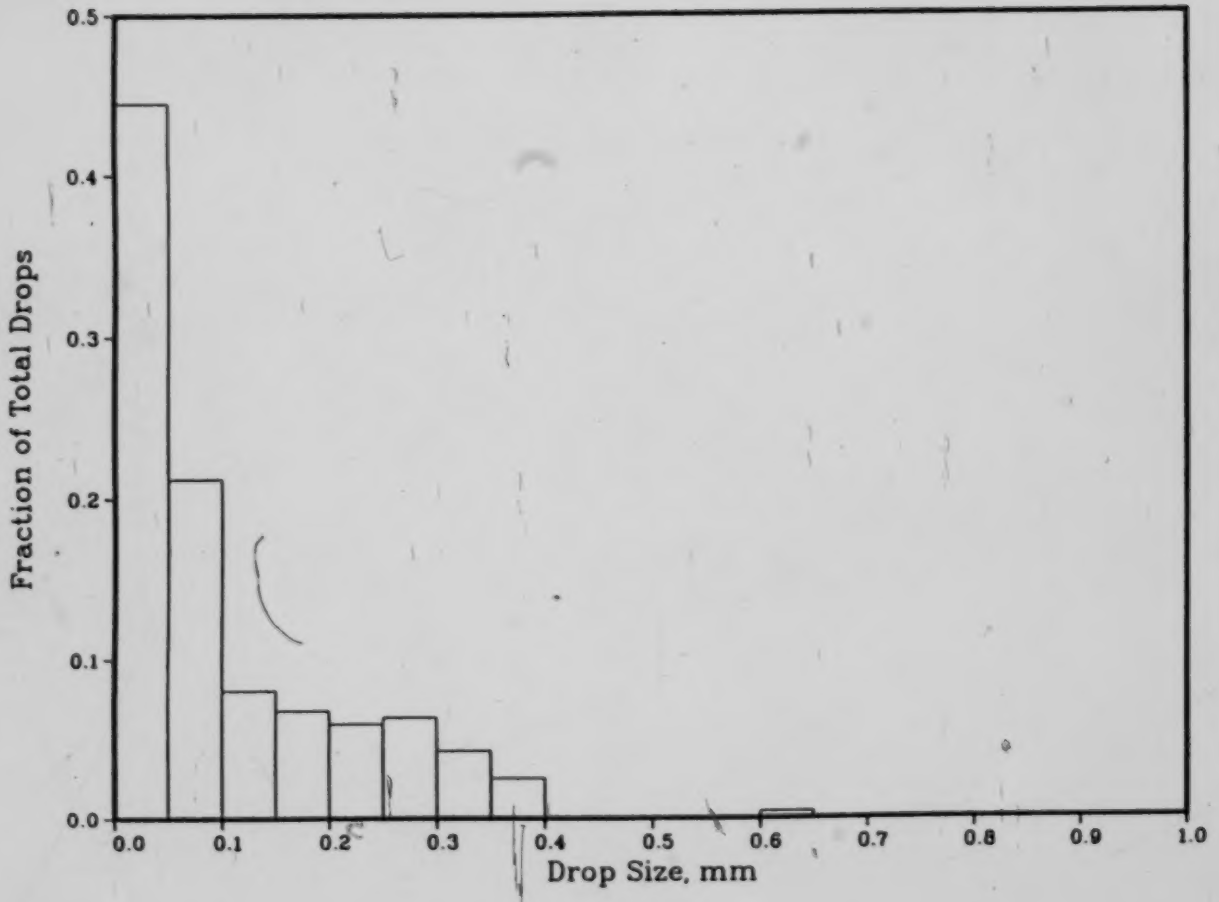

Figure 11.2.1 : Drop size distribution for a 5% paraffin oil, 95% water dispersion, 0.001M NaCl, 305 rpm

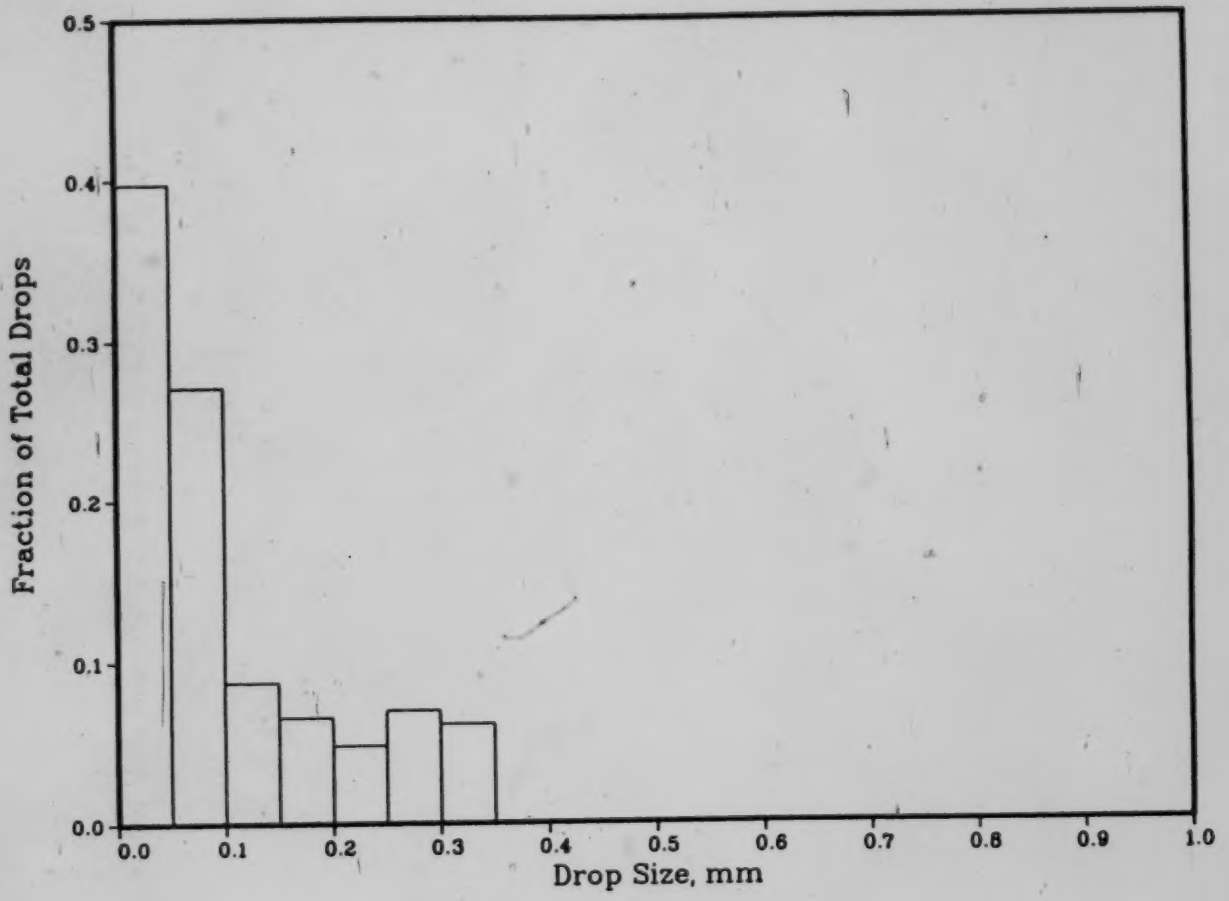

Figure 11.2.2 : Drop size distribution for a 5% paraffin oil, 95% water dispersion, 0.001M NaCl, 327.5 rpm

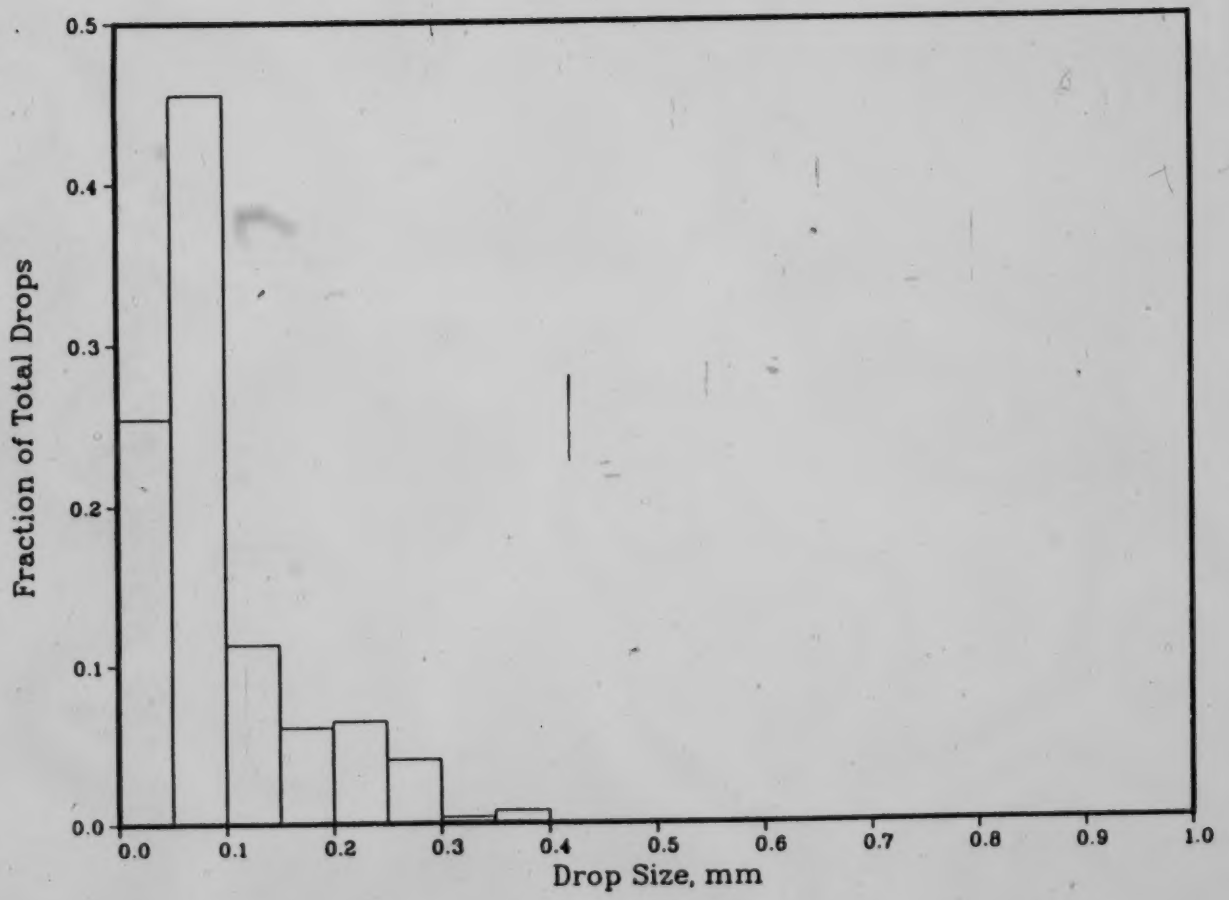

Figure 11.2.3 : Drop size distribution for a 5% paraffin oil, 95% water dispersion, 0.001M NaCl, 349 rpm

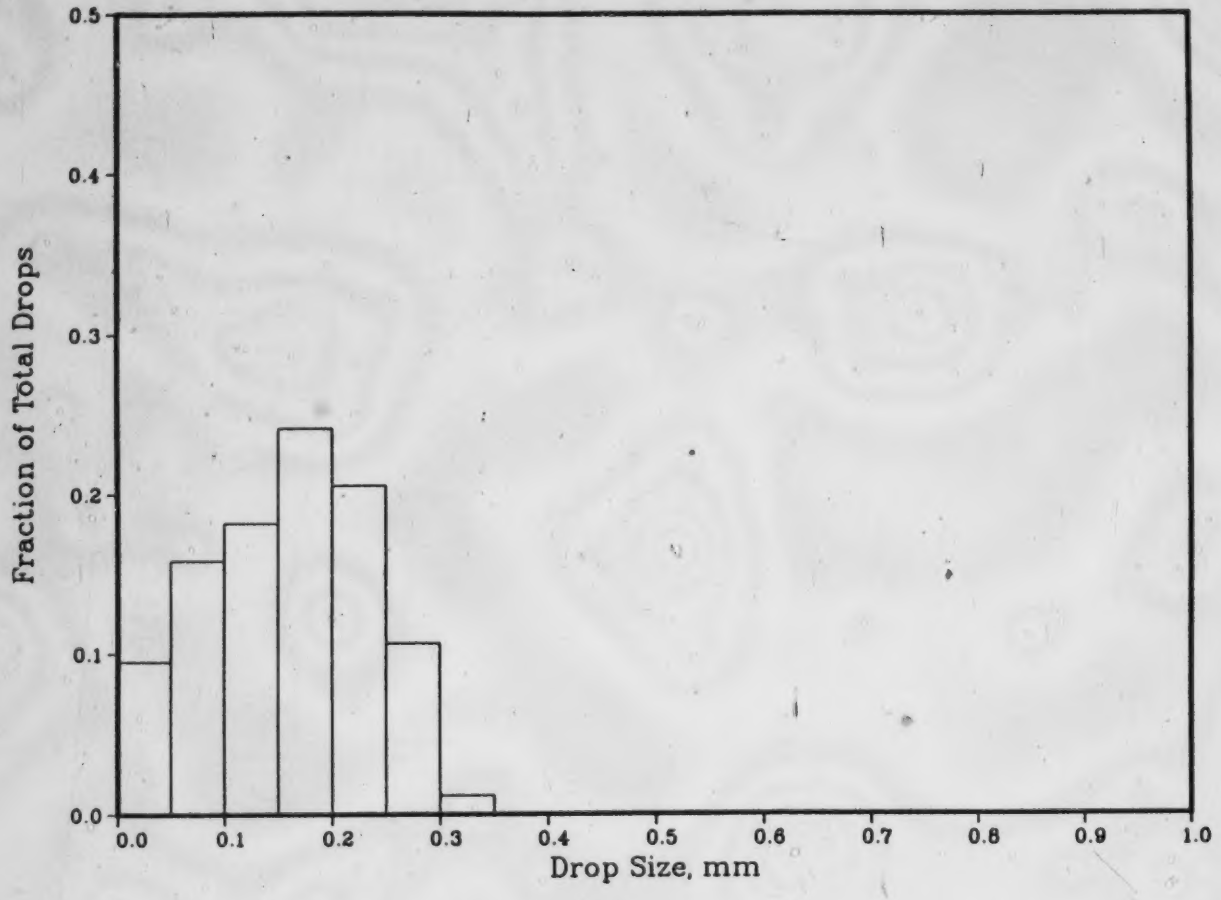

Figure 11.2.4 : Drop size distribution for a 5% paraffin oil, 95% water dispersion, 0.001M NaCl, 403 rpm

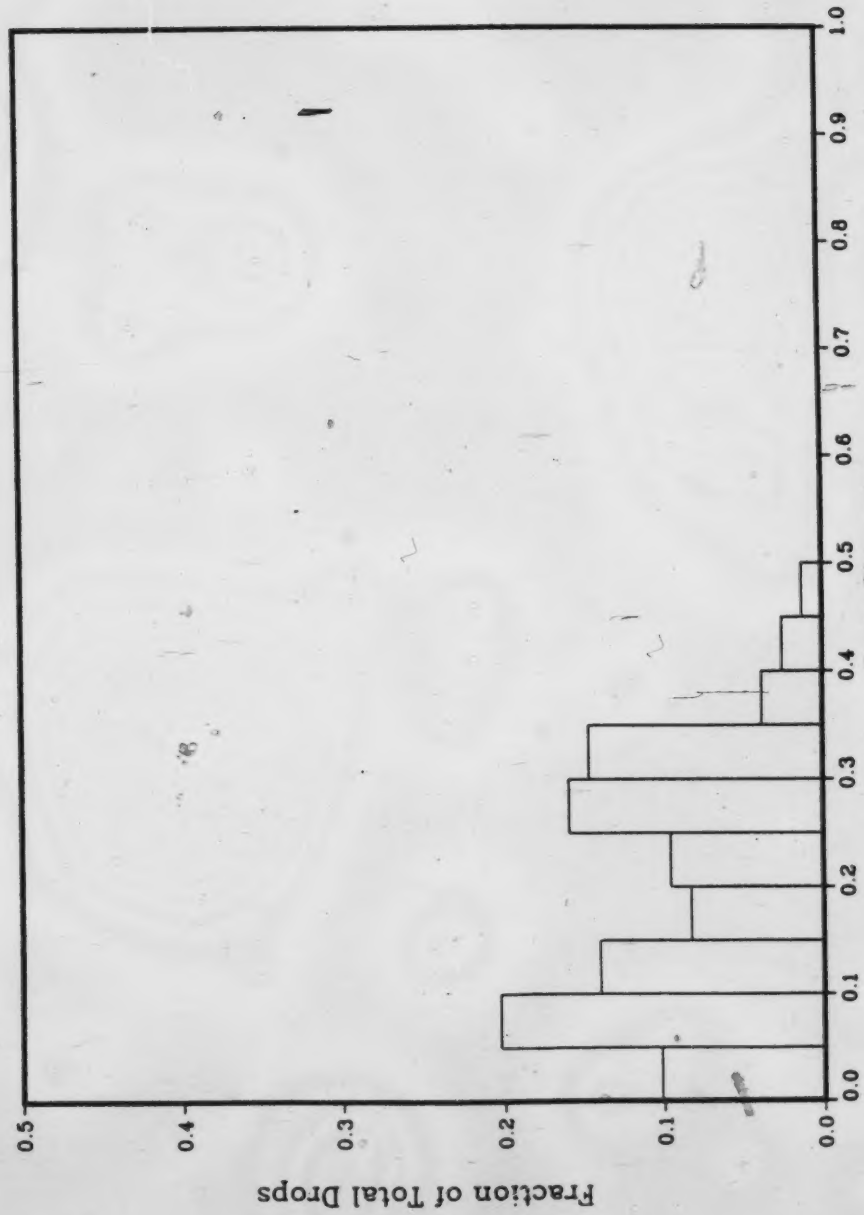

Figure 11.2.5 : Drop size distribution for a 5% paraffin oil, 95% water dispersion, 0.04 wt% kaolinite, 0.001M NaCl, 308 rpm

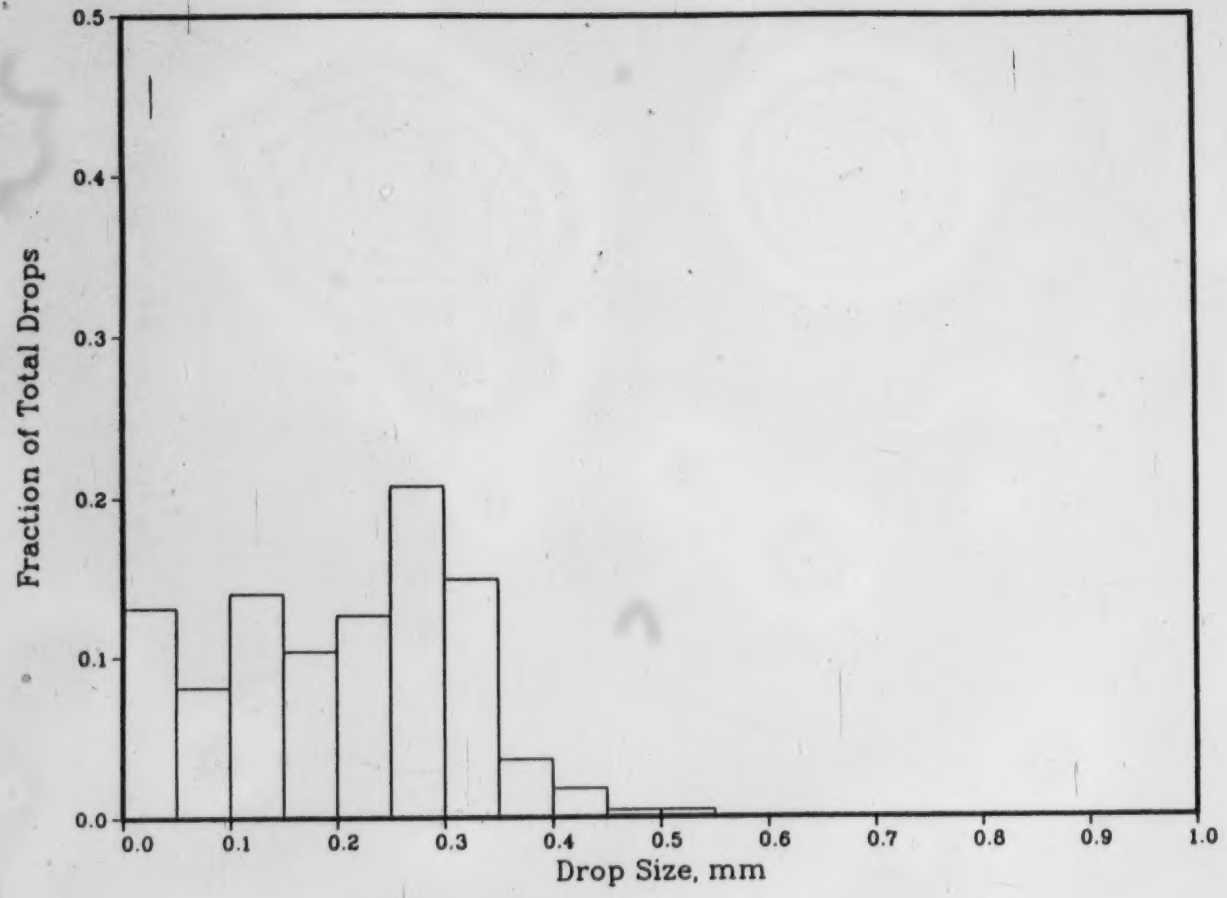

Figure 11.2.6 : Drop size distribution for a 5% paraffin oil, 95% water dispersion, 0.04 wt% kaolinite, 0.001M NaCl, 325 rpm

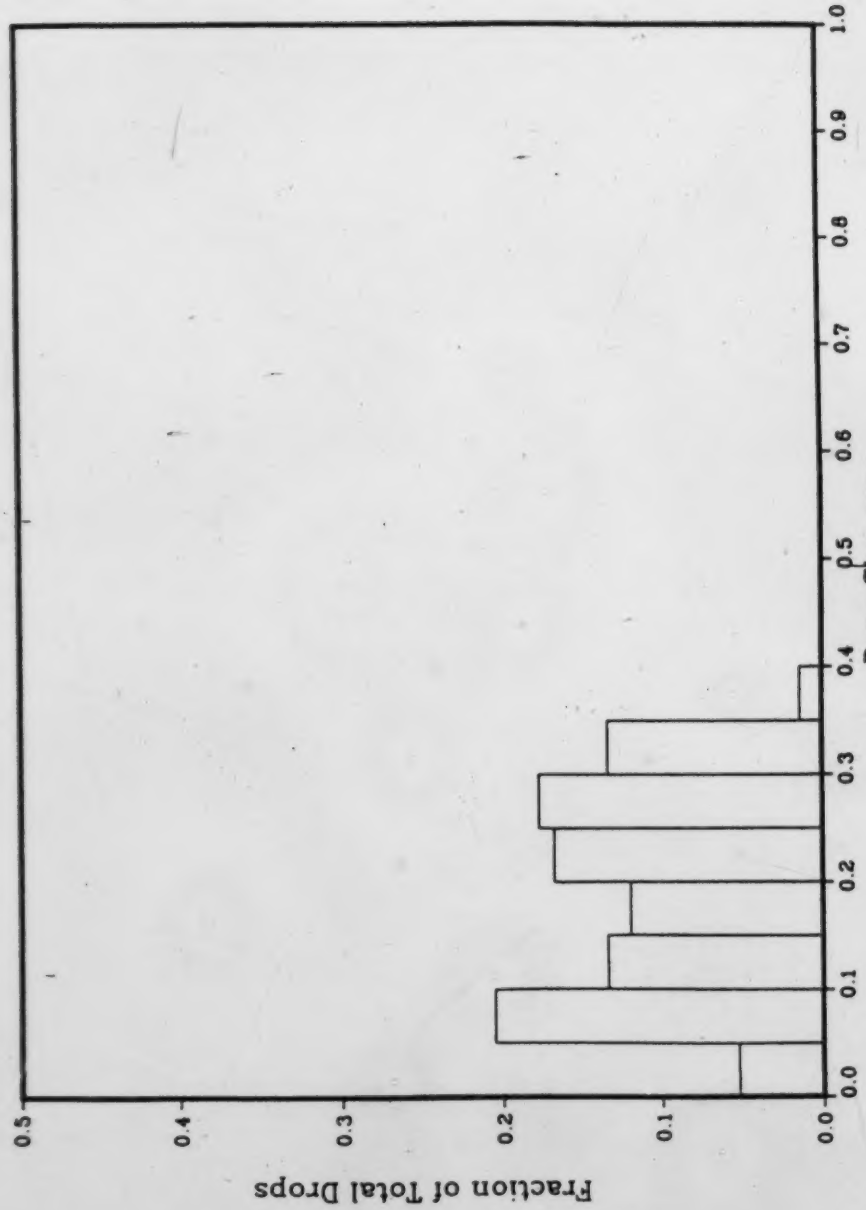

Figure 11.2.7 : Drop size distribution for a 5% paraffin oil, 95% water dispersion, 0.04 wt% kaolinite, 0.001M NaCl, 345 rpm

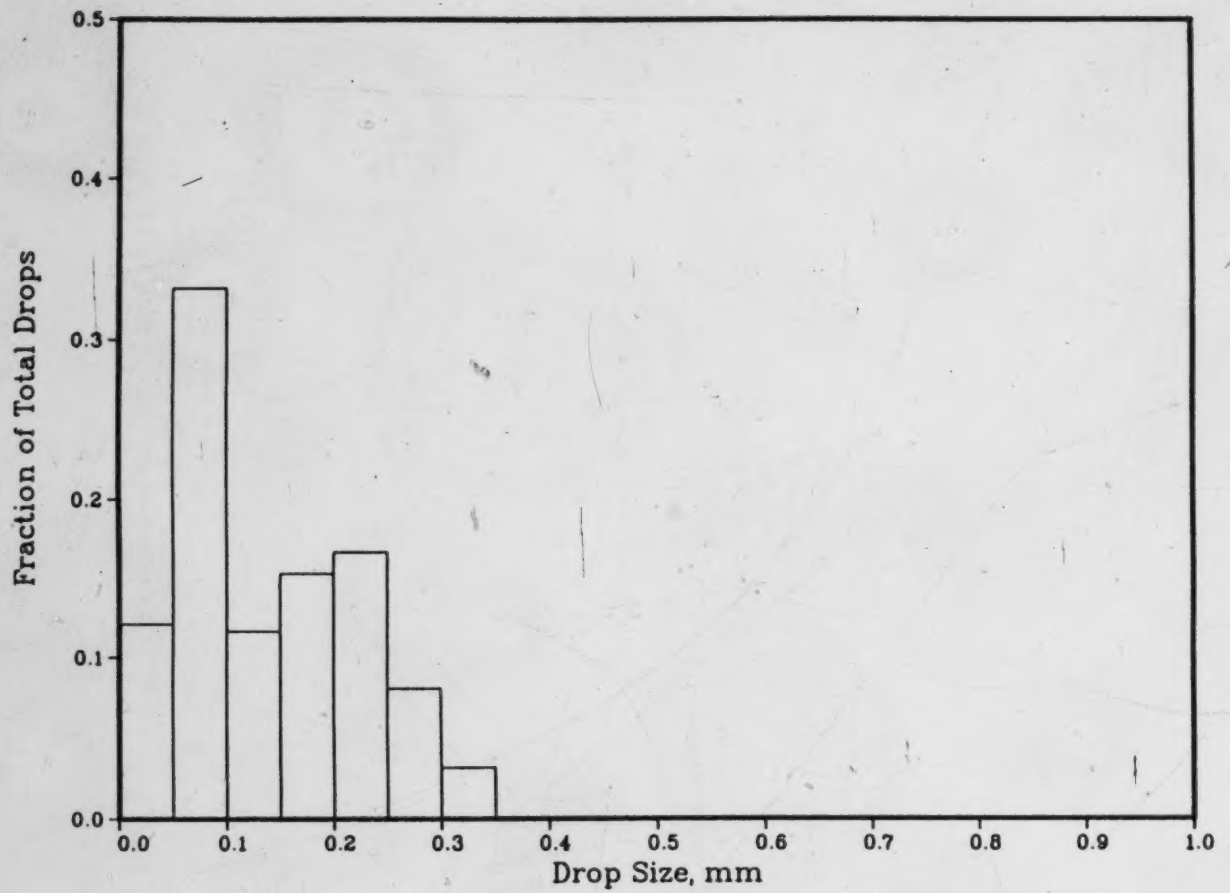

Figure 11.2.8 : Drop size distribution for a 5% paraffin oil, 95% water dispersion, 0.04 wt% kaolinite, 0.001M NaCl, 349 rpm

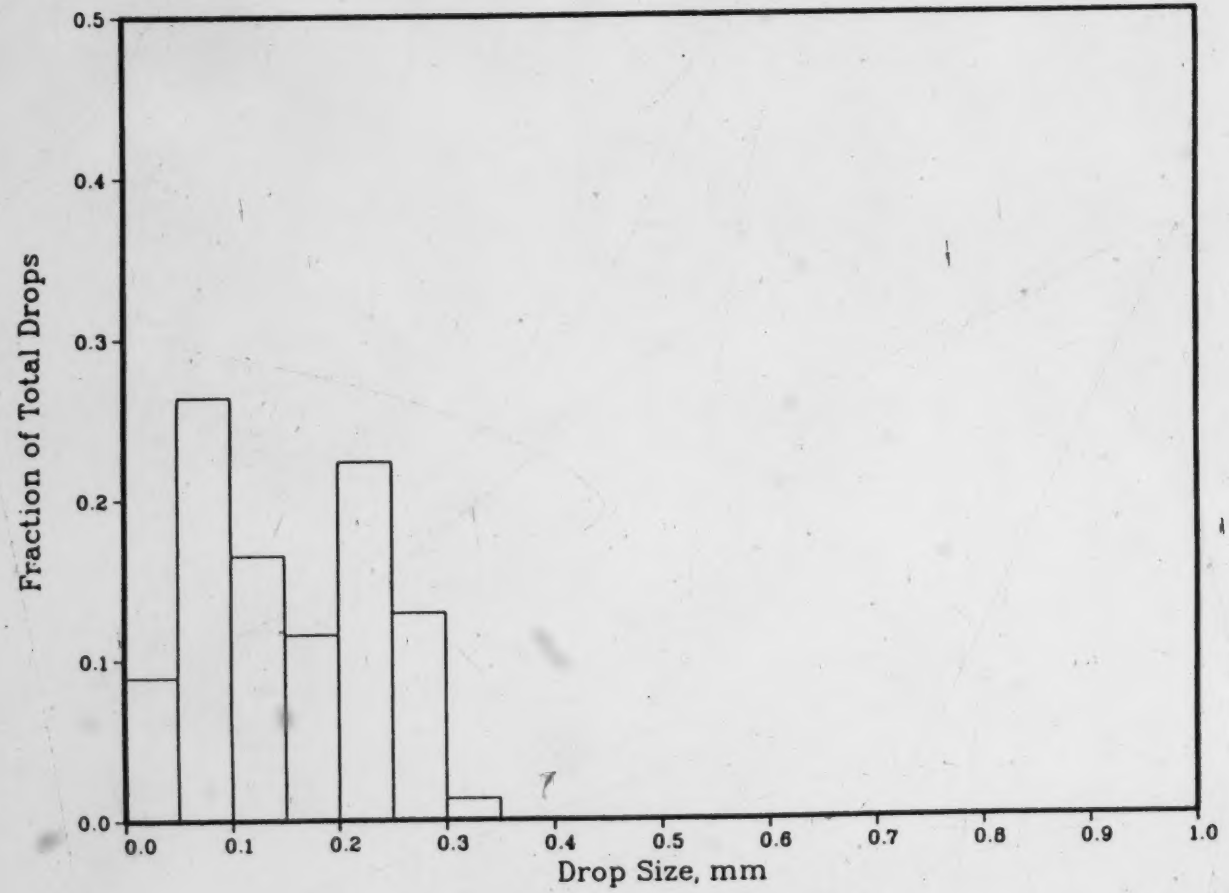

Figure 11.2.9 : Drop size distribution for a 5% paraffin oil, 95% water dispersion, 0.04 wt% kaolinite, 0.001M NaCl, 401 rpm

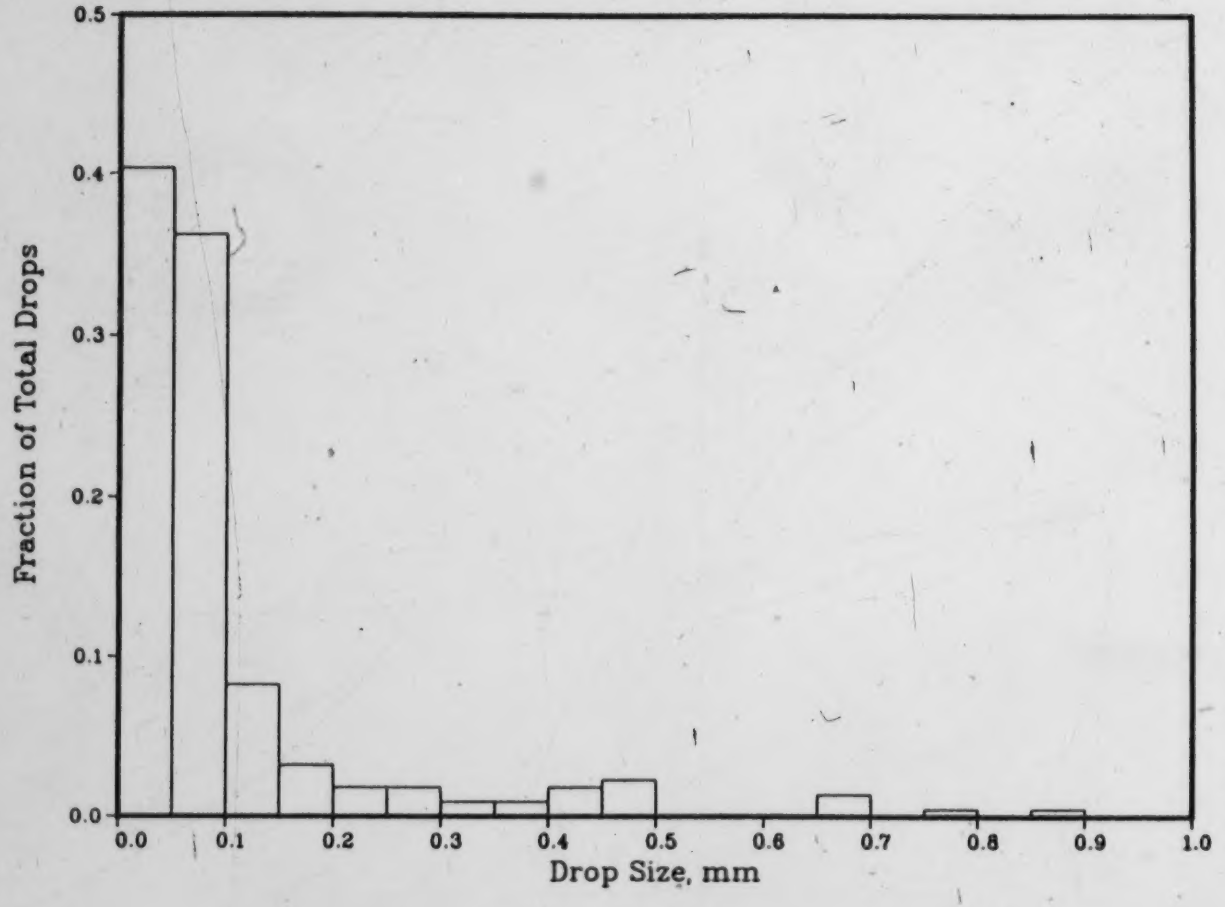

Figure 11.3.1 : Drop size distribution for a 5% bitumen, 95% water dispersion, 0.001M NaCl, 319 rpm

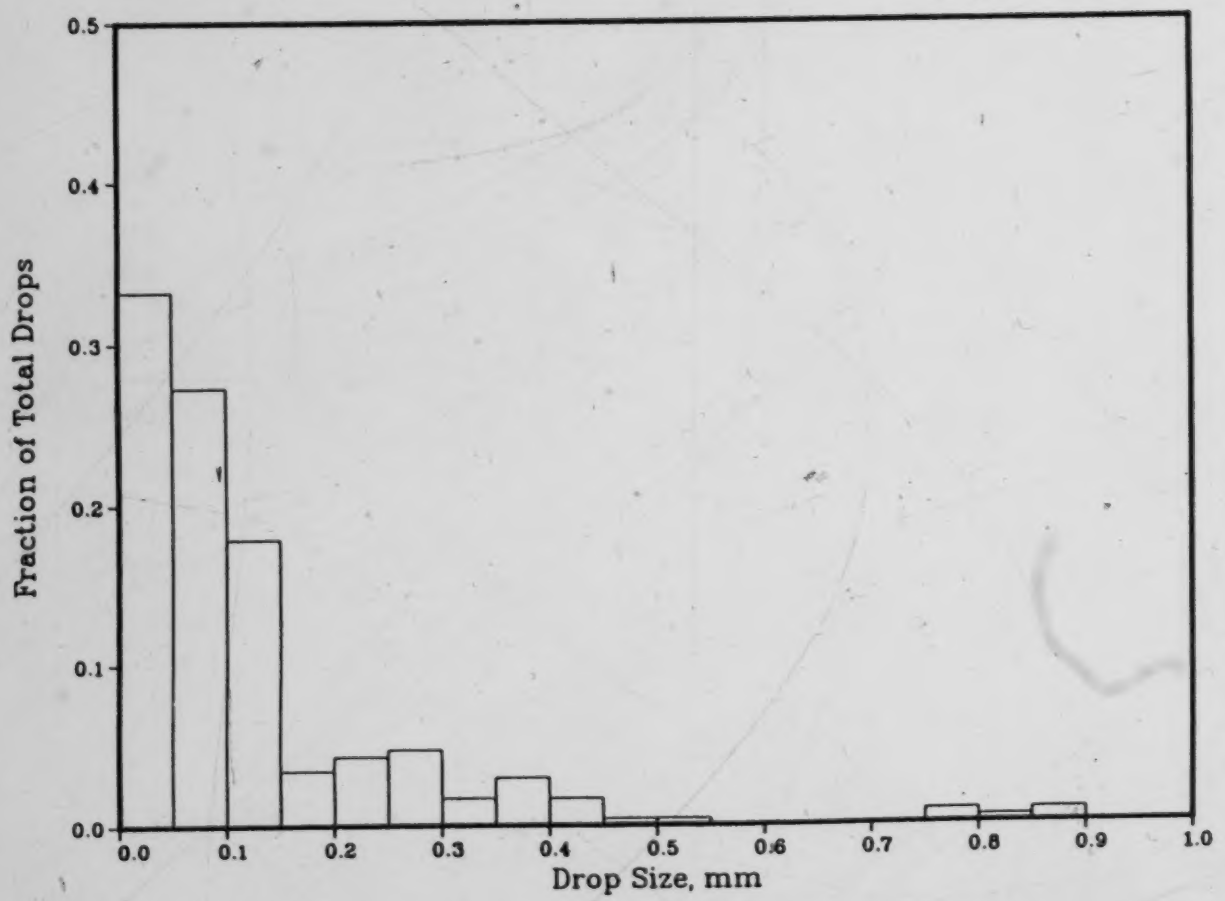

Figure 11.3.2 : Drop size distribution for a 5% bitumen, 95% water dispersion, 0.001M NaCl, 360 rpm

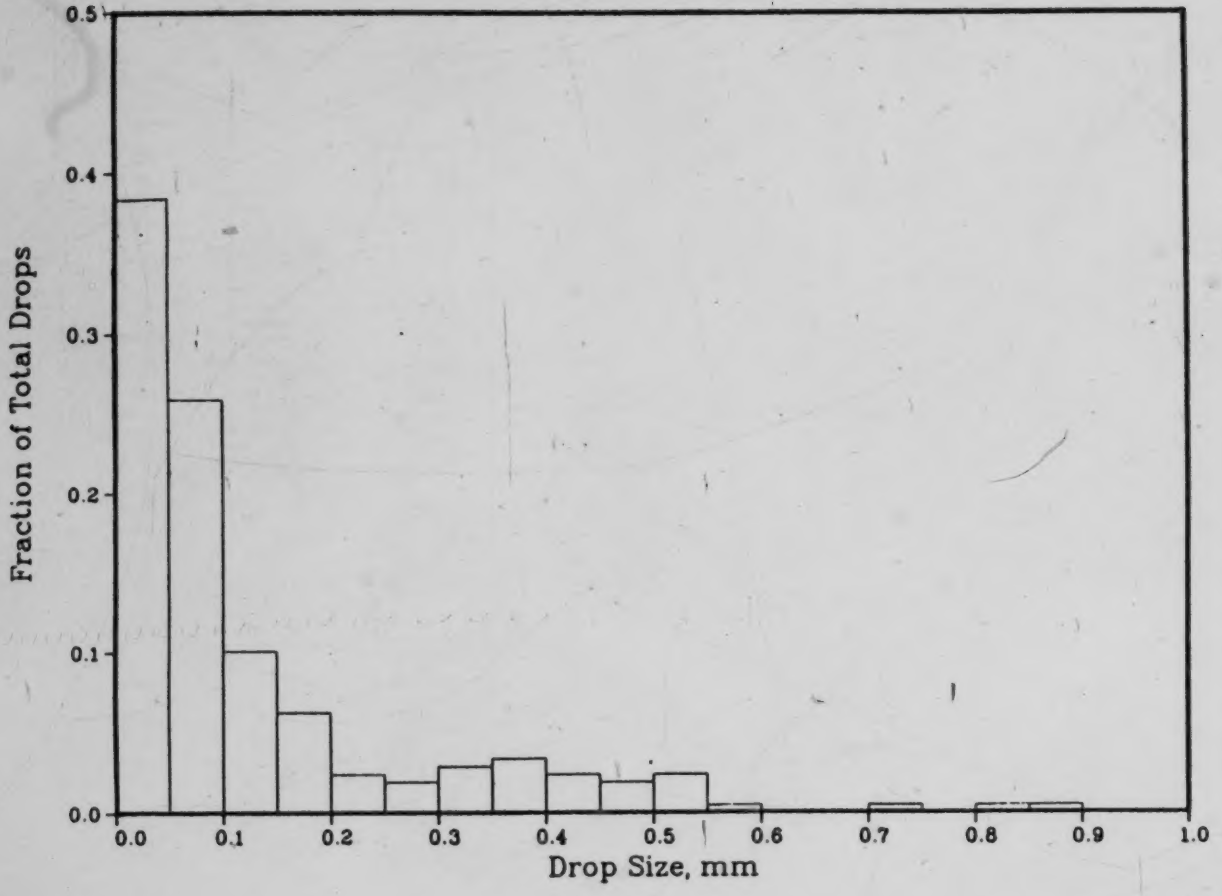

Figure 11.3.3 : Drop size distribution for a 5% bitumen, 95% water dispersion, 0.001M NaCl, 410 rpm

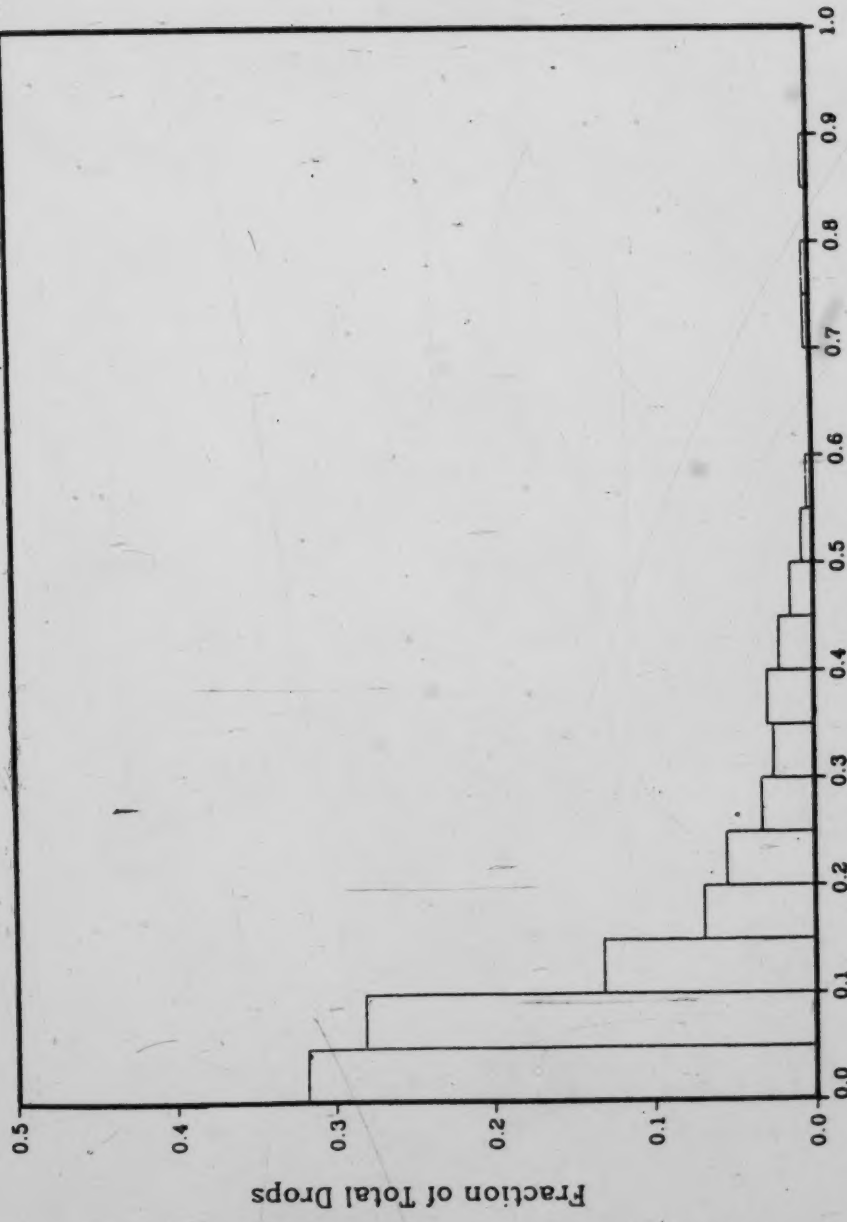

Figure 11.3.4 : Drop size distribution for a 5% bitumen, 95% water dispersion, 0.001M NaCl, 450 rpm

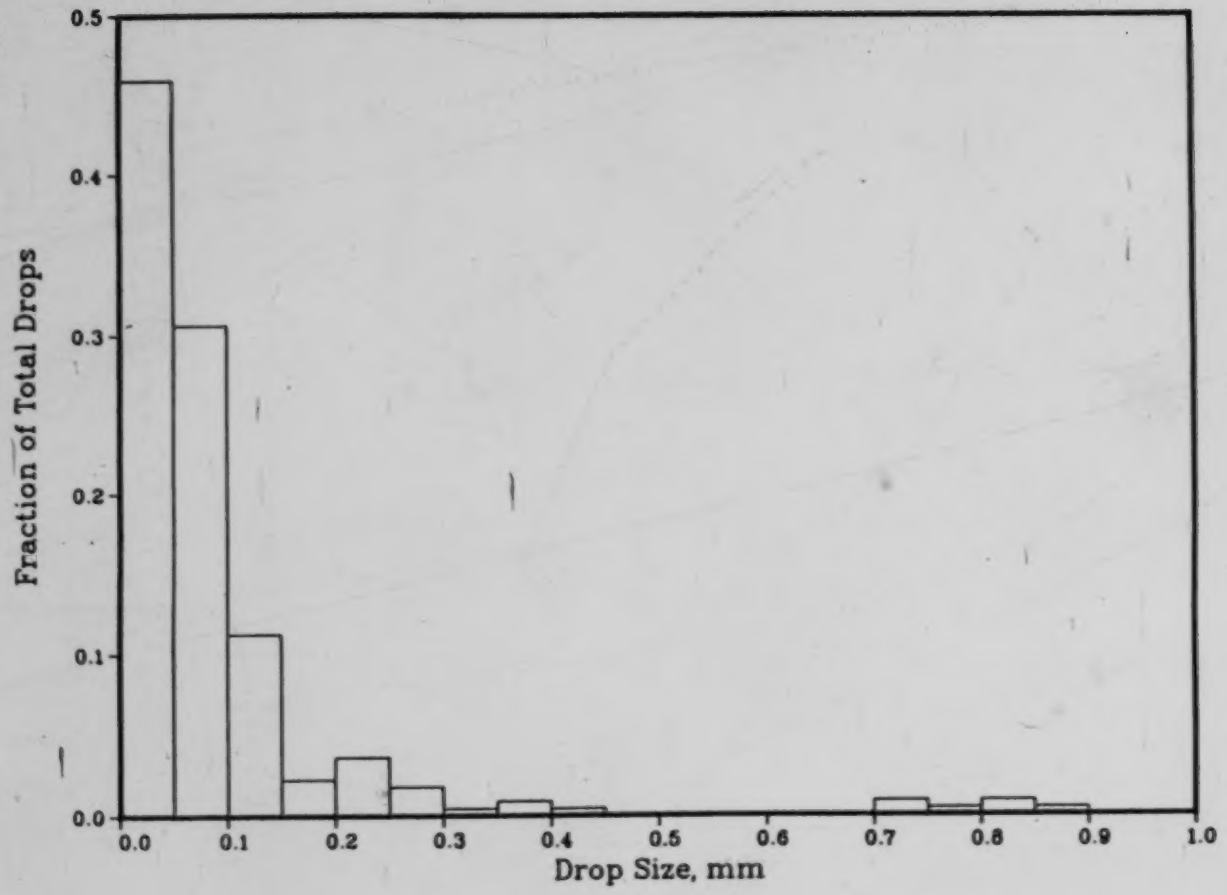

Figure 11.3.5 : Drop size distribution for a 5% bitumen, 95% water dispersion, 0.04 wt% kaolinite, 0.001M NaCl, 304 rpm

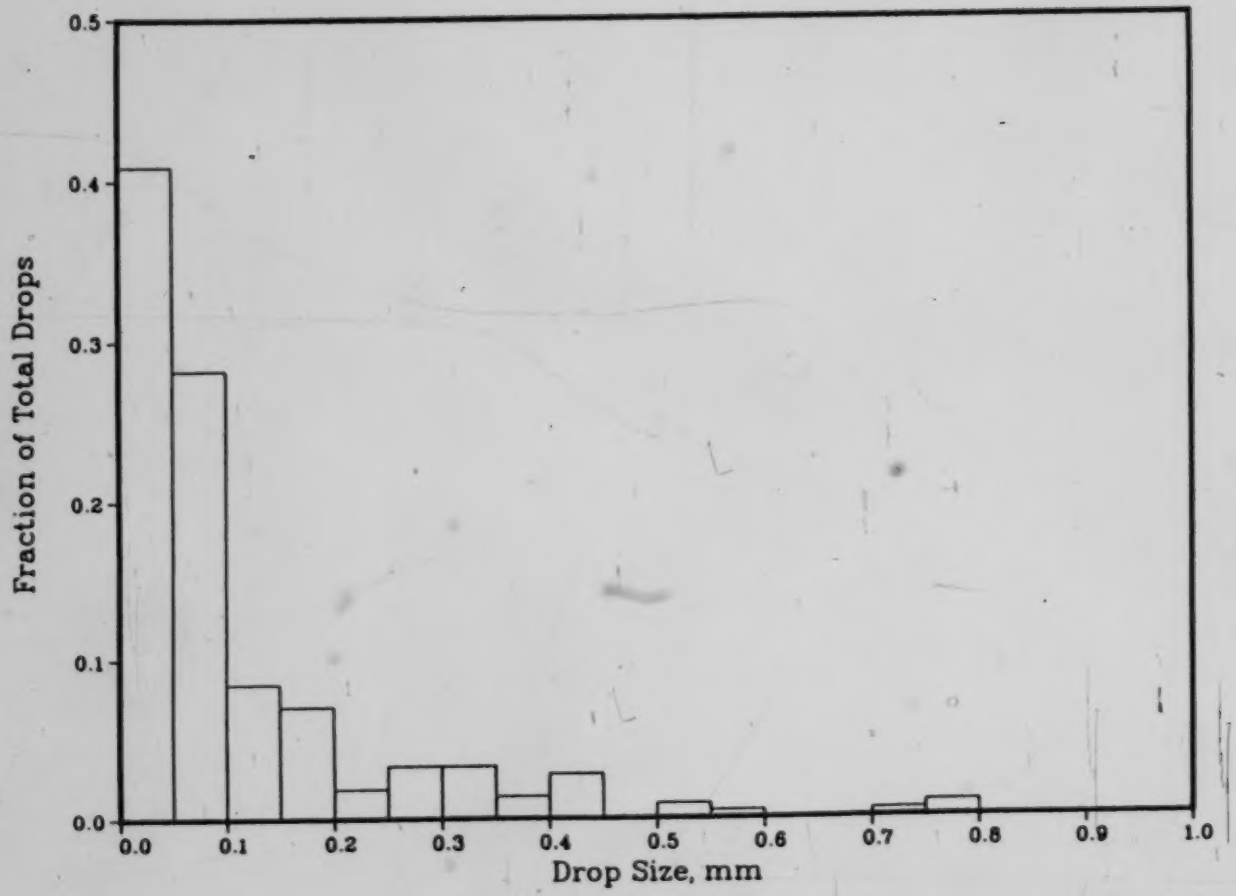

Figure 11.3.6 : Drop size distribution for a 5% bitumen, 95% water dispersion, 0.04 wt% kaolinite, 0.001M NaCl, 356 rpm

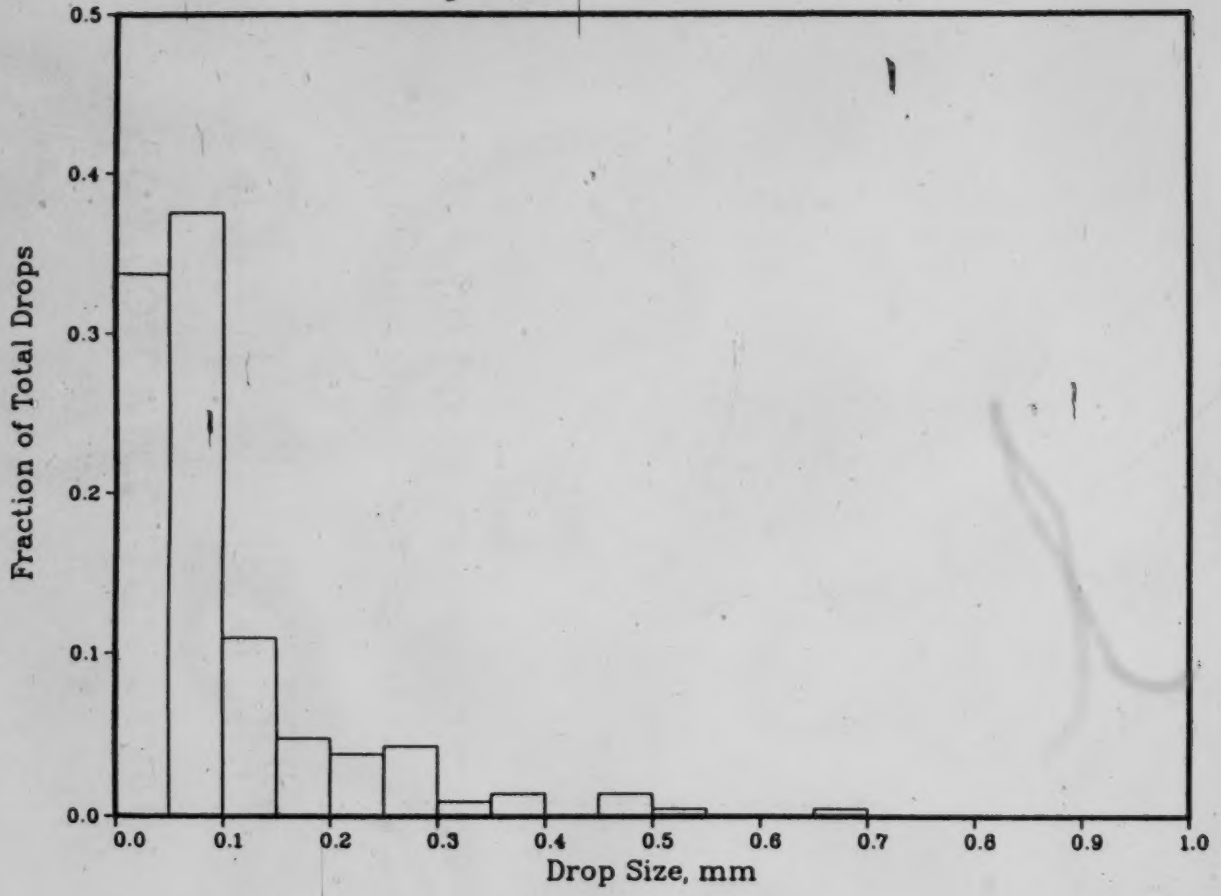

Figure 11.3.7 : Drop size distribution for a 5% bitumen, 95% water dispersion, 0.04 wt% kaolinite, 0.001M NaCl, 380 rpm

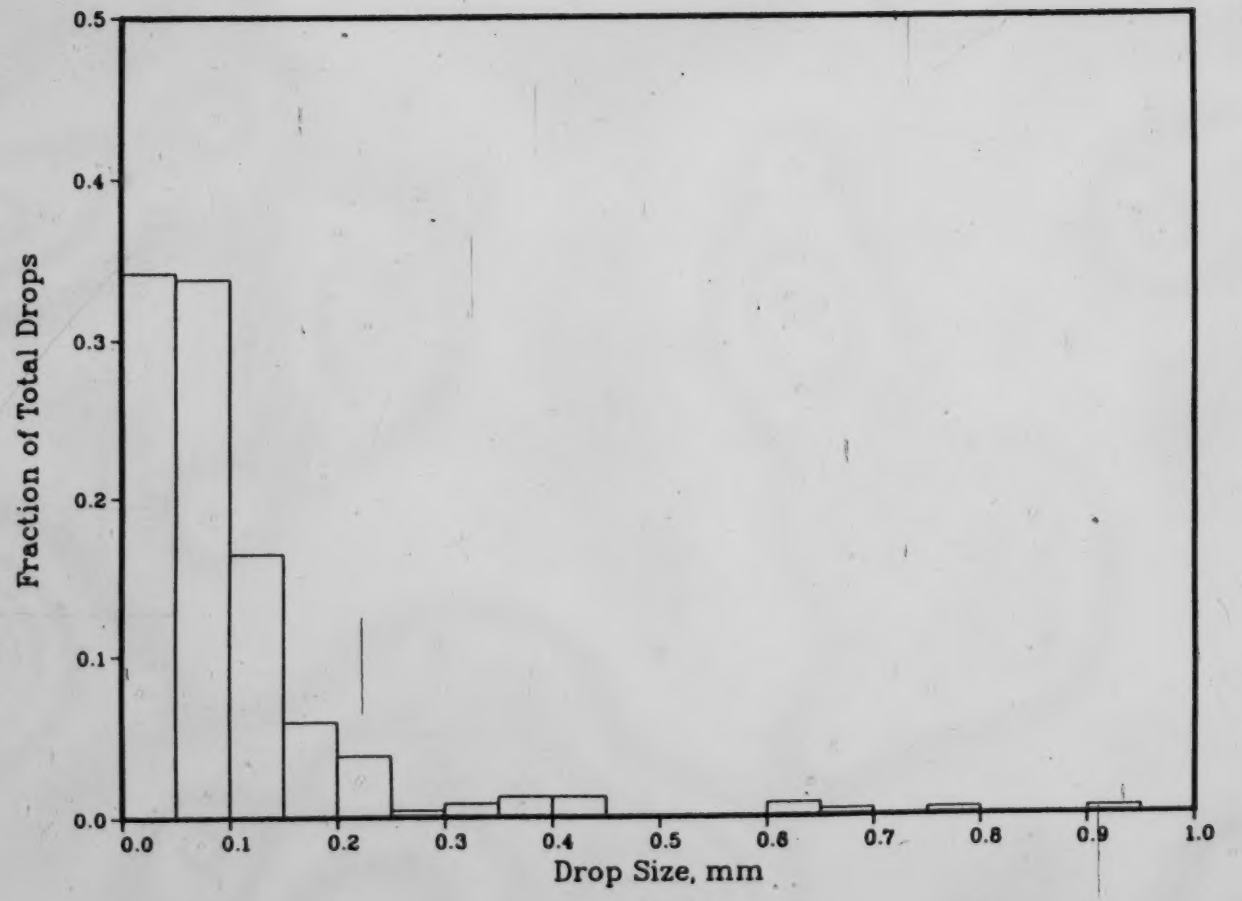

Figure 11.3.8 : Drop size distribution for a 5% bitumen, 95% water dispersion, 0.04 wt% kaolinite, 0.001M NaCl, 414 rpm

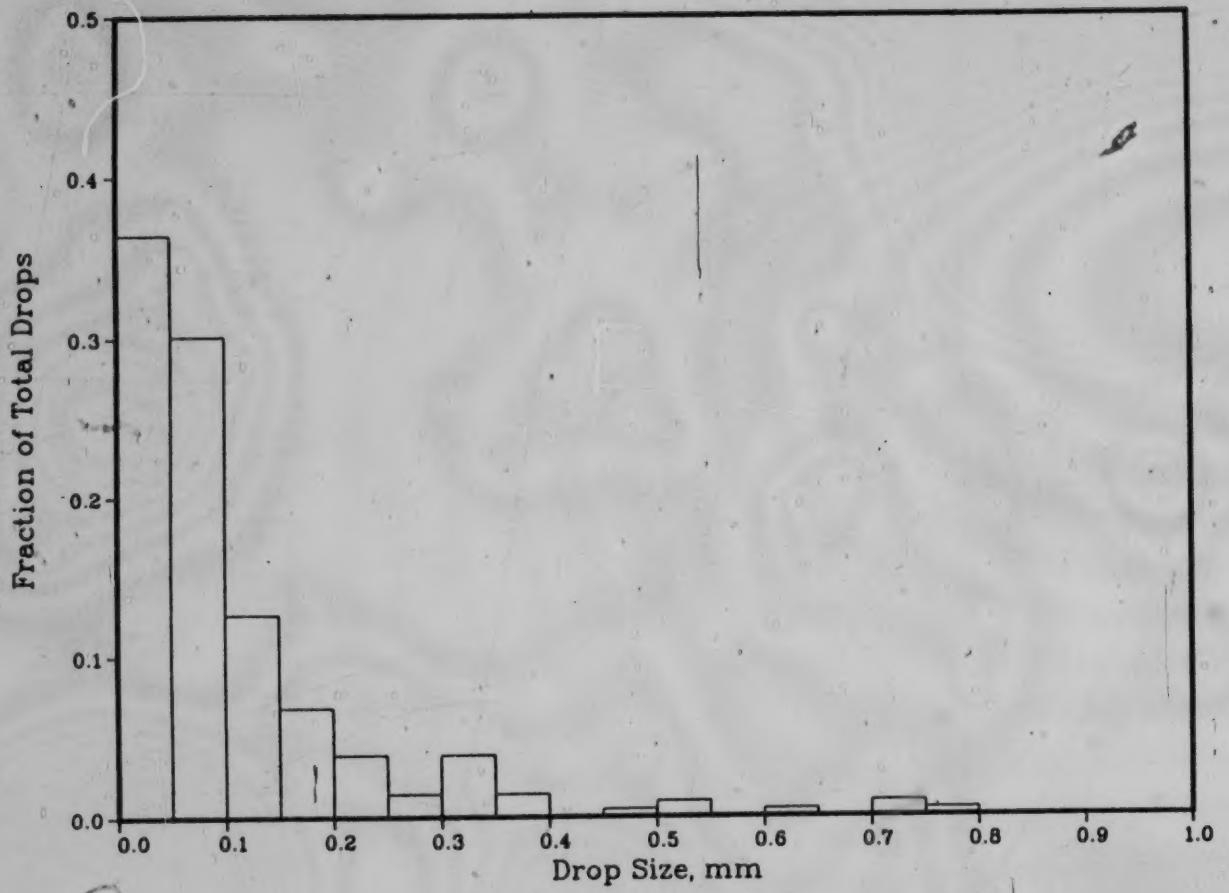

Figure 11.3.9 : Drop size distribution for a 5% bitumen, 95% water dispersion, 0.04 wt% kaolinite, 0.001M NaCl, 437 rpm